ROLE OF THE VITAMIN D RECEPTOR IN INSULIN SECRETION

AND BETA CELL FUNCTION

APPROVED BY SUPERVISORY COMMITTEE

Makoto Kuro-o

Melanie Cobb

Philipp Scherer

Joyce Repa

DEDICATION

I would like dedicate this dissertation to my parents, Særún Sigurgeirsdóttir and Guðmundur Kjalar Jónsson, and my dear husband, Svavar Sigursteinsson. I would like to thank my parents for always believing in me and teaching me that with hard work and dedication you can accomplish anything. I would like to thank my dear husband for his immense support in all areas and I am forever grateful for him staying at home and taking such good care of our son, Isak Thor Svavarsson, during the course of my study.

ACKNOWLEDGEMENT

First of all I would like to thank my mentor, Dr. Joyce Repa, for everything she has taught me. Joyce has truly gone far and beyond in training me to become a good scientist and she has taught me a great deal more than just proper bench work. I feel very blessed to have gotten my training under her guidance. I would like to thank my dissertation committee, Dr. Melanie Cobb, Dr. Makoto Kuro-o and Dr. Philipp Scherer, for their guidance and support. I also want to thank them for allowing me to interact and learn from their students and postdoctoral fellows, and for sharing reagents and equipment that were vital for the advancement of my research. I would also like to thank all my lab mates and collaborators. Especially Jen-Chieh Chuang for teaching me how to isolate primary mouse islets and Anna Taylor for all her help and for always being there when I needed her. I would also like to thank Joyce Repa, Ryan Jones, Anna Taylor and Yelenis Mari for their help in proofreading this dissertation and providing constructive criticism.

ROLE OF THE VITAMIN D RECEPTOR IN INSULIN SECRETION AND BETA CELL FUNCTION

by

LILJA KJALARSDOTTIR

DISSERTATION / THESIS

Presented to the Faculty of the Graduate School of Biomedical Sciences

The University of Texas Southwestern Medical Center at Dallas

In Partial Fulfillment of the Requirements

For the Degree of

DOCTOR OF PHILOSOPHY

The University of Texas Southwestern Medical Center at Dallas

Dallas, Texas

November, 2011

ROLE OF THE VITAMIN D RECEPTOR IN INSULIN SECRETION AND BETA CELL FUNCTION

Lilja Kjalarsdottir, Ph.D

The University of Texas Southwestern Medical Center at Dallas, 2011

Supervising Professor: Joyce Repa, Ph.D.

1,25-dihydroxyvitamin D_3 (VitD) is a ligand for the Vitamin D Receptor (VDR, NR1I1), which is a member of the family of Nuclear Hormone Receptors (NHR). Previously, the Repa lab identified VDR as the fourth most abundant NHR in mouse islets based on mRNA levels, also, VDR is clearly present in human islets [1]. In the past years multiple epidemiological studies have implicated Vitamin D deficiency in the development of Type 2 Diabetes, however no reports have described any mechanism(s) linking VitD status with pancreatic islet function. Therefore, my studies have focused on the role of Vitamin D and VDR in islet biology.

Preincubation of isolated mouse and human islets with Vitamin D results in enhanced glucose-stimulated insulin secretion (GSIS). This response is VDR-dependent, as no VitD-mediated change in GSIS is observed in islets obtained from *Vdr*-null mice. However, VitD causes no changes in gene expression of any of the major islet hormones, nor does it change glucose uptake into primary beta cells. VitD does however increase glucose-stimulated calcium uptake, suggesting that VitD affects transcription of genes involved in calcium flux into the beta cell.

To identify molecular mechanisms linking VDR activity to increased insulin secretion and increased glucose-stimulated calcium uptake, we performed global gene expression profiling by microarray in mouse and human islets. These studies identified multiple genes associated with islet function, calcium transport and insulin secretion. One of these genes is the R-type voltage-gated calcium channel, CaV2.3, which is highly upregulated by VitD in human and mouse islets. We identified a strong VDR binding element within intron 7 of the Cav2.3 gene that is conserved in mouse and man. With previous reports linking Cav2.3 activity with Type 2 Diabetes, our findings support a role for vitamin D signaling in the regulation of CaV2.3 and calcium uptake to enhance glucose-stimulated insulin secretion by beta cells of the endocrine pancreas.

A second VDR target gene we identified in the islet is *klotho*, a key regulator of phosphate homeostasis. We clearly establish that klotho mRNA and protein are detected in beta cells of mouse islets, at levels sufficient to mediate signal transduction pathways via klotho's role as a co-receptor for FGF23. By analysis of islets from *Klotho*$^{-/-}$ mice, we

also show that the sialidase activity of klotho may modulate the membrane localization of GLUT-2 to affect glucose-stimulated insulin secretion.

In summary, my studies suggest that vitamin D status may impact the beta cell's capacity to sense glucose levels and respond appropriately to secrete the anabolic hormone, insulin. Future studies involving beta cell-selective deletion of VDR, klotho, and Cav2.3 are now warranted, to elucidate the contribution of islet vitamin D signaling pathways in glucose homeostasis *in vivo*.

The results of studies for my dissertation research provide a needed mechanistic approach, which complements the current clinical and observational reports that exist, regarding potential roles for Vitamin D in the progression of Diabetes. In addition, our identification of numerous Vitamin-D regulated genes of the human and mouse islet can form the basis for future hypothesis-driven research efforts to identify novel therapeutic targets to affect insulin secretion and beta cell function.

TABLE OF CONTENTS

PRIOR PUBLICATIONS

Mansucripts:

Submitted. *"Vitamin D enhances glucose-stimulated insulin secretion in islets by affecting intracellular calcium."* **L. Kjalarsdottir**, S. Tersey, M. Vishwanath, J.-C. Chuang, B. Posner, R. Mirmira, and J. J. Repa.

Under revision. *"ChREBP is a critical effector of glucose-stinulated insulin secretion in the mouse pancreatic islet."* J-Y. Cha, J-C. Chuang, **L. Kjalarsdottir**, A.Villasenor, K. Uyeda, O. Cleaver, and J. J. Repa.

In preparation. *"Vitamin D and klotho actions in the mouse islet."* **L. Kjalarsdottir**, M. Kuro-o, and J. J. Repa.

In preparation: "*Global gene expression analysis of Vitamin D-regulated genes in mouse and human islets*." **L. Kjalarsdottir**, J. Garmey, R. Mirmira, and J. J. Repa.

In preparation: *"Role of calcium and synaptotagmin in ghrelin secretion."* J-C. Chuang, **L. Kjalarsdottir**, I. Sakata, A. Walker, A. Kuperman, S. Rovinsky, S. Osborne-Lawrence, J. J. Repa and J. M. Zigman.

In preparation. *"The role of apoD in the progression of Niemann-Pick Type C disease."* **L. Kjalarsdottir**, J. J. Repa, S. D. Turley, and J. M. Dietschy.

Invited review on Nuclear Hormone Receptors and islet biology (TEMS)

Posters:

June 2009. ADA meeting, New Orleans, LA. *"Vitamin D-regulated gene expression in the endocrine pancreas."* **L. Kjalarsdottir**, J-C. Chuang, and J. J. Repa.

Jan. 2011. Keystone meeting: Type 2 Diabetes, Insulin Resistance and Metabolic Dysfunction (J1). Keystone, CO. *"Vitamin D increases insulin secretion in mouse pancreatic islets via the voltage-gated calcium channel, CaV2.3.*" **L. Kjalarsdottir**, J-C. Chuang and J. J. Repa. <u>*Awarded Student travel scholarship to attend meeting*</u>.

Jan. 2011. Keystone meeting: Type 2 Diabetes, Insulin Resistance and Metabolic Dysfunction (J1). Keystone, CO *"Postprandial enhancement of metabolic remodeling by hepatic XBP1s, Insulin Resistance and Metabolic Dysfunction."* Y. Deng, Z. V. Wang, **L. Kjalarsdottir,** V. Pashkov, I. W. Asterholm, T. M. Wilkie, J. J. Repa, G. Liang, J. A. Hill, J. D. Horton, P. E. Scherer .

Abstract:

2010. *"Vitamin D increases insulin secretion in mouse pancreatic islets via the voltage-gated calcium channel, CaV2.3."* **L. Kjalarsdottir**, J-C. Chuang, M. Vishwanath, B. Posner, R. G. Mirmira and J. J. Repa.
Winner of 42nd Annual Sigma Xi abstract competition at UT Southwestern.

LIST OF FIGURES

LIST OF APPENDIX FIGURES

LIST OF TABLES

LIST OF APPENDICES

LIST OF ABREVIATIONS

36B4 – Acidic ribosomal phosphoprotein P0

ADAM10 – A desintegrin and metalloproteinase 10

ADAM17 – A desintegrin and metalloproteinase17

AK5 – Adenylate Kinase 5

ALOX12 – Arachidonate 12-lipoxygenase

Amigo2 – Adhesion molecule with Ig-like domain 2

ARRB2 – Arrestin Beta 2

BSEP – Bile salt efflux pump (ABCB11)

CACNA1A – Calcium channel, voltage-dependent, P/Q type, alpha 1A subunit (CaV2.1)

CACNA1B – Calcium channel, voltage-dependent, N type, alpha 1B subunit (CaV2.2)

CACNA1C – Calcium channel, voltage-dependent, L type, alpha 1C subunit (CaV1.2)

CACNA1D – Calcium channel, voltage-dependent, L type, alpha 1D subunit (CaV1.3)

CACNA1E – Calcium channel, voltage-dependent, R type, alpha 1E subunit (CaV2.3)

CACNA1F – Calcium channel, voltage-dependent, L type, alpha 1F subunit (CaV1.4)

CACNA1G – Calcium channel, voltage-dependent, T type, alpha 1G subunit (CaV3.1)

CACNA1H – Calcium channel, voltage-dependent, T type, alpha 1H subunit (CaV3.2)

CACNA1I – Calcium channel, voltage-dependent, T type, alpha 1I subunit (CaV3.3)

CACNA1S – Calcium channel, voltage-dependent, L type, alpha 1S subunit (CaV1.1)

CACNA2D1 – Calcium channel, voltage-dependent, alpha 2/delta subunit 1

CACNA2D2 – Calcium channel, voltage-dependent, alpha 2/delta subunit 2

CACNA2D3 – Calcium channel, voltage-dependent, alpha 2/delta subunit 3

CACNA2D4 – Calcium channel, voltage-dependent, alpha 2/delta subunit 4

CACNB1 – Calcium channel, voltage-dependent, beta 1 subunit

CACNB2 – Calcium channel, voltage-dependent, beta 2 subunit

CACNB3 – Calcium channel, voltage-dependent, beta 3 subunit

CACNB4 – Calcium channel, voltage-dependent, beta 4 subunit

CACNG1 – Calcium channel, voltage-dependent, gamma subunit 1

CACNG2 – Calcium channel, voltage-dependent, gamma subunit 2

CACNG3 – Calcium channel, voltage-dependent, gamma subunit 3

CACNG4 – Calcium channel, voltage-dependent, gamma subunit 4

CACNG5 – Calcium channel, voltage-dependent, gamma subunit 5

CACNG6 – Calcium channel, voltage-dependent, gamma subunit 6

CACNG7 – Calcium channel, voltage-dependent, gamma subunit 7

CACNG8 – Calcium channel, voltage-dependent, gamma subunit 8

CCND1 – Cyclin D1

CNS – Central nervous system

CSNK – Casein kappa

CYCLO – Cyclophilin

CYP24A1 – cytochrome P450, family 24, subfamily A, polypeptide 1

CYP27B1 – cytochrome P450, family 27, subfamily B, polypeptide 1

C_T: Threshold cycle

DOK5 – Docking protein 5

FABP6 – Fatty acid binding protein 6, ileal

FGF15 – Fibroblast growth factor 15

FGF23 – Fibroblast growth factor 23

FGFR1 – Fibroblast growth factor receptor 1

FXR – Farnesoid X receptor (NR1H4)

GADD45a – Growth arrest and DNA-damage-inducible, alpha

GDF10 – Growth differentiation factor 10 (BMP3b)

GLP1R – Glucagon-like peptide 1 receptor

GPBAR1 – G protein-coupled bile acid receptor 1

GPC6 – Glypican 6

GSIS – Glucose-stimulated insulin secretion

GTT – Glucose tolerance test

H2-Bl – Histocompatibility 2, blastocyst

Het INSII – Heterogeneous nuclear insulin II

HPRT1 – Hypoxanthine-guanine phosphoribosyl transferase

IBAT – Ileal bile acid transporter (SLC10A2)

IHC – Immunohistochemistry

Ildr2 – Immunoglobulin-like domain containing receptor 2

IPGTT – Intraperitoneal glucose tolerance test

IP – Intraperitoneal

ISH – *In situ* hybridization

ITT – Insulin tolerance test

KL – Klotho

LUC – Luciferase

MX2 – Myxovirus (influenza virus) resistance 2

NEDD9 – Neural precursor cell expressed, developmentally down-regulated gene 9

NHR – Nuclear hormone receptor

NTCP – Sodium-taurocholate cotransporter polypeptide (SLC10A1)

OSGIN1 – oxidative stress induced growth inhibitor 1

OSTalpha – Organic solute transporter alpha

OSTbeta – Organic solute transporter beta

PC1/3 – Proprotein convertase subtilisin/kexin type 1 (PCSK1)

PC2 – Proprotein convertase subtilisin/kexin type 2 (PCSK2)

PMSF – phenylmethanesulfonylfluoride

PRG-3 – Plasticity related gene 3 (LPPR1)

PVDF – Polyvinylidene fluoride

qPCR – Quantitative polymerase chain reaction

RAMP1 –Receptor (G protein-coupled) activity modifying protein 1

RNase4 – Ribonuclease, RNase A family, 4

RXR – Retinoid X receptor (NR2B subfamily)

SCL51094 – Unknown gene found by microarray

SGK2 – Serum/glucocorticoid regulated kinase 2

SHP – Small heterodimer partner (NR0B2)

SLITRK1 – SLIT and NTRK-like family, member 1

SST – Somatostatin

STX18 – Syntaxin 18

ST6Gal1 – ST6 beta-galactosamide alpha-2,6-sialyltranferase 1

SYTL2 – Synaptotagmin-like 2

T1DM – Type 1 diabetes mellitus

T2DM – Type 2 diabetes mellitus

TACR3 – Tachykinin receptor 3

TGFB1 – Transforming growth factor beta 1

TGR5 – G protein-coupled bile acid receptor 1 (GPBAR1)

TK – Thymidine kinase

TM4SF4 – Transmembrane 4 superfamily member 4

TMEM27 – Transmembrane protein 27

TRPV6 – Transient receptor potential cation channel, subfamily V, member 6

Ttc36 – Tetratricopeptide repeat domain 36

TSS – Transcriptional start site

VDR – Vitamin D receptor (NR1I1)

VitD– 1,25-dihydroxyvitamin D_3

CHAPTER ONE

Introduction

1.1. Vitamin D and the Vitamin D Receptor

1,25-dihydroxyvitamin D (VitD) is a ligand for the Vitamin D receptor (VDR, NR1I1), which is a member of the nuclear hormone receptor family of transcription factors (NHR). NHRs are a class of transcription factors that have a ligand-binding pocket capable of binding steroids and other lipophilic molecules. NHRs also contain a central DNA binding domain that confers sequence-specific binding to DNA sequences within target genes. Upon ligand-binding, activated NHRs recruit protein machinery that modulated gene transcription to affect development, metabolism, immune function and other biological processes. In the case of VDR, upon ligand binding it forms a heterodimer with its partner, the retinoid X receptor (RXR). The activated RXR-VDR heterodimer then binds Vitamin D receptor binding elements (VDRE) within target genes, recruits co-activators and affects transcription (Figure 1.1).

Vitamin D and VDR play an important role in plasma calcium homeostasis by increasing absorption of calcium in intestine and reabsorption in kidney. VitD impacts plasma calcium levels by activating VDR-dependent transcription of TrpV5 in the kidney and TrpV6 in intestine [2]. Increased abundance of TrpV5 in kidney increases calcium reabsorption from urine, thus reducing urinary calcium loss. By a similar mechanism, induction of TrpV6 in intestine increases calcium absorption from dietary intake.

One of the most responsive VitD target genes is *Cyp24a1*, which contains two well characterized VDREs within its proximal promoter and four additional VDREs at about 50 kb downstream of the *Cyp24a1* gene [3]. Cyp24a1 is a 24-hydroxylase that is highly expressed in kidney and acts in a negative feedback loop to inhibit VitD activity. Cyp24a1 can add a 24-hydroxyl group to both 25-hydroxyvitamin D and 1,25-dihydroxyvitamin D, rendering them inactive and unable to bind to VDR.

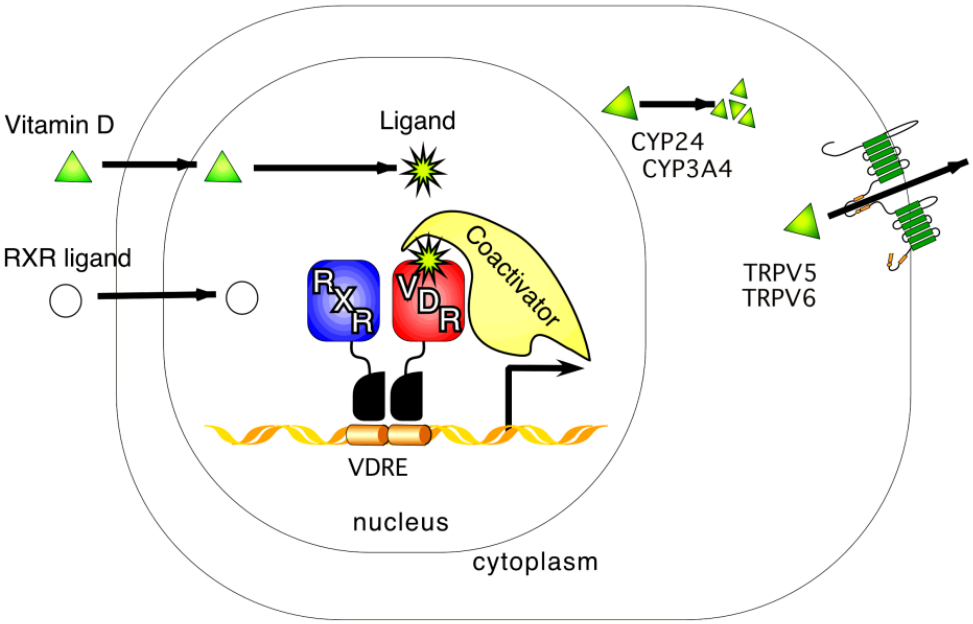

Figure 1.1. Primary action of VDR is transcriptional regulation. VitD can enter cells by diffusing through the plasma membrane. Once inside the cell, VitD binds VDR present in the nucleus as a heterodimer with its obligate partner RXR. The activated RXR-VDR dimer binds Vitamin D Receptor binding elements (VDRE) within target genes, recruits co-activators and initiates transcription. Examples of target genes given are *Cyp24a1*, *Cyp3a4*, *TrpV5* and *TrpV6* (see text for details).

For most of the well characterized VDR target genes to date, the VDRE has been identified in the proximal promoter region. However, it is becoming evident that VDR

can mediate expression of genes from VDREs located at substantial distances (10-100kb) from the transcriptional start site (TSS). Recently, a genome-wide chromatin immunoprecipitation on microarray (ChIP-chip) performed in pre-osteoblastic cells for VDR, RXR, RNA polymerase II, and histone H4 acetylation (H4ac) was performed. This study showed that VDR, RXR and H4Ac bind to distal regions 43% of the time (within gene introns 38% and exons 6% of the time) and only 13% of the time at traditional promoter regions (within 5 kb from the TSS) [4].

Vitamin D precursors can be acquired from dietary intake (Table 1.1) or from the sun's UVB rays (Figure 1.2). The best dietary sources of Vitamin D precursors are fatty fish, eggs, liver and multiple Vitamin D-fortified milk products. Table 1 gives more detailed information about the amount of Vitamin D present in 100g of various food products. Vitamin D can also be generated in skin, once the sun's UVB rays hit the skin, a Vitamin D precursor is generated from 7-dehydrocholesterol. The Vitamin D precursors (from skin or diet) travel in the circulation to the liver, where they are 25-hydroxylated by a liver 25-hydroxylase (Cyp2R1). The 25-hydroxyvitamin D forms then travel to the kidney for 1α-hydroxylation by the enzyme Cyp24a1, and this final hydroxylation generates 1,25-dihydroxyvitamin D (VitD), which is the active hormone form of Vitamin D. Figure 1.3 shows the structure of 25-hydroxyvitamin D and 1,25-dihydroxyvitamin D.

Table 1.1 Foods containing Vitamin D (IU/100g).

Foods that naturally contain vitamin D (IU/100g)			
Food	**IU/100 g**	**Food**	**IU/100 g**
Halibut liver oil (D3)	200,000	Redfish (D3)	90
Cod liver (D3)	8500	Sole (D3)	60
Sea eel (D3)	520	Tuna (D3)	200
Smoked river eel (D3)	3600	Oyster (D3)	300
Cod (D3)	50	Butter (D3)	50
Halibut (D3)	200	Margarine (D3)	300
Black halibut (D3)	600	Crème fraîche (D3)	40
Herring (D3)	1250	Calf's liver (D3)	130
Sea bass (D3)	20	Poultry liver (D3)	50
Mackerel (D3)	40	Milk (D3)	1
Sardine (D3)	300	Cheese (D3)	10–20
Salmon (D3)	650	Egg (D2 and D3)	70
Canned salmon (D3)	450	Liquid yolk (D2 and D3)	220

Table adapted from [5].

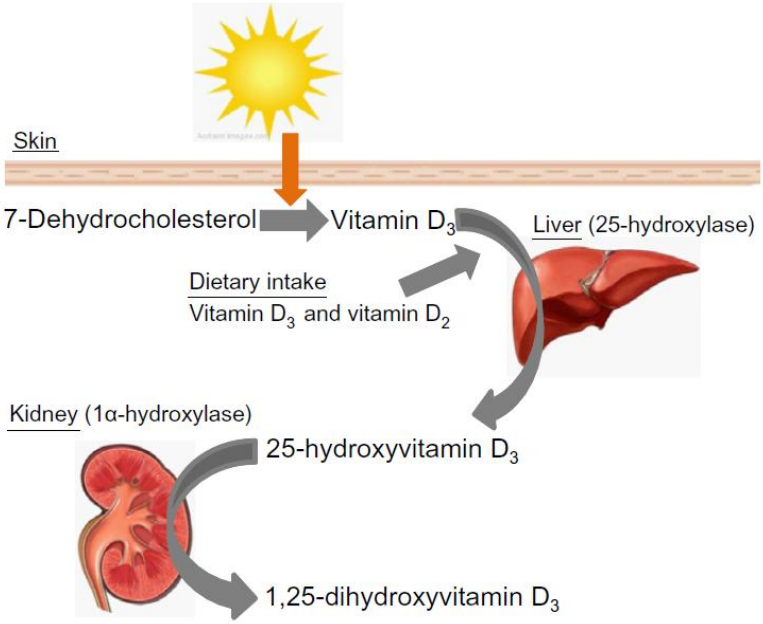

Figure 1.2. Vitamin D metabolism. Vitamin D can be acquired from dietary intake or from the sun's UVB rays. Once the sun's UVB rays hit the skin, Vitamin D precursor is generated from 7-dehydrocholesterol. The precursor is 25-hydroxylated by a liver 25-hydroxylase, then it travels to the kidney where it is 1α-hydroxylated. This final hydroxylation generates 1,25-dihydroxyvitamin D (VitD), the active hormone and ligand for VDR. Figure is taken from [6].

Vitamin D made from the sun's UVB rays is Vitamin D_3 (cholecalciferol) as is the Vitamin D obtained from animal sources. Vitamin D_2 (ergocalciferol) is generated by plants and yeast. Vitamin D_2 is structurally related to Vitamin D_3 and activates VDR. However it is less effective than Vitamin D_3 in raising and maintaining the plasma Vitamin D levels due to decreased bioavailability (Figure 1.3).

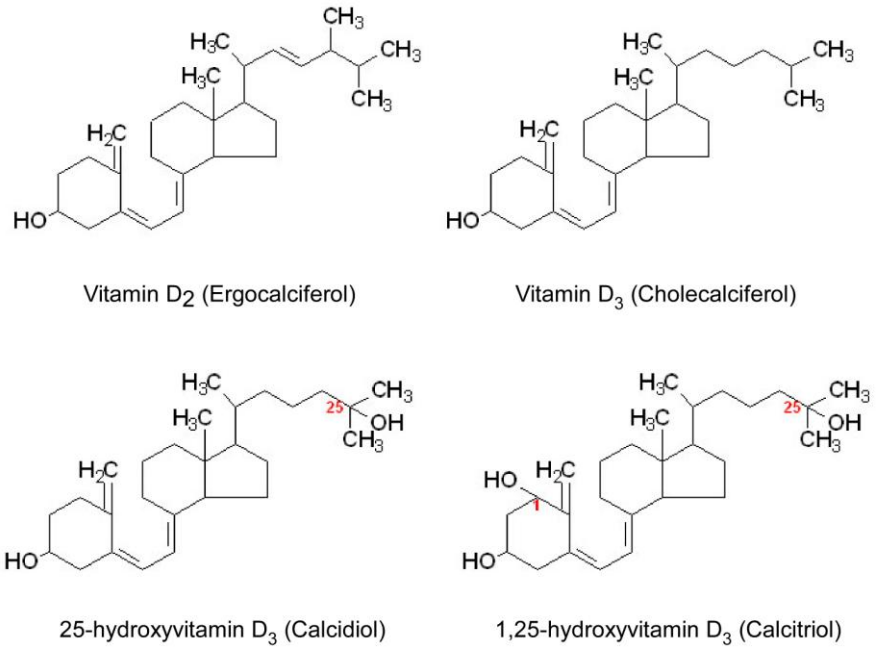

Figure 1.3. Structure of Vitamin D_2, Vitamin D_3, 25-hydroxyvitamin D_3 and 1,25-dihydroxyvitamin D_3. (Figure is adapted from http://themedicalbiochemistrypage.org/vitamins.html)

The serum concentration of 25-hydroxyvitamin D is the best indicator of Vitamin D status as it represents both ingested and endogenously produced Vitamin D. Additionally it has a quite long circulating half-life of 15 days. It is also present at sufficiently high concentration to enable clinical measurement. On the contrary,

circulating 1,25-hydroxyvitamin D is not a good indicator of vitamin D status because it has a short half-life of only 4-6 hours and its concentration is dramatically affected by parathyroid hormone, calcium, and phosphate [7-9]. Recently the Institute of Medicine concluded that nearly all people have sufficient levels of 25-hydroxyvitamin D if their serum levels fall above 20 ng/mL (50 nmol/L), despite this many other researchers concider the optimal range of 25-hydroxyvitamin D to be 30-60 ng/mL [7, 10]. According to the 2005-2006 National Health and Nutrition Examination Survey , more than 40% of the adult US population is Vitamin D deficient (≤20 ng/mL) [11]. As the skin pigment melanin absorbs sunlight, darker skinned people cannot synthesize as much Vitamin D from the sunlight as light skinned people. Therefore it is not surprising that Vitamin D deficiency is much more prevalent in African Americans (82%) than Caucasians (31%) [11].

1.2. Vitamin D and Diabetes

Vitamin D has long been known to be important for proper bone health and regulation of serum calcium and phosphate levels. However, it is coming more apparent that Vitamin D has a much broader role in physiology, affecting immune function, muscle strength, cancer progression and cardiovascular health [12]. Furthermore, multiple epidemiological studies have implicated Vitamin D deficiency in the development of Type 2 Diabetes. First, there are a number of recently published longitudinal observational studies that suggest people with low Vitamin D status have increased risk of developing Type 2 Diabetes [13-15]. Secondly, several randomized trials of Vitamin D and glycemic outcome suggest that people with glucose intolerance or

Type 2 Diabetes may benefit from Vitamin D supplementation [16-18]. Finally, the only clinical study that assessed insulin secretion during a glucose tolerance test reported a significant improvement in beta cell function after only 16 weeks of Vitamin D supplementation [18]. When the authors calculated the disposition index (the product of insulin secretion and insulin sensitivity), they detected a significant improvement that was independent of calcium intake (Figure 1.4). However, these results need to be confirmed by similar studies using larger cohorts to establish if vitamin D supplementation is an effective intervention to delay the progression from pre-diabetes to Type 2 Diabetes.

Combined, these studies suggest that Vitamin D supplementation with or without combined calcium supplementation delays and even improves Type 2 Diabetes in individuals with established glucose intolerance. However, higher powered trials are needed to fully establish if Vitamin D has an effect on Type 2 Diabetes progression and, if confirmed, to establish the optimal range of plasma 25-dihydroxyvitamin D achieve this effect.

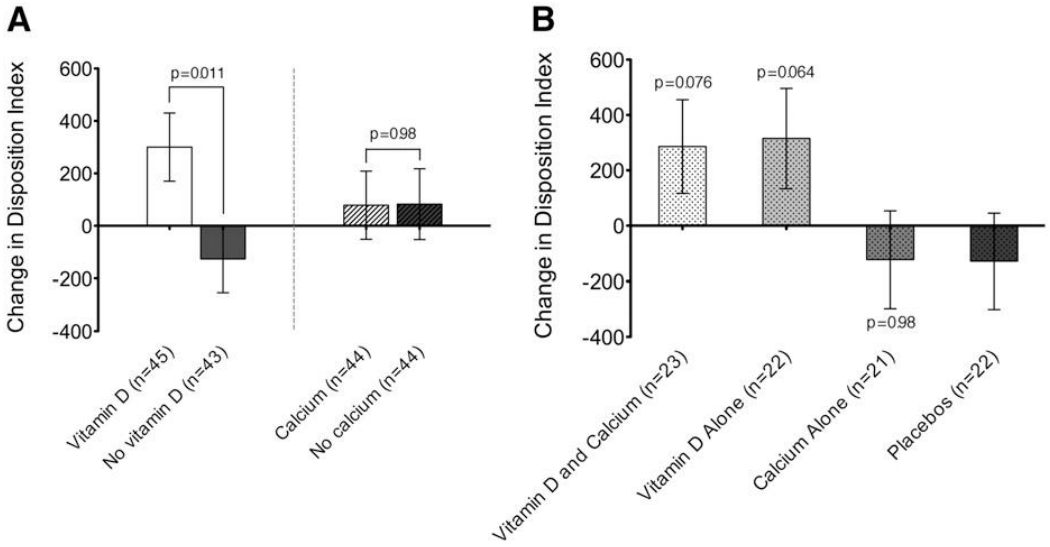

Figure 1.4. Vitamin D supplementation improves insulin status. Results from a human clinical trial (n=88), testing effect of 16-week Vitamin D supplementation with or without calcium on insulin status. All data are least squares means adjusted for stratified variables (age and BMI), the baseline value of the outcome variable, race, and time of study entry. A: Changes in the disposition index between vitamin D (white bar) and no vitamin D (grey bar) or between calcium (hatched white bar) and no calcium (hatched grey bar). P values are for the ANOVA test for differences in means between vitamin D and no vitamin D or between calcium and no calcium. B: Changes in the disposition index for vitamin D and calcium (crosshatched white bar) compared with vitamin D alone (crosshatched grey bar) compared with calcium alone (crosshatched grey bar) compared with placebo (crosshatched dark grey bar). P values are for the ANOVA test for differences in means compared with placebo. P = 0.92 for the vitamin D calcium interaction. Disposition index = product of insulin secretion and insulin sensitivity. Figure taken from [18]

In addition to promising clinical data, there are several reports showing that Vitamin D deficiency has unfavorable effects on insulin secretion in rodents. In 1980, Vitamin D deficient rats were shown to have reduced insulin secretion compared to Vitamin D sufficient controls [19]. Subsequent studies suggested that this effect was independent of the changes in serum calcium caused by the Vitamin D deficiency [20, 21].

According to the literature summarized here above, there is a strong trend suggesting that vitamin D might exert positive effects on beta cells in mice and humans.

However, the mechanism(s) of action of Vitamin D and how it may impact gene transcription to improve beta cell function remains to be elucidated.

1.3. Type 2 Diabetes

Diabetes is rapidly becoming a pandemic with no signs of abatement. Type 2 Diabetes is the most common form of diabetes, representing more than 90% of all cases. Type 2 Diabetes develops when beta cells of the endocrine pancreas cannot secrete sufficient insulin to lower blood glucose, either because of overt peripheral insulin resistance and/or beta cell failure and death. Persistent high blood glucose can result in many micro- and macro-vascular complications that increase the risk of blindness, kidney disease, heart disease and neuropathy. The disease is associated with increased morbidity and mortality. Thus with the rapidly increasing numbers of Type 2 Diabetic patients with multiple other complications, it is becoming the most costly disease in the western world. According to data from the 2011 National Diabetes Fact Sheet, total medical cost for diabetes in 2007 was $116 billion [22]. This report also states that in 2004, 68% of diabetes-related death resulted from heart disease and 16% resulted from stroke. In addition, diabetes is the leading cause for new cases of blindness in adults; 44% of all new cases of kidney failure in 2008 were because of diabetes; and 60% of nontraumatic lower-limb amputations occur in people with diabetes. Lastly, about 60% to 70% of people with diabetes have mild to severe forms of nervous system damage presenting as pain or tingling sensation in hands and feet.

Type 2 Diabetes is both caused by beta cell dysfunction and insulin resistance so treatment strategies can target either one or both of these processes. Insulin resistance is

normally reversible with a change in diet and exercise but recovery from beta cell failure and death is more difficult. As suggested by Weir et al (2004), there are 5 stages of evolving beta cell dysfunction during diabetes [23]. At stage 1, compensation occurs, and beta cells need to secrete more insulin because of increasing insulin resistance. At this point, compensation can also include expansion of beta cell mass to meet the increased demand for insulin. Stage 2 occurs when glucose levels start to rise: then beta cell mass starts to decrease and beta cells start to become dysfunctional as evidenced by reduced acute glucose stimulated insulin secretion. Stage 3 is transient and unstable: this is where glucose level rises relatively rapidly, because at some critical point beta cell mass becomes inadequate. At stage 4, individuals become overtly hyperglycemic but can normally secrete enough insulin to escape ketoacidosis. At this point, beta cell mass has been reduced by 50% and the remaining beta cells are not functioning properly. For many type 2 diabetes patients, stage 4 lasts throughout the remainder of their life; but for some, the beta cell destruction is so severe that they end up in stage 5, where the beta cell loss is so great that they are dependent on exogenous insulin for survival. Individuals on the path to diabetes can remain at stage 2 for a very long time, but once they reach stage 3 there is normally a rapid progression to stage 4. Therefore earlier interventions are better; because, if beta cell function and survival can be improved at early stages, there will be far fewer cases of Type 2 Diabetes.

1.4. Endocrine pancreas and insulin secretion

The pancreas is a glandular organ in the digestive and endocrine system of vertebrates that is located in proximity to the liver, stomach and small intestine (Figure 1.5a). The pancreas is divided into an endocrine pancreas that produces several important hormones, such as insulin, glucagon and somatostatin, and an exocrine pancreas that acts as a digestive organ, producing and secreting digestive enzymes into the small intestine. Collectively, endocrine and exocrine pancreas aid in movement of nutrients from food in the digestive tract to cells of the body.

The endocrine pancreas is made up of several cells types that cluster together to form islets of Langerhans [24]. The islets occupy only about 2% of the volume in the pancreas and they are spread across the exocrine pancreas (Figure 1.5b). The four major cell types that make up an islet are: beta cells, alpha-cells, PP-cells (also called F-cells) and delta-cells. Beta cells, which secrete insulin, are the most abundant cell type and occupy 65-80% of the islet mass. Alpha-cells that secrete glucagon come thereafter, and they occupy about 15-20% of the islet mass. Delta-cells secrete somatostatin and occupy 3-10% of the islet mass. Lastly, pp-cells make up 3-5% of the islet mass and secrete pancreatic polypeptide.

Insulin and glucagon play a crucial role in controlling blood glucose levels in response to fasting and feeding. In response to meals, insulin lowers blood glucose by enhancing cellular uptake of glucose into the cells of the body. Taking skeletal muscle as an example: when insulin binds to the insulin receptor, signaling events are initiated that dictate transport of vesicles containing the glucose transporter, Glut4, to the plasma membrane [25]. The increase of Glut4 at the plasma membrane allows for rapid uptake of

glucose and that reduces blood glucose levels. Contrary to insulin, glucagon is secreted from alpha-cells when blood glucose level drop. Glucagon binds to glucagon receptors (GCGR) in the liver to enhance gluconeogenesis, thereby keeping the blood glucose from dropping dangerously low. Somatostatin and pancreatic polypeptide are not as critical in maintaining glucose levels within normal range. Somatostatin can, however, impact both glucagon and insulin secretion. In addition to being produced in the delta-cells of the islet, somatostatin is also generated by some regions of the central nervous system (CNS) and the digestive tract. In general, somatostatin inhibits secretion of a wide variety of hormones, and in the islet, somatostatin inhibits the secretion of glucagon and insulin. The absence of somatostatin results in increased insulin secretion and blocks the nutrient-induced suppression of glucagon secretion [26]. Pancreatic polypeptide is found in the digestive tract and in islet, some of the known functions of pancreatic polypeptide include: pancreatic secretion, gastric emptying, intestinal motility and appetite [27].

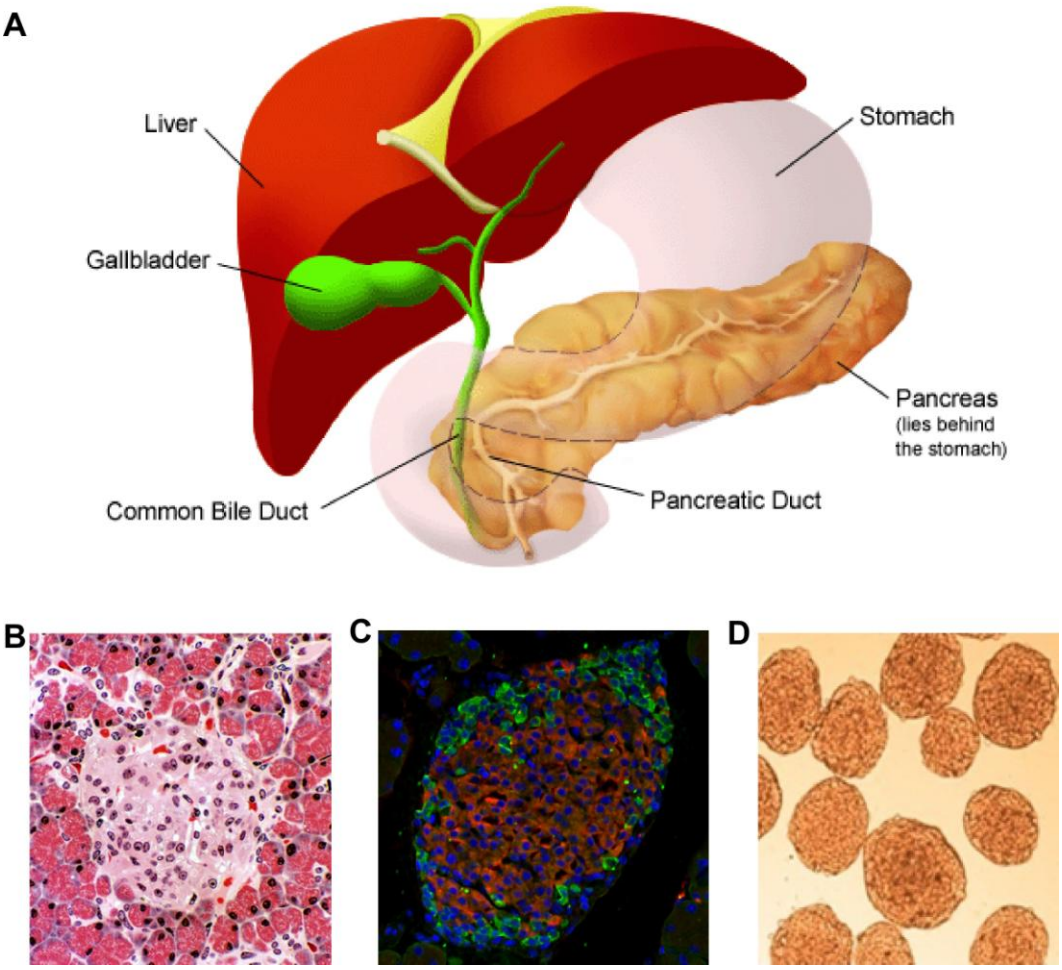

Figure 1.5. Endocrine pancreas structure and organization. A. The pancreas lies behind the stomach and is attached to the small intestine via the pancreatic duct, where pancreatic juice is secreted from exocrine pancreas into the digestive tract. B. Hematoxilin and Eosin staining of pancreatic section showing a cross-section of an islet surrounded by exocrine pancreas. Multiple blood vessels are seen embedded in the islet, the islet reads the glucose level in these blood vessels and responds by secreting the proper hormone that is then carried by the blood vessels to the rest of the body. C. Insulin (red) and glucagon (green) immunohistochemistry of a mouse pancreatic section. Dapi stains the nucleus blue D. Image of isolated mouse islets in culture media after overnight recovery.
Figure A was taken from http://www.yalemedicalgroup.org/stw/images/125548.jpg
Figure B was taken from http://education.vetmed.vt.edu/Curriculum/VM8054/Labs/Lab20

To study islet biology, it is essential to be able to isolate islets and culture them *in vitro*. Figure 1.1c shows an example of how isolated islets look under a microscope. Primary islets, cultured for up to a week *in vitro*, maintain many of their *in vivo* characteristics including glucose stimulated insulin secretion (GSIS) and thus provide an ideal model to investigate the intricate islet physiology [28].

Isolation of primary islets has made it possible to unravel some of the key components of GSIS. Figure 1.6 describes these key components; however, it is necessary to keep in mind that this is a simplified rendition of insulin secretion as many other factors have been identified that can impact the GSIS pathway at each point. GSIS is normally activated after feeding. Quickly after ingesting a meal, glucose level rises and glucose is transported into the beta cell via the glucose transporter, GLUT-2. The enzyme Glucokinase rapidly phosphorylates glucose, which allows glucose to enter the glycolysis pathway. Each molecule of glucose generates two molecules of pyruvate that can enter the citric acid cycle and, subsequently, the electron transport chain, leading to enhancement of ATP generation. This sequence of events increases the ATP/ADP ratio, which closes the ATP-sensitive K^+ channel and depolarizes the beta cell. The depolarization activates voltage-dependent Ca^{2+} channels that allow Ca^{2+} to flow from the extracellular environment into the cytosol. This increases the cytosolic concentration of Ca^{2+} and activates a variety of second messengers, such as cAMP, that initiate exocytosis of insulin-containing vesicles.

Insulin secretion occurs in two distinct phases. First-phase insulin secretion is initiated as soon as blood glucose level rises, this phase is generated by insulin granules that are docked and ready for release at the plasma membrane. After the first phase-

insulin-secretion-peak, the second phase of insulin secretion begins. The insulin secreted during the second phase is located in cytoplasmic insulin granules that need to be transported to the plasma membrane for secretion. The second phase is sustained until normoglycemia is restored.

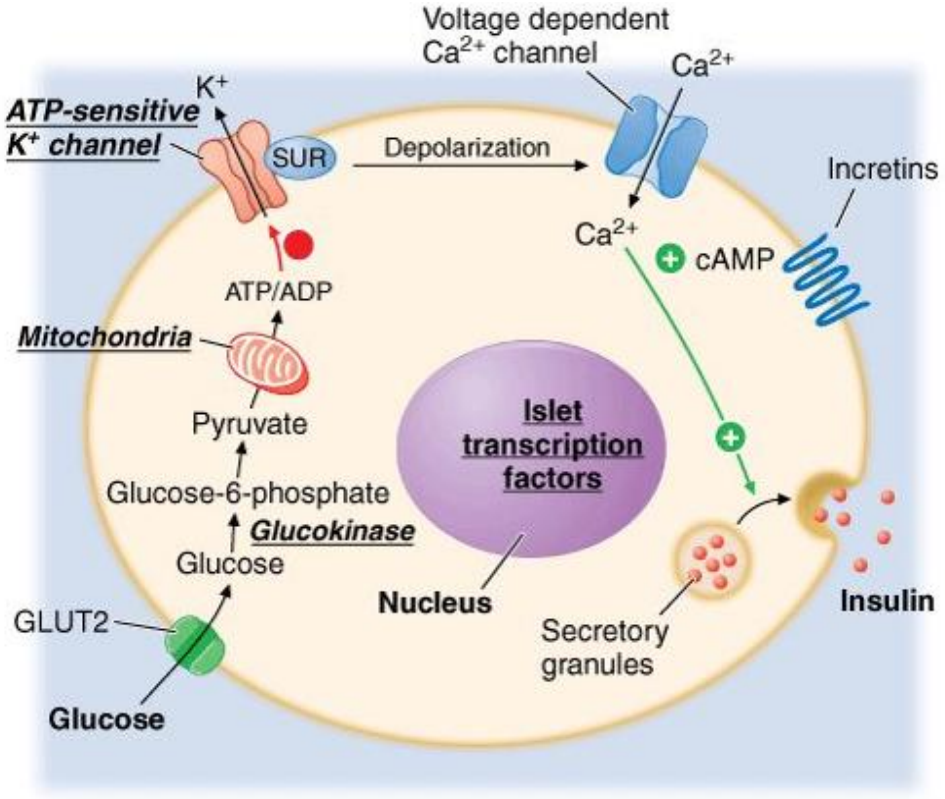

Figure 1.6. Glucose-stimulated insulin secretion by the beta cell of the endocrine pancreas. After a meal, glucose levels rise, and glucose is transported into the beta cell via the glucose transporter, GLUT-2. Glucose is then metabolized by the glycolysis pathway to pyruvate, which enters the citric acid cycle and subsequently the electron transport chain where ATP is generated. This increases the ATP/ADP ratio, which causes closing of the ATP-sensitive K+ channel and depolarization of the beta cell. The depolarization activates voltage-dependent Ca^{2+} channels that open to increase the cytosolic concentration of Ca^{2+}, to initiate exocytosis of insulin-containing granules. Figure was taken from Fauci et al. Harrison's Principles of Internal Medicine, 17 edition: http://accessmedicine.com

My dissertation work has focused on the role(s) of VDR in beta cell biology. I have focused on elucidating what genes, and thereby what pathways, are under the control of VDR in endocrine pancreas. Figure 1.7 summarizes the hypothesis I have worked on during my dissertation.

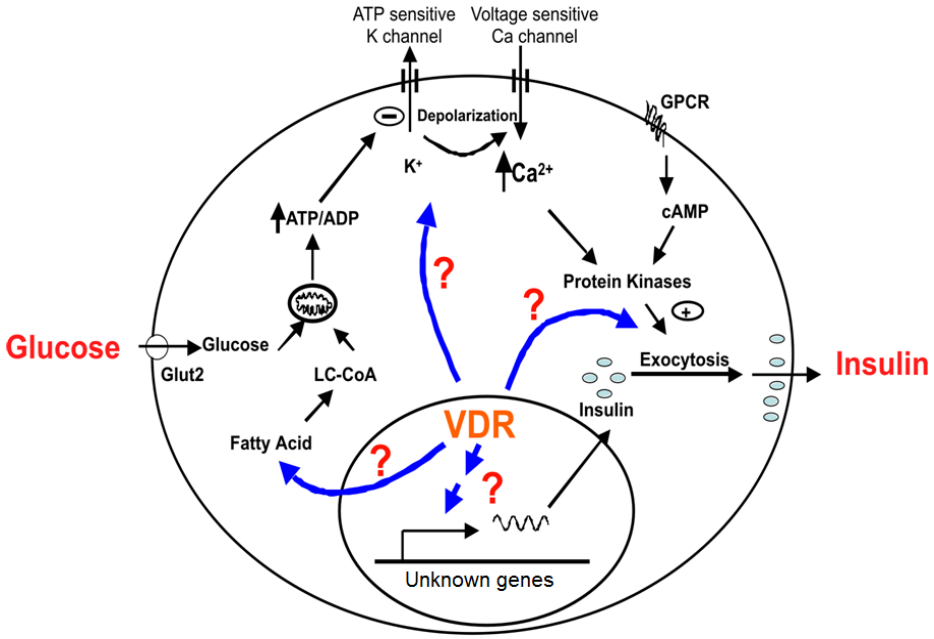

Figure 1.7. Hypothetical model showing where VDR target genes might act in the beta cell. VDR might be working through multiple genes in the beta cell to enhance beta cell function and increase insulin secretion.

CHAPTER TWO

Vitamin D enhances glucose-stimulated insulin secretion in mouse and human islets

2.1 Abstract

In the United States it is estimated that up to 40% of the adult population do not have sufficient Vitamin D levels. Recent epidemiological studies suggest that poor Vitamin D status is associated with increased incidence of diabetes. 1,25-dihydroxyvitamin D_3 (VitD) is a ligand for the Vitamin D Receptor (VDR), which is highly expressed in islets. In studies presented here, we establish that VDR mRNA is upregulated in isolated mouse islets exposed to a glucose challenge suggesting an increased need for Vit D signaling when glucose level rises. VitD pretreatment of isolated mouse and human islets results in enhanced glucose-stimulated insulin secretion (GSIS). This response is VDR-dependent, as no VitD-mediated change in GSIS is observed in islets obtained from *Vdr*-null mice. VitD pretreatment has no effect on total insulin pool nor does it enhance glucose uptake into primary beta cells, however, it does enhance glucose-stimulated calcium influx. Therefore, proteins that aid in the movement of calcium across the plasma membrane are likely candidates for the VitD-enhanced GSIS.

To identify molecular mechanisms behind the VitD-enhanced GSIS, we performed global gene expression profiling by microarray in human islets. This study identified several genes involved in calcium regulation. One of these genes is the R-type voltage-gated calcium channel, CaV2.3, which is highly upregulated by VitD in human and mouse islets. Furthermore, *in silico* analysis along with reporter studies identified a conserved VDRE in intron 7 of the mouse and human CaV2.3 gene. To account for any

discrepancies between VitD-induced transcriptional regulation in mouse and human islets, we performed a survey of all members of the voltage-gated calcium channel family in mouse islets. This analysis identified another calcium channel subunit, Cacna2d3, upregulated by VitD. This report clearly demonstrates that VitD enhances GSIS in both mouse and human islets and suggests that VitD-induced transcriptional regulation of genes of the voltage-gated calcium channel family are involved in that process.

2.2 Introduction

1,25-dihydroxyvitamin D_3 (VitD), is a ligand for the vitamin D receptor (VDR), which is a member of the nuclear hormone receptor (NRH) family. NHRs are ligand-activated transcriptional factors that bind steroid hormones and other lipophilic compounds. In the case of VDR, the ligand (VitD) enters the cell and binds VDR that is located in the nucleus. Upon ligand binding VDR interacts with its heterodimer partner, the retinoid X receptor (RXR) and together they find vitamin D receptor binding elements (VDRE) within target genes. Traditionally, VDREs are thought to be located within the proximal promoter of target genes. However, recent studies have suggested that genes may have multiple VDREs located far upstream or far downstream to a gene, within introns and even within coding regions [3, 4, 29, 30]. One of the most responsive VDR target genes is *cyp24a1*. The product of this gene participates in a negative feedback loop, to control serum levels of VitD, by adding a 24-hydroxyl group to VitD and inactivating it [3].

Vitamin D has long been known to be important for proper bone health and regulation of serum calcium and phosphate levels. However, it is becoming more

apparent that Vitamin D has a much broader role in physiology affecting: immune function; muscle strength; cancer progression and cardiovascular health [12]. Additionally, multiple epidemiological studies implicate Vitamin D deficiency in the development of Type 2 Diabetes [31, 32]. In the United States up to 40% of the adult population is suggested to be Vitamin D deficient [11]. However, to date there are no mechanistic studies linking VitD action to improved glycemia or delayed development of diabetes.

Our lab has identified VDR to be the fourth most abundant NHR in the mouse islet based on mRNA levels (figure 2.1) and VDR is clearly present in human islets [1]. Therefore, Vitamin D actions may occur directly by altering beta cell function. In this study we evaluated the effects of VitD on islet function, and elucidated molecular mechanisms linking VDR activity and GSIS.

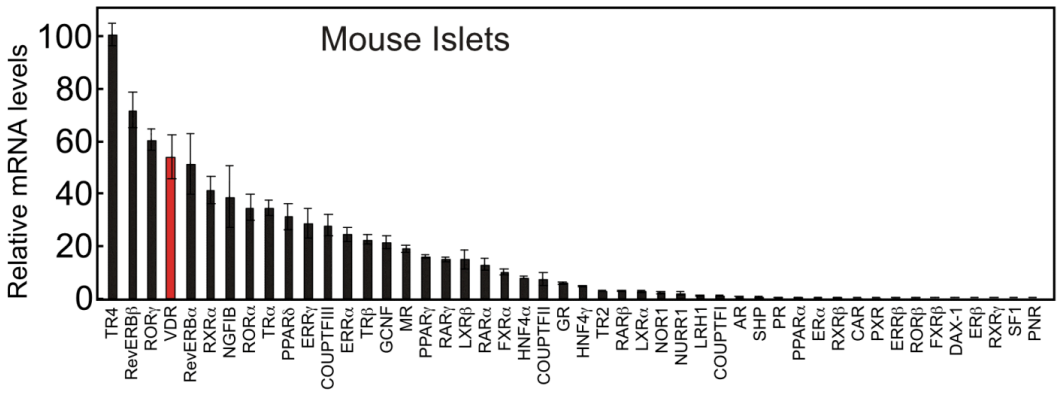

Figure 2.1. Rank order of Nuclear Hormone Receptor expression in mouse islets. Figure taken from [1].

2.3 Materials and methods

Materials

1,25-dihydroxyvitamin D_3 (>99.0 % by HPLC) was purchased from Sigma-Aldrich, and was resuspended in tissue-culture grade DMSO. This VDR ligand is referred to as "VitD" hereafter in this manuscript. The fluorescent glucose analog 2-NBDG (2-(*N*-(7-nitrobenz-2-oxa-1,3-diazol-4-yl)amino)-2-deoxyglucose) was obtained from Invitrogen/Molecular Probes. Liberase (CAT#1815032) and Collagenase P (CAT# 11213857001) for islet isolation were obtained from Roche. Collagen I and Poly-L-Lysine were purchased from BD Bioscience (CAT#354249) and Sigma-Aldrich (CAT#P7890). Oligonucleotides were obtained from Integrated DNA Technologies. Real-time PCR reagents were purchased from Applied Biosystems. Guinea pig anti-insulin polyclonal antibody was purchased from DakoCytomation (CAT#A0564) and anti-guinea pig TRITC secondary antibody from Jackson (CAT#706026148)

Animals

All tissues and islets were obtained from 3-5-month-old mice in the fed-state. The *Vdr*$^{-/-}$ mice were generously provided by Marie DeMay (Harvard Medical School [33]); but have now been backcrossed for greater than 10 generations onto an A129/SvJ strain background. Mice were maintained in a temperature-controlled room (23 ± 1°C) on a 12-h light (0700 h–1900 h), 12-h dark cycle with *ad libitum* access to water and a standard rodent diet (Harlan Teklad Premier Laboratory Diet no. 2016), and housed with sanitized wood-chip bedding (Sani-Chips, P.J. Murphy Forest Products, Montville, NJ). All animal experiments were approved by the Institutional Animal Care and Use

Committee of the University of Texas Southwestern Medical Center, which assures that all animal use adheres to federal regulations as published in the Animal Welfare Act, the Guide for the Care and Use of Laboratory Animals, the Public Health Service Policy, and the US Government Principles Regarding the Care and Use of Animals (http://www.utsouthwestern.edu/utsw/cda/ dept41600/files/54634.html).

Cell culture

The mouse insulinoma cell line Beta-TC-6 ([CRL-11506], [34]), the adenoma-derived mouse glucagonoma cell line alpha-TC1-clone 9 ([CRL-2350], [35]), and human kidney cell line HEK293 [CRL-1573] were obtained from American Type Tissue Culture. The MIN6 mouse insulinoma cell line [36] was kindly provided by Melanie Cobb (UT Southwestern Medical Center). Cells were maintained in their optimal culture conditions unless indicated otherwise. HEK293 cells were cultured in DMEM media with 10% fetal bovine serum, 100 IU/ml penicillin and 100 μg/ml streptomycin at 37°C and 5% CO_2. Beta-TC-6 cells were routinely cultured in DMEM (4.5g/L glucose, 4 mM glutamine) with 15% heat-inactivated FBS. MIN6 cells were maintained in DMEM (4.5g/L glucose), 2 mM L-glutamine, 1 mM sodium pyruvate and 10% heat-inactivated FBS. Alpha-TC1 cells were cultured in DMEM-based media, containing: 4 mM L-glutamine, 1.5 g/L sodium bicarbonate, 3 g/L glucose, 10% heat-inactivated dialyzed FBS, 15 mM HEPES, 0.1 mM non-essentail amino acids and 0.02% BSA.

Human Islets and Microarray

Human pancreatic islets were obtained from a cadaveric donor (49 yo Caucasian male, islet purity at 90%) and immediately placed in RPMI medium containing 11 mM glucose and 10% FBS. Islets (200/well) were then cultured for 16h in the presence of 20 nM Vit D or vehicle (DMSO) with duplicate biologic samples prepared for each condition. Total RNA was isolated, and microarray analysis was performed using the Human Affymetrix U133 Plus 2.0 array platform. Comparative gene expression was done using GeneSifter software with fold-change cut-off at ≥ 2 and $p \geq 0.05$. Further interrogation of the microarray data was performed using Ingenuity Pathway Analysis (www.ingenuity.com).

Mouse Islet isolation

The mouse islet isolation method has been previously described [1]. Briefly, the mouse pancreas was perfused and digested with Liberase RI (Roche, CAT#11815032001) or Collagenase P enzyme (Roche, CAT#1121857001). Islets were then isolated using Ficoll gradient centrifugation and hand-selection under a stereomicroscope for transfer to RPMI 1640 medium (11.1 mM glucose) supplemented with 10% (vol/vol) heat-inactivated fetal bovine serum (FBS), 100 IU/ml penicillin, and 100 μg/ml streptomycin (Invitrogen, Carlsbad, CA). Islets used for tissue distribution analysis had RNA harvested after an overnight recovery (37°C, 5% CO_2). For all other experiments, islets were allowed to recover overnight and then were treated with 20 nM VitD or vehicle (DMSO, 0.1% v/v) for an additional 16 hours before RNA or protein isolation, or functional assay.

Human islet glucose-stimulated insulin secretion

Human islet glucose-stimulated insulin secretion has been described elsewhere [37]. Human islets from three independent donors were maintained at 37°C with 5% CO_2 in media made up of: RPMI 1640, 10% fetal bovine serum, 100 units/ml penicillin and 100 μg/ml streptomycin. Approximately 50 islets/well were preincubated overnight in 20 nM VitD or vehicle After 16 hours of incubation in 20 nM VitD or vehicle (DMSO, 0.1% v/v), islets were transferred to Krebs-Ringer buffer, pH 7.4, containing 134 mM NaCl, 4.7 mMKCl, 1.2 mM KH2PO4, 1.2 mM MgSO4, 1.0 mM CaCl2, 5 mM NaHCO3, 10 mM HEPES, 0.1% BSA and 2.5 mM (low glucose) or 25 mM (high glucose) for one hour. Culture media were obtained and islets collected for determination of insulin content using an ELISA (Alpco, #80-INSHU-E01.1].

Mouse islet glucose-stimulated insulin secretion

Islets were pre-incubated in 20 nM VitD (or vehicle, DMSO at 0.1% v/v) for 16 hours in 11 mM glucose medium unless otherwise stated. Islets were then conditioned for 1 hour at 37°C in secretion assay buffer (SAB): pH 7.4, containing 114 mM NaCl, 4.7 mMKCl, 1.2 mM KH2PO4, 1.16 mM MgSO4, 2.5 mM CaCl2, 25.5 mM NaHCO3, 20 mM HEPES, 0.2% BSA and 0 mM glucose. Subsequently, islets were incubated for 60 min in SAB containing either 5 or 17.5 mM glucose. The media and islets from this final incubation were collected, and insulin content was measured using a rat sensitive insulin radioimmunoassay (Millipore).

Total islet insulin

Islets were suspended in 100 µl phosphate-buffered saline (PBS) and sonicated using a Bioruptor XL sonicator (Diagenode). Sonication was done with power setting at high in a 4°C waterbath, using 2 cycles (30 sec on, 30 sec off). Samples were diluted 1000 fold to assure that insulin levels fell within the linear range of a Rat Sensitive Insulin RIA (Millipore)

Total pancreatic insulin content in mice receiving vitamin D treatment

Male mice, 3-5 months of age, were assigned to one of the following four treatment groups: wild-type vehicle-injected, wild-type VitD-injected, *Vdr*$^{-/-}$ vehicle-injected and *Vdr*$^{-/-}$ VitD-injected (n=7/group). Every other day over a 5 day period, mice received VitD or vehicle (ip injection, VitD at 0.5 ng/g body weight). The last injection was performed 12 hours before pancreas removal. Pancreata were excised from mice, weighed and placed in acidic ethanol (75% ethanol, 0.2M HCl) on ice. Thereafter, pancreata were homogenized and kept at 4°C over night. The next day, the pancreatic slurry was centrifuged. The supernatant was transferred to a new tube to be stored at -20°C, while the remaining slurry was homogenized again in a fresh solution of acidic ethanol and kept at 4°C over night. On the third day, the pancreatic slurry was centrifuged, and the supernatant was transferred to the tube at -20°C. Then, the remaining slurry was homogenized again in a fresh solution of acidic ethanol, centrifuged and all extraction supernatants for a given sample were pooled and diluted 10,000 fold for measuring insulin using a Rat Sensitive Insulin RIA (Millipore).

Quantitative real-time PCR (qPCR) measurement of RNA

RNA was isolated from tissue samples, cultured islets or cell lines using RNA STAT-60 (Tel-Test Inc., Friendswood, TX), and RNA quality and quantity were assessed spectrophotometrically using a Nanodrop 1000 (Thermo Scientific). For each sample, 2 μg of total RNA was treated with ribonuclease-free deoxyribonuclease (Roche), and then reverse transcribed with random hexamers using SuperScript II (Invitrogen), as previously described in detail [38]. qPCR was performed using an Applied Biosystem Prism 7900HT sequence detection system (Applied Biosystems, Foster City, CA) and SYBR-green chemistry [38, 39]. Gene-specific primers were designed using D-LUX primer design software (www.invitrogen.com) and validated by analysis of template titration and dissociation curves [1]. Primer sequences are reported in Appendix B. qPCRs (10 μl) contained 25 ng of reverse-transcribed RNA, 150nM each of forward and reverse primers, and 5 μl of 2x SYBR Green PCR master mix (Applied Biosystems). Multiple housekeeping genes were evaluated in each assay to ensure that their RNA levels were invariant under the experimental conditions of each study. Results of qPCR were evaluated by the comparative Ct method [user bulletin no. 2, PerkinElmer Life Sciences [38]] using hypoxanthine-guanine phosphoribosyl transferase (HPRT), acidic ribosomal phosphoprotein P0 (36B4) and cyclophilin as housekeeping control genes, as appropriate.

Glucose uptake assay

A 96-well plate (Greiner CAT#655090) was prepared by incubating for 1 hour at 37°C with 50 μl/well of a solution containing 10μg/mL Collagen I and 0.1 mg/mL Poly-

L-Lysine. The plate was washed twice with PBS and allowed to air-dry for 1 hour. Mouse islets were dispersed into single cells by 20 minute incubation in Accutase (Innovative Cell Technologies, AT104) at ambient temperature. Accutase solution was removed by aspiration after a short, low-speed spin, and dispersed islet cells were washed once with culture media. Dispersed islet cells were seeded at 40,000 cells/well onto a precoated plate, and the plate was spun down at 30xG. VitD (20 nM) or vehicle (DMSO, 0.1% v/v) was added to wells. 16 hours later, cells were washed with secretion assay buffer (SAB) without glucose and then exposed to the fluorescent glucose analog 2-NBDG (2-deoxy-2-[(7-nitro-2,1,3-benzoxadiazol-4-yl)amino]-D-glucose, 500 μM) for 0, 2, 4, 6, or 8 minutes. The plate was rapidly chilled on ice and washed with ice-cold SAB buffer to stop 2-NBDG uptake into cells, then fluorescent imaging was performed using the BD pathway 855 Bioimaging system using a FITC filter, 10x objective and 4x4 montages. After imaging, cells were post-fixed with 4% formaldehyde for 15 minutes, blocked for 1 hour at RT with PBS containing 5% Goat serum and 5% Donkey serum, and then subjected to immunostaining using a guinea pig anti-Insulin primary antibody (1:300) and anti-guinea pig TRITC secondary antibody (1:300). Single cells that stained positive for insulin were selected for graphing, Over 100 cells/group met this criterion for a given experiment, and results were confirmed in two independent experiments.

Intracellular Calcium measurement

As described above, dispersed islet cells were plated on a 96-well plate precoated with Collagen I and Poly-L-Lysine. After 16 hour incubation in 20 nM VitD or vehicle, cells were loaded with 5μM Fura-2 AM for 1 hour (37°C and 5% CO2). The cells were

then washed with KRH buffer (119 mM NaCl, 4.7 mM KCl, 2.5 mM CaCl, 1.2 mM MgCl2, 1.2 mM KH2PO4, 10 mM HEPES, 2.0 mM D-Glucose) and 100µl/well of KRH was added. Intracellular calcium was monitored with the BD pathway 855 Bioimaging system (at 37°C), using a 10x objective and 4x4 montages. 6 images were collected at baseline (2 mM glucose), then 25 µL of 0.092M glucose in KRH was injected to the well for a final concentration of 20 mM glucose. Images were collected for the following 8 minutes. 25 µl 0.156 M KCl was then injected for a final concentration of 30 mM KCl and images were collected for another 1.5 minutes. After imaging, cells were fixed and stained with insulin as described above. Single cells that stained positive for insulin, had stable baseline and responded to the addition of glucose and KCl were selected for graphing. Over 150 cells/group met these criteria for each experiment, and results were confirmed in three independent experiments.

Plasmids

The expression plasmids pCMX-mouseVDR and pCMX-mouseRXRα, and the pCMX-β-galactosidase plasmid (used to control for transfection efficiency) were obtained from David Mangelsdorf (UT Southwestern Medical Center). Putative Vitamin D response elements (VDRE) within novel VDR target genes were identified using the algorithm, NHR-scan [40]. Oligonucleotides containing these putative VDRE sites, as well as the positive control VDRE of the mouse Cyp24a1 promoter, were annealed and subcloned into the HindIII site upstream of the thymidine kinase promoter of the luciferase plasmid, pTK-LUC [41]. Plasmid construction was confirmed by DNA sequencing, and plasmids containing two copies each of the respective VDRE were

chosen for use in transfection experiments. Oligonucleotide sequences are available in Appendix B.

Transfections

HEK-293 cells were seeded into a 96-well plate and allowed to reach ~80% confluence. Cells in each well were transfected with 40 ng pCMX-VDR, 20 ng pCMX-RXR, 15 ng pCMX-β-Gal, and 75 ng luciferase reporter plasmid, using Lipofectamine 2000 (Invitrogen). 5-8 hours later, vehicle (DMSO) or 20 nM VitD was added at a final volume of 0.1%. 24 h after addition of ligand, cells were harvested, lysed, and analyzed for luciferase (FLUOstar OPTIMA, BMG Labtech) and β-galactosidase (PowerWave XS, BioTek) activity. Results are expressed as relative luciferase units (RLU), following correction for transfection efficiency using β-gal activity.

Statistics

All results are expressed as the means ± SEM for each treatment group. Two-tailed Student's *t*-tests were performed to compare differences between two groups. 1-way and 2-way ANOVA, with Bonferroni's multiple comparisons post test were used to compare samples in experiments with 3 or more groups. All statistical tests were performed using GraphPad Prism software (GraphPad, San Diego, CA). Significance was established at $P < 0.05$ and is represented with an asterisk (*) for t-tests, or different groups are represented by different letters for ANOVA.

2.4 Results

VDR is expressed in mouse islets and is upregulated by incubation in high glucose.

Our previous survey of nuclear hormone receptor expression in cells of the endocrine pancreas revealed that the vitamin D receptor (VDR, NR1I1) was the most abundant receptor in islets, among those receptors for which a bona fide ligand has been identified. In this case, 1,25-dihydroxyvitamin D_3 (VitD) is known to bind VDR with an estimated dissociation coefficient of 0.1-1 nM

Relative transcript abundance of a gene often reflects the importance of that gene in a given tissue. Therefore, we determined the tissue distribution of mouse *Vdr* mRNA levels in an array of mouse tissues including the Vitamin D target organs, kidney and small intestine (Figure 2.2a). As expected VDR mRNA levels are most abundant in kidney and small intestine, but, *Vdr* mRNA levels in islets were quite high. All other tissues tested had negligible amounts of VDR mRNA compared to islets, even though some of them have been reported to respond to VitD. The pattern seen in this tissue distribution analysis suggests that VDR has an important role in islets.

The ability to sense changes in plasma glucose and respond in a proper manner is vital for the beta cell. Thus, we tested if VDR expression in isolated mouse islets was sensitive to glucose levels in the media. Incubation of isolated primary mouse islets in 17.5 mM glucose, versus 5 mM glucose, resulted in a significant (73%) increase in VDR mRNA levels (Figure 2.2b). To confirm and extend these findings, a time-course study was performed using the Min6 insulinoma cell line. A significant (2-fold) increase in VDR mRNA level was observed by 3 hours after glucose administration, and was maintained for 10 hours (Figure 2.2c).

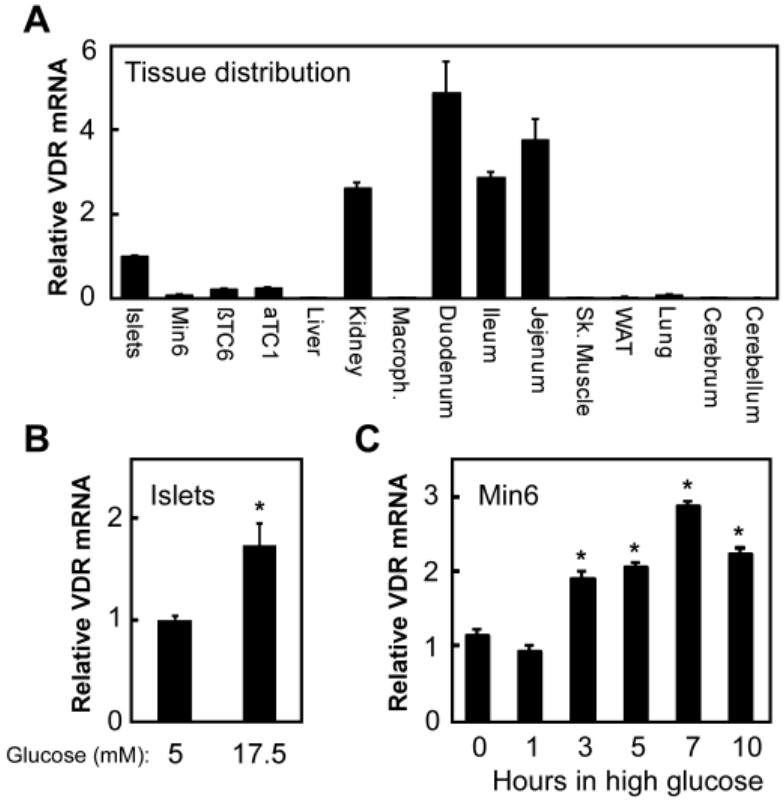

Figure 2.2. VDR is expressed in pancreatic islets and is upregulated by high glucose. A: Tissue distribution of VDR mRNA in male A129/SvJ mice (3 months old, male, chow-fed) and mouse beta cell lines (Min6, βTC6 and αTC1) (n=3). VDR mRNA values are normalized against the housekeeping gene cyclophilin. B: Mouse islets were cultured in 3 mM glucose for 8 hours, then transferred to media containing low (5 mM) or high (17.5 mM) glucose for 16 hours. RNA was isolated and measured by qPCR. VDR mRNA levels were normalized against the housekeeping gene HPRT. C: Min6 cells were incubated in 3 mM glucose for 24 hours and were then transferred to media containing 25 mM glucose for indicated times. Relative VDR levels were measured by qPCR using HPRT as the invariant control gene. All values depict the mean ± SEM of 3-4 individual samples or cultures. *$p<0.05$ compared to low-glucose control by Student's t-test (B) or ANOVA (C) with Dunnett's post-hoc analysis.

Vitamin D induces insulin secretion in mouse and human islets.

To test if physiological concentrations of VitD have an effect on insulin secretion, we performed a GSIS assay on islets pretreated with various doses of VitD (Figure 2.3a). Our choice of VitD concentrations was based on the following: in biochemical assays, 1,25-dihydroxyvitamin D_3 (VitD) binds to VDR with a dissociation

constant of ~0.1 nM; plasma levels of this active hormone are reported to be 0.2 nM in mice and humans [42, 43]; and in cell-based assays of VDR activity, VitD concentration ranges of 10-100 nM are frequently used to assure saturation of the VDR [44-46]. Isolated islets from wildtype A129/Sv mice were pretreated with vehicle, 0.2 nM VitD, 2 nM VitD or 20 nM VitD for 16 hours in regular islet media to allow enough time for VDR to turn on transcription of target genes. Thereafter, glucose-stimulated insulin secretion was performed in SAB secretion buffer. VitD pretreated islets show a trend towards increased insulin secretion using as low as 0.2 nM VitD. Islets pretreated with 2 nM VitD have approximately 2-fold insulin secretion with high glucose compared to vehicle-treated islets. Lastly, incubation in 20 nM VitD shows an even further enhancement of insulin secretion with high glucose of approximately 2.5-fold compared to vehicle treated islets. Importantly, no effect of VitD was observed under low-glucose conditions.

In order to investigate if the VitD-enhanced GSIS is dependent on VDR, islets from wildtype or *Vdr*$^{-/-}$ mice were pretreated for 16 hours in 20 nM VitD or vehicle and then used in a GSIS assay (fig 2.3c). Results show that in high glucose VitD-pretreated wildtype islets secrete twice the amount of insulin as the vehicle-treated wildtype islets. Furthermore, VitD enhanced GSIS is entirely dependent on VDR as no further enhancement of insulin secretion is seen with VitD pretreatment in *Vdr*$^{-/-}$ mouse islets.

To test if the VitD-enhanced GSIS is mouse strain-dependent, we performed the GSIS assay on isolated islets from C57Bl/6 and A129/Sv mice for a side-by-side comparison (Figure 2.3b). Islets were pretreated for 16 hours in 20 nM VitD or vehicle and then used for a GSIS assay. Again, VitD had no effect on insulin secretion under low

glucose conditions; however, when glucose concentration was elevated to 17.5 mM VitD-pretreated islets exhibited 2-fold insulin secretion compared to vehicle-treated islets. These results are independent of strain background, as both VitD-treated islets from C57Bl/6 and A129/Sv mice show approximately 2-fold enhancement of insulin secretion under the high glucose condition. GSIS performed in a perifusion system (Figure 2.3d) confirm the VitD-enhanced GSIS observed in the static incubation GSIS experiments (Figure 2.3a-c).

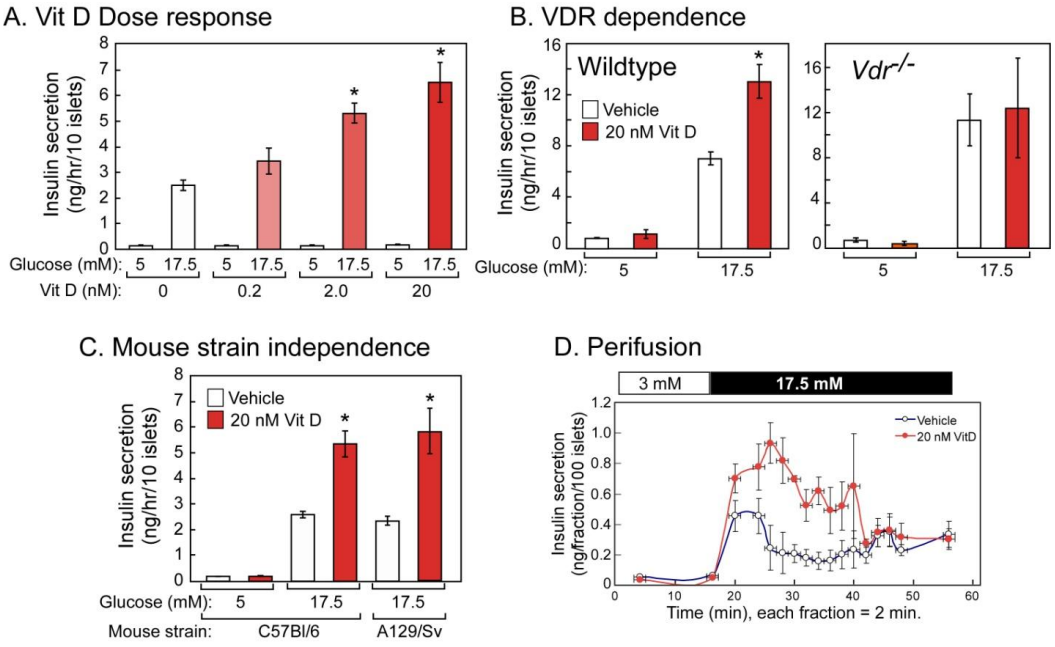

Figure 2.3. VitD enhances glucose stimulated insulin secretion in mouse islets. A. Isolated islets from wildtype A129/Sv mice were incubated in, 0 nM, 0.2 nM, 2 nM or 20 nM VitD for 16 hours, and then a glucose stimulated insulin secretion was performed in either 5 mM or 17.5 mM glucose. B. Islets from wildtype or *Vdr*$^{-/-}$ mice were pretreated for 16 hours in 20 nM VitDor vehicle and then used for a glucose stimulated insulin secretion assay. C. Islets from C57Bl/6 or A129/Sv mice were pretreated for 16 hours in 20 nM VitD or vehicle and then used for glucose stimulated insulin secretion assay. D. A perifusion experiment confirmed the previous observations evaluating GSIS by static incubation. All data are shown as the mean ± S.E. (n = 3). Asterisk denotes a significance from the vehicle treated high glucose bar (p-value ≤ 0.05)

In addition to VitD, the bile acid lithocholic acid (LCA) is another physiological ligand for VDR [47]. In order to confirm that the increase in GSIS was through VDR, LCA was tested. Isolated islets from wildtype and *Vdr*$^{-/-}$ mice were pretreated in 10mM LCA for 16 hours and were then immediately used for a GSIS experiment. Pretreatment of wildtype islets results in 2.5-fold induction of GSIS compared to vehicle treated islets. When the same is done in *Vdr*$^{-/-}$ islets, the induction is only 1.6-fold (Figure 2.4). When the results are expressed as fold induction (LCA/vehicle) of insulin secretion in 17.5 mM glucose shows that half of the LCA-enhanced insulin secretion is dependent on VDR. The other half is likely due to other bile acid receptors present in islets (see appendix A).

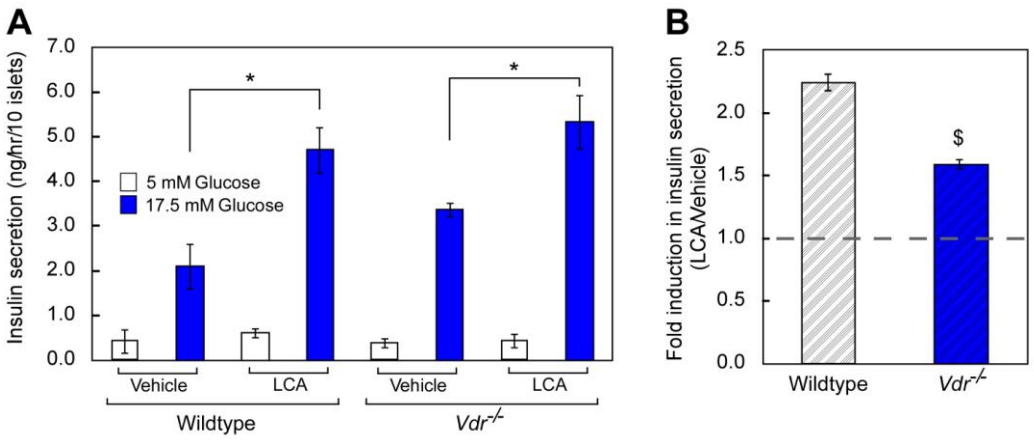

Figure 2.4. LCA enhances GSIS greater in wildtype compared to *Vdr*$^{-/-}$ islets. A: Islets from wildtype or *Vdr*$^{-/-}$ mice were pretreated for 16 hours in 10 mM LCA or vehicle and then used for a glucose-stimulated insulin secretion assay (GSIS). B: Ligand-induced GSIS in wildtype and *Vdr*$^{-/-}$ islets expressed as ratio of high glucose induced insulin secretion in LCA-treated versus vehicle-treated islets. All data are shown as the mean ± S.E. (n = 4). Vehicle versus VitD pretreated high glucose groups were compared using Two-tailed Student's *t*test. *, data indicate statistical difference from high glucose vehicle treated samples ($p \leq 0.05$) compared high glucose VitD-treated samples. $, data indicate statistical difference ($p < 0.05$) of HG/LG ratio compared with vehicle treated-islets.

VitD-pretreatment augments insulin secretion in human islets.

Multiple cross-sectional and follow up human clinical studies have shown a connection between Vitamin D status and Type 2 Diabetes [13-18]. Furthermore, some studies have shown an improvement in insulin secretion after Vitamin D treatment [18]. Therefore, we also tested if cultured human islets were as responsive to VitD in a GSIS assay as mouse islets.

Isolated human islets from 3 different donors were independently pretreated with 20 nM VitD or vehicle for 16 hours and then used for a glucose-stimulated insulin secretion assay. All three donor islets showed an improvement in beta cell function after VitD pretreatment (Figure 2.5a). Either by increasing high glucose-stimulated insulin secretion (donor 1 and donor 3; 2-fold and 2.5-fold increase respectively) or by decreasing stress-induced low glucose stimulated insulin secretion (donor 2 and donor 3; 2-fold and 3-fold decrease respectively). Average response between all three donors shows a 2-fold increase in high glucose stimulated insulin secretion when islets were pretreated with VitD (Figure 2.5b). Furthermore, the average stimulation index (high glucose/low glucose stimulated insulin secretion) for vehicle-treated human islet was 2-fold, and that response was increased to 12-fold in human islets pretreated with 20 nM VitD (Figure 2.5c).

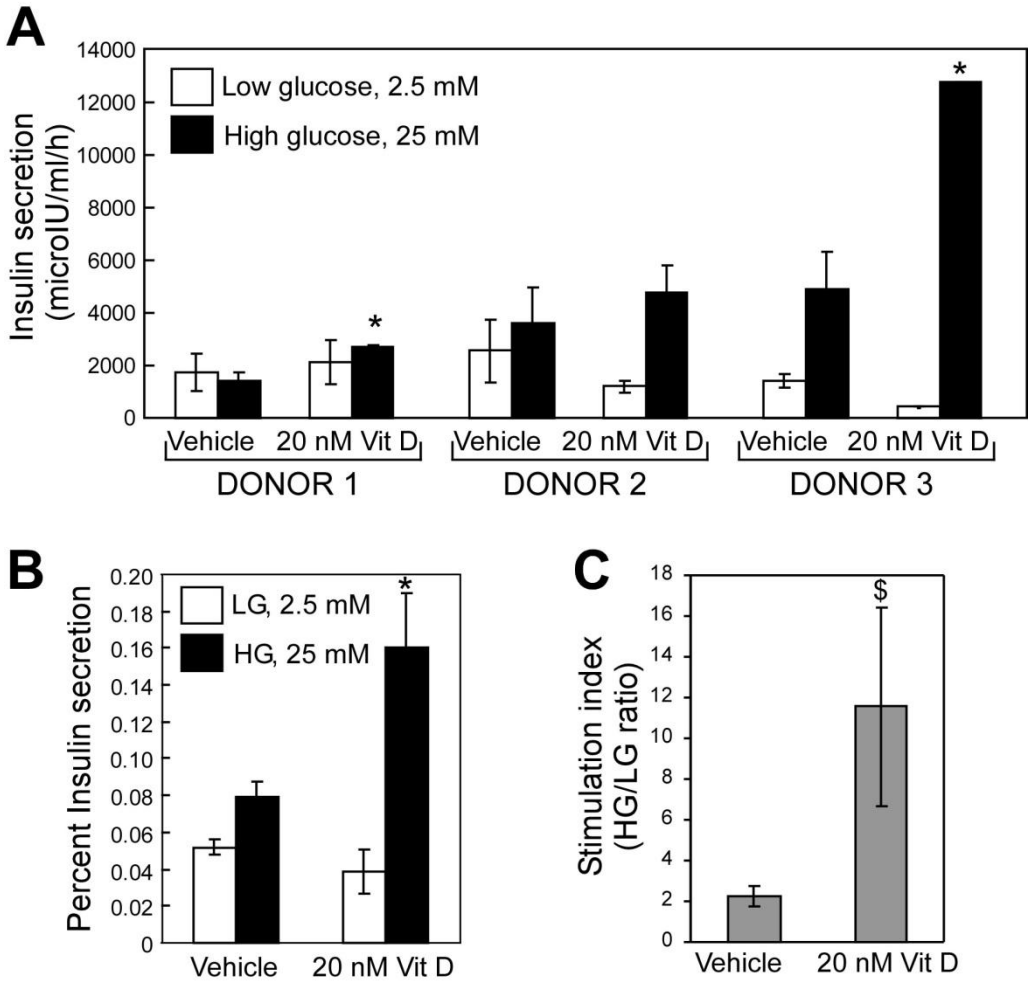

Figure 2.5. VitD-pretreatment improves insulin secretion in human islets. A: human islets were exposed to 2.5 or 25 mM glucose for 1 h after 16 h of preincubation with VitD (20 nM) or vehicle (DMSO 0.1% v/v). B: Summary data from three donors, expressed as percent secreted insulin. C: Summary data from three donors, expressed as stimulation index (HG/LG) of insulin secretion. Insulin secretion was measured by enzyme-linked immunosorbent assay and normalized to total insulin content. All data are shown as the mean ± S.E. (n = 3). Vehicle versus VitD pretreated high glucose groups were compared using Two-tailed Student's $t$test. *, data indicate statistical difference ($p < 0.05$) compared with islets pretreated with VitD. $, data indicate statistical difference ($p < 0.05$) of HG/LG ratio compared with vehicle treated islets.

VitD pretreatment increases glucose stimulated calcium uptake and has no effect on glucose uptake or quantity of islet hormones.

A candidate approach was taken to identify pathways involved in insulin secretion that might be affected by VitD. First, the relative quantity of islet hormones was assessed by mRNA level. Isolated mouse islets were cultured for 16 hours in the presence of vehicle or 20 nM VitD, and then mRNA levels of islet hormones were measured by qPCR (Figure 2.6a). mRNA levels of insulin I/II, heterogeneous nuclear insulin II, somatostatin and glucagon were unchanged by VitD-treatment. The heterogeneous nuclear insulin II (het-Ins) is a transient version of insulin transcript that represents newly generated transcripts from the Insulin II gene. Therefore the het-Ins transcript is often used to represent transcriptional activity of the insulin promoter. With no change seen in the het-Ins transcript or the Ins I/II transcript, it can be concluded that VitD does not affect transcriptional activity of the insulin gene.

Despite the lack of change in mRNA levels of insulin, total insulin pool in islets pretreated with vehicle or VitD was also evaluated. Total insulin content from 10 islets was measured at the end of a GSIS from wildtype and *Vdr*$^{-/-}$ islets that had been pretreated with vehicle or 20 nM VitD for 16 hours (Figure 2.6b). Neither VitD treatment nor genotype affected total insulin pool in isolated islets. Furthermore, total pancreatic insulin was not affected by VitD treatment in wildtype or *Vdr*$^{-/-}$ mice (Figure 2.6c).

Glucose uptake is the first step in the initiation of glucose stimulated insulin secretion. To test if glucose uptake was altered by VitD pretreatment a glucose uptake assay was performed. Dispersed primary mouse islet cells were cultured for 16 hours in the presence of vehicle or 20 nM VitD. At the end of incubation, cells were washed with

a buffer containing 0 mM glucose and then incubated in 500μM 2-NBDG for 0, 2, 4, 6, or 8 minutes. Intracellular 2-NBDG fluorescence was imaged using the BD pathway 855 Bioimaging system. After imaging, cells were stained with Insulin antibody and only cells that stained positive for insulin were selected for graphing. The results show that VitD pretreatment has no effect on glucose uptake into primary beta cells (Figure 2.6d).

Lastly, glucose-stimulated calcium uptake was assessed in dispersed primary beta cells. Calcium influx, via voltage-gated calcium channels, is an important component of glucose-stimulated insulin secretion. Here, dispersed primary mouse islet cells were cultured for 16 hours in the presence of vehicle or 20 nM VitD. At the end of incubation, cells were loaded with FURA-2 AM and imaged using BD Pathway 855 Bioimaging system using dual excitation at 340nm and 380nm. Baseline measurements were taken at 2 mM glucose, and then glucose was injected to a final concentration of 20 mM. Lastly cells were depolarized using 30 mM KCl. Post fixation and insulin staining allowed for selection of purely beta cell population for graphing. The results show a very significant enhancement of glucose stimulated calcium influx with VitD pretreatment (Figure 2.6e). Notably there was no change in baseline calcium intracellular concentration with VitD pretreatment.

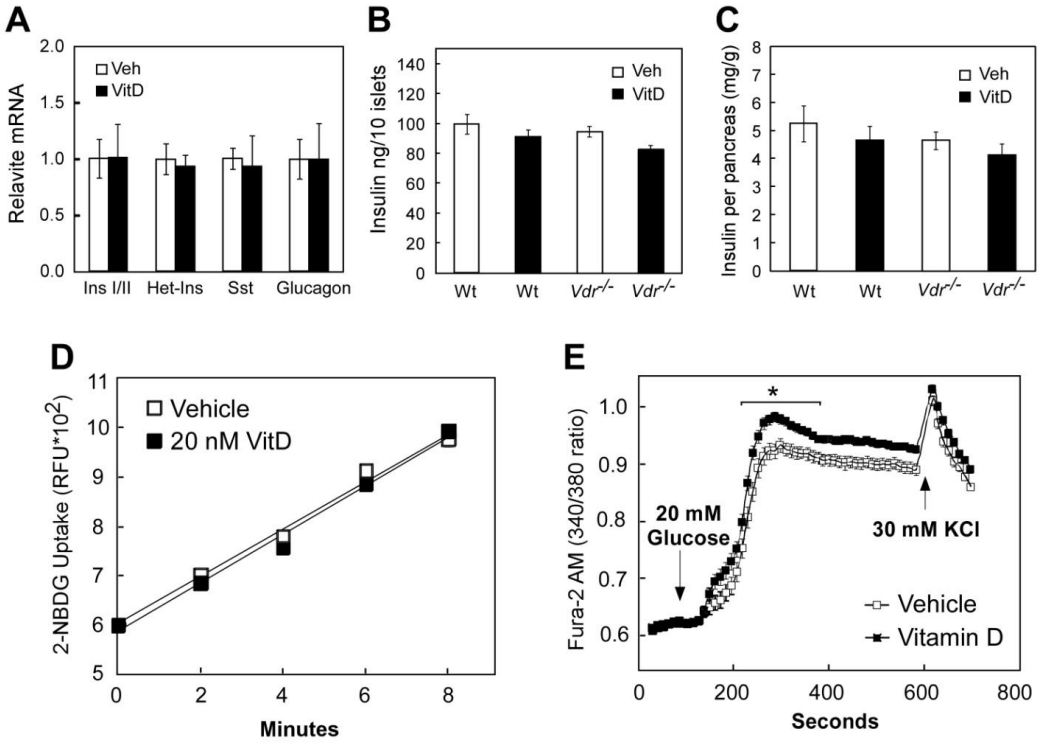

Figure 2.6. VitD pretreatment increases glucose stimulated calcium uptake and has no effect on glucose uptake or quantity of islet hormones. Isolated mouse islets were cultured for 16 hours in the presence of vehicle or 20 nM VitD (A,B): A. mRNA levels of islet hormones were measured by qPCR. InsI/II: mature Insulin I/II, Het-Ins: heterogeneous nuclear insulin II, Sst: somatostatin and glucagon. B. Total insulin content from 10 islets was measured at the end of a GSIS from wildtype and *Vdr*$^{-/-}$ islets. C. Wildtype and *Vdr*$^{-/-}$ mice were IP injected with VitD (0.5ng/g bodyweight) every other day for 5 days and then pancreatic insulin was quantified. Dispersed primary mouse islet cells were cultured for 16 hours in vehicle or 20 nM VitD (D, E): D. Cells were incubated in 500µM 2-NBDG for 0, 2, 4, 6, or 8 minutes, and then 2-NBDG uptake imaging was done using the BD pathway 855 Bioimaging system. Single cells that stained positive for insulin were selected for graphing (n=500 cells) E. Cells were loaded with FURA-2 AM and imaged using BD Pathway 855 Bioimaging system using dual excitation at 340nm and 380nm. Six baseline measurements at 2 mM glucose were taken before glucose was injected to a final concentration of 20 mM. Glucose induced calcium influx was monitored for 8 minutes and then cells were depolarized using 30 mM KCl. Insulin staining allowed for selection of beta cells for graphing. Asterisk denotes a significant difference ($p < 0.05$) between vehicle and VitD treatment calculated using 2-way Anova with Bonferroni's multiple comparisons post test. All data are shown as the mean ± S.E.

Microarray using human islets identifies CaV2.3 as a VDR-regulated gene.

As VitD enhances GSIS in mouse and human islets, we performed a microarray using human islets treated with VitD or vehicle and validated potential target genes using qPCR in mouse islets. RNA from human islets treated with vehicle or 20 nM VitD for 16 hours (n=2) were subjected to a microarray. Downstream analysis revealed 300 genes upregulated 2-fold or greater with VitD (p-value cut-off was set at ≤ 0.05). The 300 upregulated genes were analyzed using Ingenuity Pathway Analysis (IPA), which identified calcium signaling to be the most significantly affected canonical pathway (p-value of 0.0016). Next, an IPA-generated list of all genes related to calcium signaling and transport was overlaid with the human islet microarray data, and this comparison revealed 30 calcium genes that were upregulated by VitD treatment (Figure 2.7a).

As glucose enhanced calcium influx is increased in VitD-pretreated beta cells, we focused on the 5 genes encoding plasma membrane calcium channels (*Cacna1e=CaV2.3, ATP2b2, ATP2b3, TrpV6* and *Cacnb1*). The top candidates to explain VitD effects in beta cells were *TrpV6,* which is a previously identified target gene of VitD [48], and the 2 members of the voltage-gated calcium channel family that are important components of the insulin secretion machinery, *cacna1e* (CaV2.3) and *cacnb1* [49].

According to qPCR results using mouse islets, CaV2.3 is the strongest candidate with approximately 6-fold enrichment after 16 hour VitD treatment (fig 2.7b). The *ATP2b2* and *ATP2b3* genes encode for plasma membrane calcium pumps that export calcium from the cell. Thus their increase would be inconsistent with our observations using calcium imaging. qPCR results in mouse islets treated with VitD showed no increase in transcript level of these genes (data not shown).

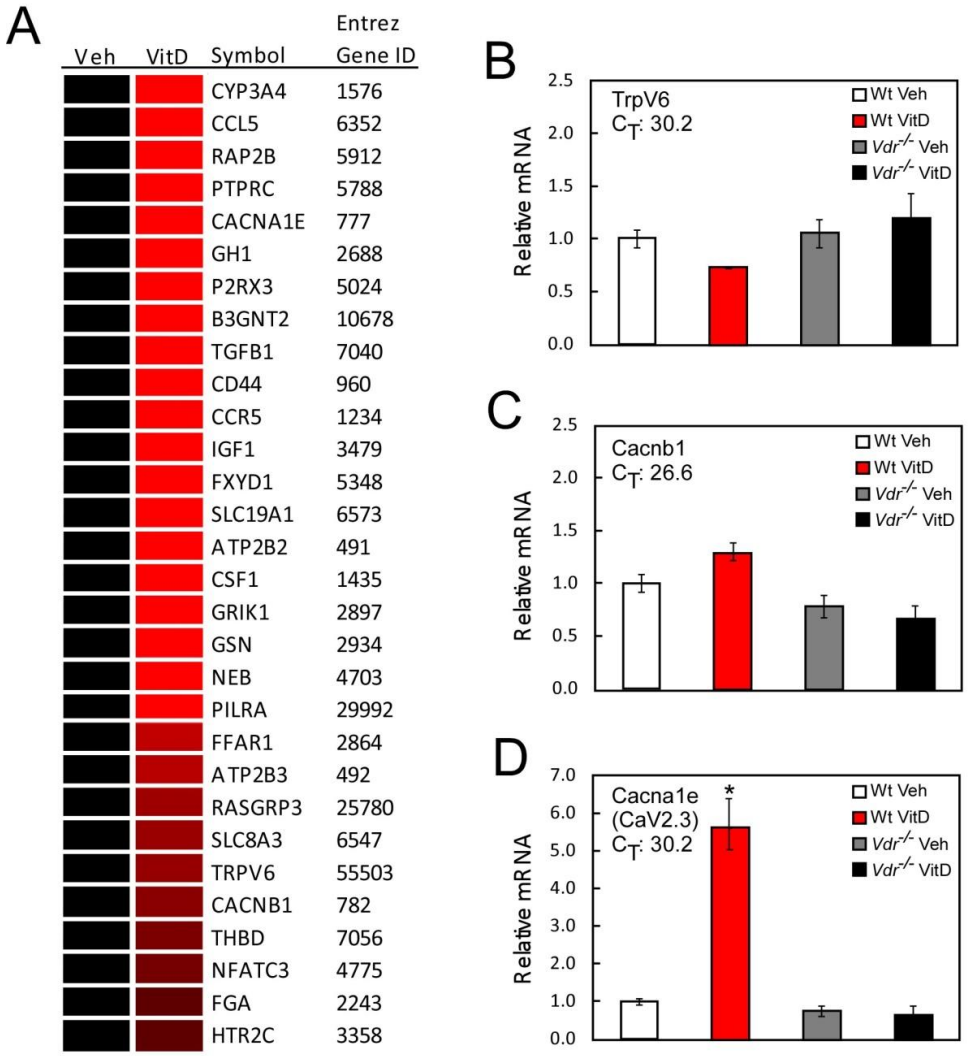

Figure 2.7. Microarray on human islets and downstream analysis identify CaV2.3 as being a strong candidate for the VitD-enhanced GSIS. Microarray results from human islet samples treated with vehicle or 20 nM VitD for 16 hours (n=2) revealed 300 genes that were upregulated ≥2 fold (p-value cut-off was set at ≤ 0.05). The Ingenuity Pathway Analysis (IPA) software was used to analyze the 300 upregulated genes. The IPA analysis identified calcium signaling to be the most significant canonical pathway. A: Heat map showing 30 genes upregulated in the human islet microarray that are related to calcium signaling and transport (data from IPA analysis). B-D: The three genes encoding for plasma membrane calcium channels that transfer calcium into the cell were validated as target genes using wildtype and *Vdr*$^{-/-}$ mouse islets. Islets were incubated in media containing 11 mM glucose and vehicle or 20 nM VitD. All data are shown as the mean ± S.E. (n = 2).

qPCR analyses on all members of the voltage-gated calcium channel family uncover another VitD upregulated gene in mouse islets.

As two members of the voltage-gated calcium channel (VGCC) family were identified in the human islet microarray and only one of them was confirmed to be upregulated by VitD in mouse islets, we decided to look at all members of the family in mouse islets. Isolated islets from A129/Sv mice were incubated in 20 nM VitD or vehicle for 16 hours. Thereafter, RNA was harvested, reverse transcribed and analyzed by qPCR (Figure 2.8a-d). This analysis is the first report for a quantitative, comparative assessment of all voltage-gated calcium channel subunits in the islet. This analysis also identified another VitD-regulated gene, *cacna2d3*. CaV2.3 and Cacna2d3 show upregulation by VitD (which is represented by overlaid crosshatched boxes in Figure 2.8); while all other genes showed no significant change with VitD incubation.

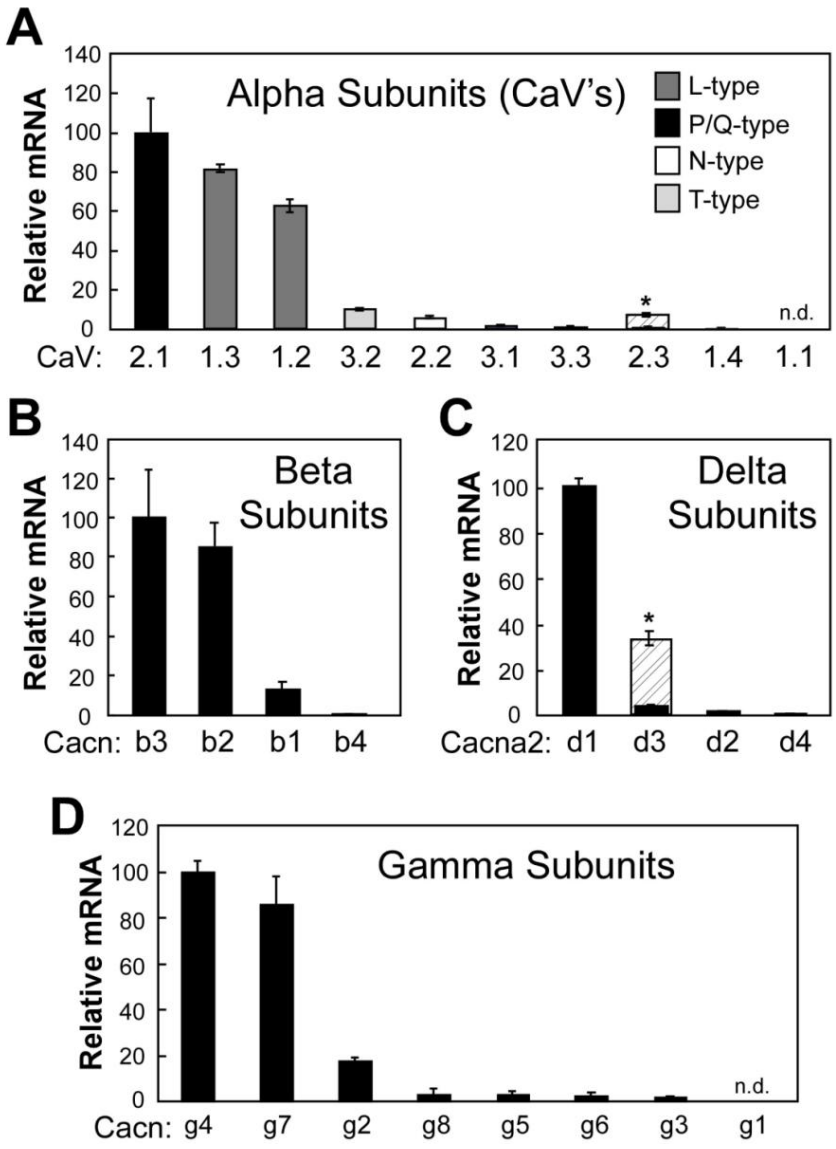

Figure 2.8. qPCR analyses of all subunits of the Voltage gated calcium channel family demonstrates that CaV2.3 and cacna2d3 are upregulated by VitD in mouse islets. qPCR results from primary mouse islets incubated in 20 nM VitD or vehicle for 16 hours. A: Members of the alpha subunit that form the transmembrane channel. B: Members of the beta regulatory subunit. C: Members of the alpha-2-delta regulatory subunit. D: Members of the gamma regulatory subunit. Overlaid crosshatched boxes on CaV2.3 and Cacna2d3 show upregulation by VitD. No significant change was observed with VitD incubation in other genes. All data are shown as the mean ± S.E. (n = 4).

The cacna1e gene contains conserved VDREs.

As CaV2.3 was the only gene in the voltage-gated calcium channel family shown to be upregulated by VitD in both mouse and human islets and since it has prior connections to insulin secretion and Type 2 Diabetes [50-52], we considered CaV2.3 to be a very likely candidate behind the VitD-enhanced GSIS. Therefore, we scanned the *cacna1e* locus for VDREs using an *in silico* analysis approach. Using NHR-scan [40], four potential VDREs were found in the mouse *cacna1e* locus and five potential VDREs were found in the human *cacna1e* locus (Figure 2.9a). Three of these VDREs were conserved between mouse and human, and are located in intron 7, exon 13 and exon 18. The additional VDRE in mouse was located in intron 25, while the two VDREs in human were located in intron 6 and the 3'UTR. Tk-Luc plasmids were made that contained two copies of the VDRE of interest inserted just upstream of the minimal thymidine kinase promoter to drive expression of the *luciferase* gene. Transfected cells were exposed to VitD or vehicle for 16 hours and then assayed for Luciferase activity (Figure 2.9b). Results show that of the three potential conserved VDREs identified by this *in silico* method, only the VDRE in intron 7 is functional. Two additional functional VDREs were identified that are not conserved between mouse and humans, one in mouse intron 25 and the other in human 3'UTR region.

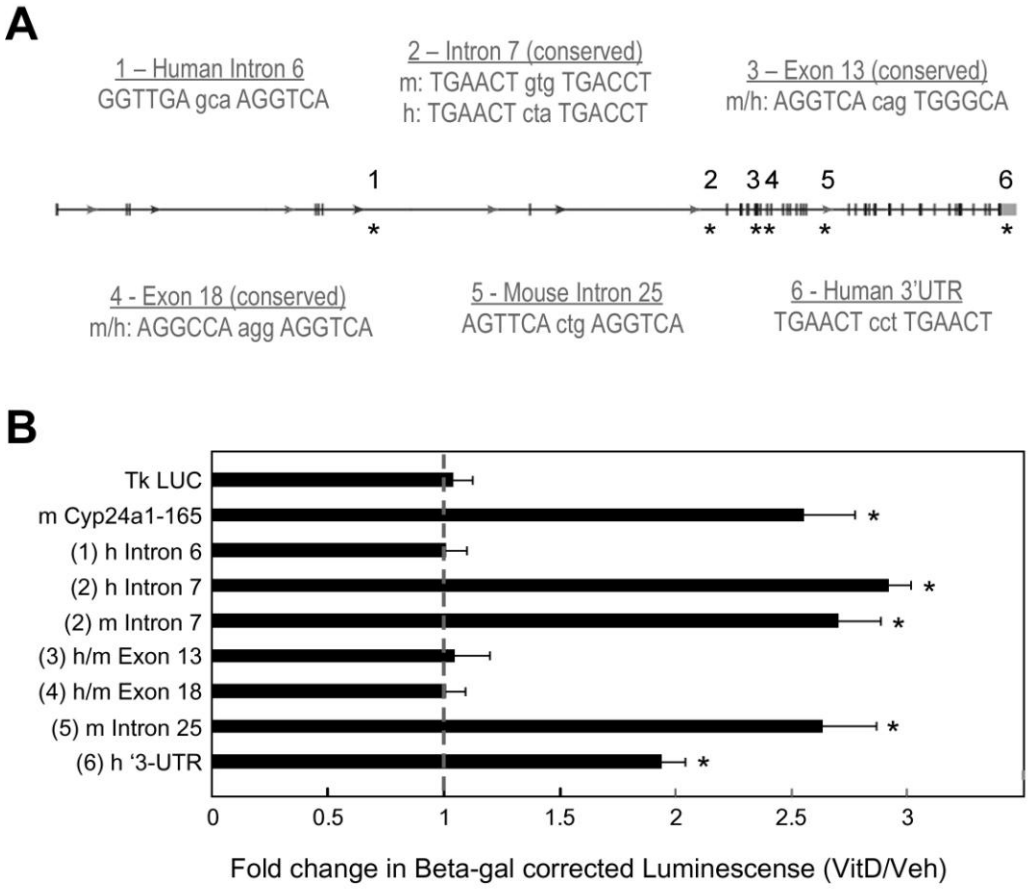

Figure 2.9. The human and mouse Cav2.3 gene contains conserved VDREs. A: *In silico* analysis of the CaV2.3 gene was used to identify potential VDREs [40]. Four potential VDREs were found in the mouse CaV2.3 gene and five potential VDREs were found in the human CaV2.3 gene. Three of the VDREs were conserved and were located in intron 7, exon 13 and exon 18. One additional VDRE was found in intron 25 in the mouse CaV2.3 gene and two additional VDREs were found in the human CaV2.3 gene, in intron 6 and the 3'UTR. B: Cell reporter assays were performed in HEK293 cells. Plasmids containing two copies of each VDRE upstream of the Thymidine kinase minimal promoter and luciferase gene were transfected along with CMV-Beta-Galactosidase (to correct for transfections efficiency) and CMV-VDR and CMX-RXR into HEK293 cells. Transfected cells were exposed to VitD or vehicle for 16 hours and then assayed for luciferase activity.

2.5 Discussion

The connection between Vitamin D levels and insulin secretion was first introduced in 1980, when Vitamin D deficient rats were shown to have reduced insulin secretion compared to Vitamin D sufficient controls [19]. Subsequent reports suggested that this effect was independent of the changes in serum calcium caused by the vitamin D deficiency [20, 21]. However, there have been no reports describing VitD-enhanced GSIS in murine or human islets. Multiple epidemiological studies have followed that reported a link between vitamin D deficiency and Type 2 Diabetes [13-15]. More relevant to our findings, several small clinical studies have reported improved glucose tolerance and beta cell function after following a vitamin D supplementation regimen [16-18].

In this report, we clearly show that pretreating mouse and human islets with 20 nM VitD for 16 hours increases GSIS over vehicle controls. Lower concentrations of VitD (2 nM) and a different VDR ligand (LCA) are also capable of producing the same effect. We also show that VDR is highly expressed in islets, and that its expression level is comparable to what is seen in kidney and intestine. As the transcript abundance of a gene often reflects it importance in a given tissue, it is likely that VDR plays an important role in islets. In addition, VDR expression is glucose-responsive, suggesting an increased need for Vit D signaling when glucose level rises.

VitD pretreatment had no effect on glucose uptake or total insulin level;, however, glucose-stimulated calcium influx was significantly enhanced. In search for a mechanism behind the increased insulin secretion and calcium influx, we took an unbiased approach by using microarray analysis of human islets treated with vehicle or VitD. As we observe VitD-enhanced GSIS in both human and mouse islets, it is possible

that the same mechanism is conserved between species. Therefore we used mouse islets to validate results from the human islet microarray. Ingenuity Pathway Analysis of the microarray identified calcium signaling to be the most significantly affected canonical pathway. Several candidates were tested by qPCR in mouse islets. Thereby, we identified the *cacna1e* gene encoding for the R-type voltage-gated calcium channel (CaV2.3) to be upregulated by VitD in mouse and human islets. CaV2.3 was a likely target gene as it has previously been shown to affect insulin secretion [50] and because we had previously observed an increased glucose-induced calcium influx by VitD pretreatment. Identification of a conserved VDRE in intron 7 of the mouse and the human *cacna1e* gene supports the upregulation of cacna1e seen by microarray and qPCR. In addition to the conserved VDRE, we discovered one additional VDRE in both human *cacna1e* (located in the 3'UTR) and mouse *cacna1e* (located in intron 25).

We did not observe the VitD-induced enhancement in *cacnb1* expression in mouse islets, as seen in human islets. This prompted us to look at transcript levels of all members of the voltage-gated calcium channel family in VitD-treated mouse islets. In addition to providing information on the expression levels of all members of the VGCC family, we also found another subunit, *cacna2d3*, to be highly VitD responsive in mouse islets. Upregulation of Cacna2d3 adds further complexity to VitD enhanced GSIS, because Cacna2d3 has been shown to increase current density of both CaV1.2 and CaV2.3 channels [53]. Therefore it is likely that more than one type of VGCC is affected by VitD treatment. The same holds true for human islets as *cacnb1* transcript levels were also affected in addition to *cacna1e*. Cacnb1 is an auxiliary subunit that can increase peak

calcium current of L-type calcium channels by controlling membrane targeting and shifting the voltage dependence of activation and inactivation [54, 55].

In summary, we demonstrate for the first time that VitD pretreatment increases GSIS in mouse and human islets. Furthermore, we have uncovered a potential mechanism behind the VitD-enhanced GSIS. Our results suggest that VitD activates transcription of the R-type voltage gated calcium channel, CaV2.3 (in mouse and human islets) and other auxiliary subunits (cacna2d3 in mouse and cacnb1 in human). As CaV2.3 has prior connection to insulin secretion, and we observe an increase in glucose-stimulated calcium uptake in primary beta cells, the increased abundance of these channels is a plausible mechanism for the VitD-enhanced GSIS.

CHAPTER THREE

Vitamin D regulation of Klotho in the beta cell

3.1 Abstract

Klotho (Kl) is a single-pass transmembrane protein that was first identified as an aging suppressor gene. Mice that lacked *Klotho* had shortened lifespan, while mice that overexpressed *Klotho* exhibited increased longevity. The shortened lifespan of *Klotho*$^{-/-}$ mice has largely been attributed to the effects of hyperphosphatemia. Membrane-bound Klotho functions as an obligate co-receptor with fibroblast growth factor receptor 1c (FGFR1c) to mediate the effects of Fibroblast Growth Factor 23 and affect phosphate retention in the kidney. The extracellular domain of Klotho can be cleaved, a process enhanced by the presence of insulin. The cleaved Klotho fragment contains sialidase activity, allowing it to remove terminal sialic acids from the glycan posttranslational modifications of proteins. By this mechanism, Klotho has also been found to modify the surface retention of transmembrane channels involved in phosphate transport, such as TrpV5 in the kidney.

In addition to altered phosphate balance, mice with modified *Klotho* expression display a metabolic phenotype. *Klotho*$^{-/-}$ mice are extremely insulin-sensitive, have reduced pancreatic insulin content and exhibit low circulating insulin and glucose levels. Reciprocally, *Klotho* transgenic mice are insulin-resistant and display elevated plasma insulin levels. In light of the metabolic phenotype of these mice, our goal was to determine whether Klotho plays a role in the endocrine pancreas. We established that Klotho is abundantly expressed in beta cells, at levels sufficient to mediate FGF23

signaling. Klotho is transcriptionally regulated by VitD treatment and plays a role in VitD-enhanced glucose-stimulated insulin secretion. Finally, others have reported that the beta cell glucose transporter GLUT-2 is modified by sialic acid residues. We establish that islets from *Klotho*$^{-/-}$ mice exhibit reduced plasma membrane localization of GLUT-2, thus affecting their ability to sense external glucose to initiate insulin release. These observations again link Klotho to the aging process, as reduced GLUT-2 activity and appropriate glucose-stimulated insulin secretion by islets declines with age. Our findings suggest that vitamin D supplementation, by upregulating Klotho, may relieve these effects in the aging islet.

3.2 Introduction

Klotho is a type-1 transmembrane protein localized to the plasma membrane of cells, with a large N-terminal domain facing into the extracellular space. Klotho is primarily expressed in kidney, parathyroid gland, and certain regions of the brain. Klotho was initially identified in a mouse strain as the gene interrupted by the random insertion of a transgene [56]. This *Klotho*$^{-/-}$ mouse strain exhibited multiple aging phenotypes, including: shortened lifespan; muscle and skin atrophy; pulmonary emphysema; osteopenia; infertility; hyperphosphatemia; and vascular and soft tissue calcification. It was confirmed that the phenotype of these mice was entirely due to the interruption of Klotho, and not a result of the transgene. Further confirmation of this Klotho phenotype was obtained upon finding that mouse lifespan is extended 20-30% when Klotho is overexpressed [57].

The *Klotho* gene encodes a transmembrane protein of 1014 amino acids in mice (1012 in humans) that shares high sequence similarity with family 1 glycosidases. The intracellular domain is merely 11 amino acids in length; the transmembrane is 21 amino acids; and the remainder is extracellular (Figure 3.1). There are two internal repeat sequences in the extracellular domain, KL1 and KL2, which are linked by 14 amino acids. Membrane-localized Klotho can be cleaved to release a Klotho fragment, containing KL1 and KL2. This cleavage is mediated by proteases of the A desintegrin and metalloproteinase family, ADAM10 and ADAM17, and the cleavage is stimulated by insulin [58].

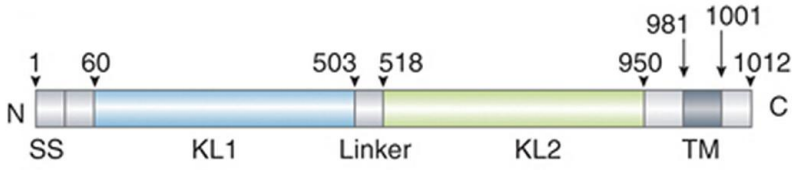

Figure 3.1. Structure of the human KLOTHO protein. The intracellular carboxy-terminal domain of KLOTHO contains 11 amino acids, the transmembrane domain (TM) is 20 amino acids. The amino-terminal extracellular domain of Klotho is comprised of a signal sequence (SS) and two internal repeats, KL1 and KL2, which share sequence similarilty with family 1 glycosidases. Figure is taken from [59]

Klotho was known to modify N-glycans of the renal epithelial Ca^{2+} channel TrpV5 and thereby increase cell-surface abundance of the channel. However, only recent reports have demonstrated that Klotho alters N-glycan branches of TrpV5 by using its sialidase activity. By removing terminal sialic acids of the N-glycan branch the underlying galactose-N-acetylglucosamine (LacNAc) disaccharides are exposed. LacNAc disaccharides are ligands for galactose-binding lectin, Galectin-1 (Lgals1). Binding of exposed LacNAc to Galectin-1 stabilizes TrpV5 at the membrane, and endocytosis is

reduced. Furthermore, only α2.6-linked sialic acids, but not α2.3-linked sialic acids, can be removed by Klotho. This was demonstrated when Klotho was rendered unable to affect cell surface retention of TrpV5 by knockdown the β-galactoside α2.6-sialyltransferase (ST6Gal-1). Furthermore, another model was used; a cell line that did not express St6Gal-1 endogenously, where Klotho was unable to affect TrpV5 cell surface retention. When St6Gal-1 was transfected into this cell line, Klotho became able to affect TrpV5 membrane localization. This demonstrated that Klotho was able to specifically remove α2.6-linked sialic acids of TrpV5 glycan modifications to affect its retention at the membrane (Figure 3.2) [60].

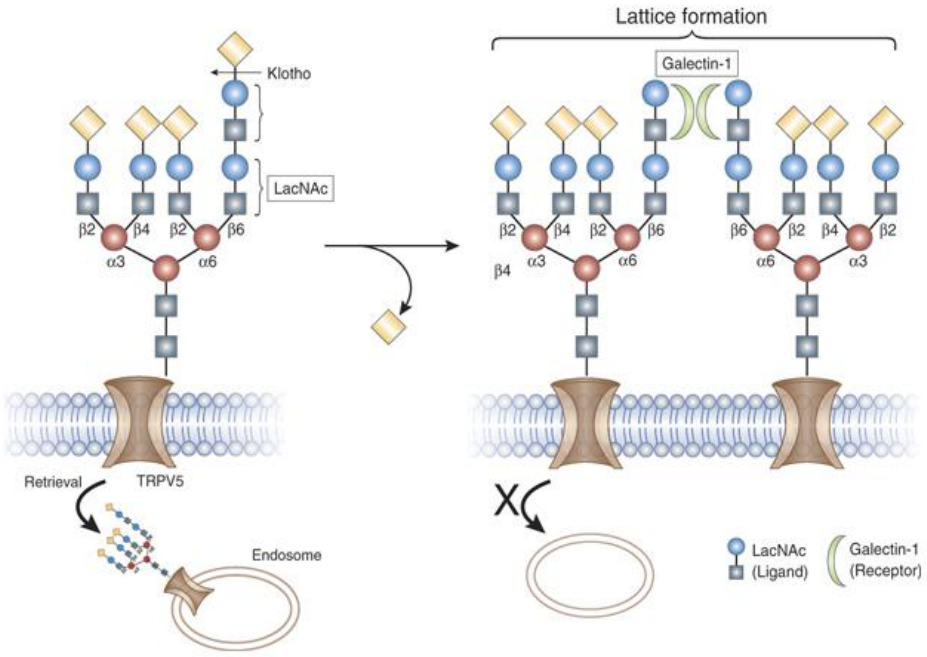

Figure 3.2. Secreted Klotho increases TrpV5 half-life at the plasma membrane by cleaving of terminal sialic acids from the N-glycan modification of TrpV5. LacNAc (N-acetyllactosamine) is a ligand for Galectin-1. If terminal α2,6-linked sialic acids are present LacNAc is unable to bind to galectin-1. Removal of sialic acids from the N-glycan of TRPV5 channel by secreted Klotho allows LacNAc binding to galectin-1. This prevents endocytosis of the channel. Sialic acid (yellow diamond), Galactose (blue ball), Mannose (red ball) and N-Acetylglucosamine (blue square). Figure is taken from [59]

Many other proteins are affected by their N-glycan modifications, one such example is Glucose transporter 2 (GLUT-2). GLUT-2 is regulated in a similar manner to TrpV5 with regards to the importance of its N-glycosylation on membrane retention. Mice lacking Mgat4a, which is a glycosyltransferase that synthesizes a β4 *N*-acetylglucosamine linkage on α3-mannose (see figure 3.2), do not exhibit membrane-localized GLUT-2 in islet beta cells, because this protein does not have fully developed glycan branching [61]. GLUT-2 is an important component of the beta cell insulin secretion machinery, as its low-affinity, high-capacity allows for rapid extracellular/intracellular equilibration of glucose to impact insulin secretion. Thus *Mgat4a*$^{-/-}$ islets exhibit diminished glucose-stimulated insulin secretion. It should be noted that unlike Klotho, which works from the outside of the cell to modify the terminal sialic acid residues of N-glycan branches, Mgat4a functions intracellularly, in the golgi, to generate the N-glycan branch.

In addition to the enzymatic activity associated with cleaved Klotho fragments, membrane-bound Klotho also functions as a co-receptor with Fibroblast Growth Factor Receptor 1 (FGFR1) to facilitate fibroblast growth factor 23 (FGF23) signaling. Prior to the discovery of FGF23 and Klotho, it was thought that Vitamin D and parathyroid hormone (PTH) were the sole hormonal regulators of serum phosphate homeostasis. It is now recognized that FGF23 is a bone-derived phosphaturic hormone that participates in a negative feedback loop with Klotho and Vitamin D (Figure 3.3). FGF23 is upregulated by 1,25-dihydroxyvitamin D (Vit D) in bone, then it enters the bloodstream and signals to kidney by binding to the FGFR1/Klotho co-receptor. This turns on a signaling pathway that leads to inhibition of *cyp27b1* transcription and enhancement of *cyp24a1*

transcription. Cyp27b1 is a kidney enzyme responsible for generating the active 1,25-dihydroxyvitamin D, which is a ligand for the Vitamin D Receptor (VDR), and Cyp24a1 is a kidney enzyme that is responsible for inactivating 1,25-dihydroxyvitamin D by 24-hydroxylation. Therefore, FGF23 acts in a negative feedback loop to reduce serum levels of 1,25-dihydroxyvitamin D by enhancing inactivation and decreasing production of the active 1,25-dihydroxyvitamin D (VitD).

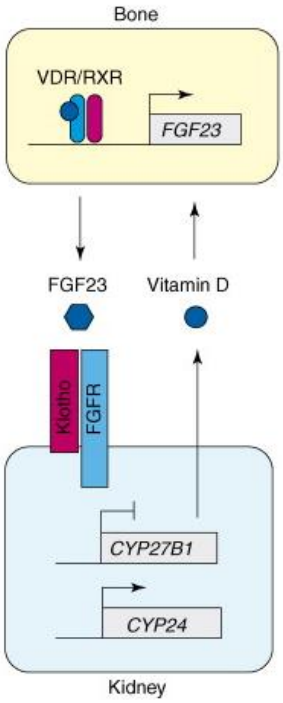

Figure 3.3. Vitamin D, Klotho and FGF23 participate in a negative feedback loop. VitD controls transcription of FGF23 in bone by binding to VDR. The VDR/RXR heterodimer turns on transcription of FGF23 that is then secreted into the bloodstream. FGF23 binds to a Klotho/FGFR1 co-receptor in kidney and activates a signal transduction pathway that eventually inhibits transcription of *cyp27b1* and increases transcription of *cyp24a1*. This reduces VitD levels and therefore expression of FGF23.
Figure taken from http://www.landesbioscience.com/curie/images/chapters/Kuro-o3color.jpg

This negative feedback loop is an important component in serum phosphate regulation. When serum phosphate levels increase; FGF23 reduces VitD levels and thus

blocks the VitD-dependent enhancement of intestinal phosphate uptake. In addition to regulating transcription of Vitamin D-metabolizing enzymes FGF23/Klotho signaling also reduces transcription of the sodium-dependent phosphate transporters, Npt2a and Npt2c, which are responsible for phosphate retention in the kidneys. This increases phosphate wasting by increasing urinary phosphate excretion and lowers serum phosphate levels (Figure 3.4).

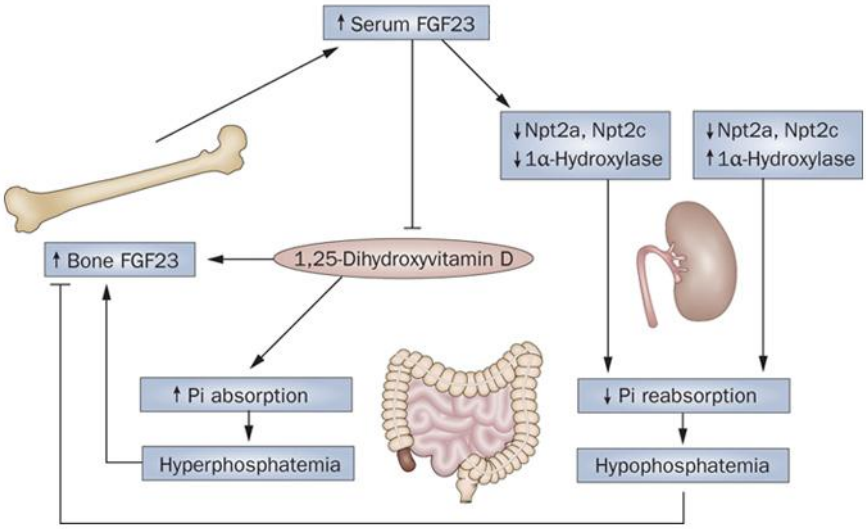

Figure 3.4. The role of FGF23 and VitD in phosphate homeostasis. VitD (1,25-dihydroxy vitamin D) increases phosphate absorption in the intestine. Both elevated phosphate and VitD turn on transcription of FGF23. Serum FGF23 inhibits production of active VitD and lowers expression of the sodium phosphate transporters Npt2a and Npt2c in kidney causing reduced phosphate uptake and elevated urinary phosphate excretion. Figure is taken from [62]

The majority of the aging-related phenotypes of *Klotho*$^{-/-}$ mice can be attributed to hyperphosphatemia, and "rescue" can be achieved by feeding these animals a low-phosphate diet. However, these mice also exhibit a metabolic phenotype as *Klotho*$^{-/-}$ mice are very insulin sensitive, have reduced pancreatic insulin and have low circulating

insulin and glucose levels [56, 63, 64]. Furthermore, *Klotho*-null mice have increased expression of a key gluconeogenesis gene in liver, phosphoenolpyruvate carboxylase (PEPCK) [64]. Reciprocally, *Klotho* transgenic mice are insulin-resistant and have elevated plasma insulin [57]. In light of the metabolic phenotypes of mice with altered Klotho expression, because the original report of Klotho [56] contained data indicating that Klotho was expressed in pancreas; and because Klotho appeared in microarrays we performed on VitD-treated islets, we performed the following studies to elucidate the role(s) of Klotho in the endocrine pancreas.

3.3 Materials and methods

Materials

1,25-dihydroxyvitamin D_3 (>99.0 % by HPLC) was purchased from Sigma-Aldrich, and was resuspended in tissue-culture grade DMSO. This VDR ligand is referred to as "VitD" hereafter in this manuscript. Recombinant FGF23 protein and recombinant Klotho was kindly provided by Makoto Kuro-o (UT Southwestern medical center). The fluorescent glucose analog 2-NBDG (2-(*N*-(7-nitrobenz-2-oxa-1,3-diazol-4-yl)amino)-2-deoxyglucose) was obtained from Invitrogen (CAT#N13195). Collagenase P (CAT#11213857001) for islet isolation was obtained from Roche. Collagen I and Poly-L-Lysine were purchased from BD Bioscience (CAT#354249) and Sigma-Aldrich (CAT#P7890), respectively. Oligonucleotides were obtained from Integrated DNA Technologies. Real-time PCR reagents were purchased from Applied Biosystems.

Rat anti-Klotho antibody (KM2119) was kindly provided by Makoto Kuro-o (UT Southwestern Medical Center) and mouse monoclonal GTU-88 to gamma tubulin

(Abcam, CAT#ab11316) were used in conjunction with IRDye 800CW-modified IgG (LI-COR, anti-rat = CAT# 926-32219, anti-mouse = CAT#926-32210) for western analyses. Guinea pig anti-insulin polyclonal antibody (DakoCytomation, CAT#A0564), rabbit anti-glucagon polyclonal antibody (Millipore, CAT#AB932), and rabbit anti-GLUT-2 polyclonal antibody (Millipore, CAT# 07-1402) were used for immunohistochemistry, in conjunction with secondary antibodies TRITC-conjugated goat anti-Guinea pig (Jackson ImmunoResearch) and FITC-conjugated donkey anti-Rabbit (Jackson ImmunoResearch). Images were acquired on a Zeiss Axio Imager Z1 microscope with Apotome accessory using AxioCam MRm camera from Zeiss.

Animals

All tissues and islets were obtained from 3-5-month-old, A129/SvJ mice. Mice were maintained in a temperature-controlled room (23 ± 1 C) with 12-h light (0700 h–1900 h), 12-h dark cycle and *ad libitum* access to water, a standard rodent diet (Harlan Teklad Diet 2016) or a rodent diet with only 0.2% phosphorus (Harlan #TD09073), and housed with sanitized wood-chip bedding (Sani-Chips, P.J. Murphy Forest Products, Montville, NJ). Tissues were harvested and islets were isolated in the morning with mice in the fed state. All experiments were performed with the approval of the Institutional Animal Care and Use Committee of the University of Texas Southwestern Medical Center, which assures that all animal use adheres to federal regulations as published in the Animal Welfare Act, the Guide for the Care and Use of Laboratory Animals (Guide),

the Public Health Service Policy, and the US Government Principles Regarding the Care and Use of Animals (http://www.utsouthwestern.edu/utsw/cda/dept41600/files/54634.html).

Islet isolation

The islet isolation method used has been described before [1]. Briefly, the mouse pancreas was perfused and digested with Collagenase P (Roche, Indianapolis, IN). Islets were then isolated using Ficoll gradient centrifugation and hand-selection under a stereomicroscope for transfer to RPMI 1640 medium (11.1 mM glucose) supplemented with 10% (vol/vol) heat-inactivated fetal bovine serum (FBS), 100 IU/ml penicillin, and 100 μg/ml streptomycin (Invitrogen, Carlsbad, CA). Islets were allowed to recover overnight (°, 5% CO_2). For tissue mRNA distribution studies, RNA was isolated from islets on day 2. For all other experiments VitD was added in the afternoon of day 2 and 16 hours later, islets were used for RNA isolation or functional assays.

Plasmids

The expression plasmids pCMX-mouseVDR and pCMX-mouseRXRα, and the pCMX-β-galactosidase plasmid (used to control for transfection efficiency) were obtained from David Mangelsdorf (UT Southwestern Medical Center). Putative Vitamin D response elements (VDRE) within novel VDR target genes were identified using the algorithm, NHR-scan [40]. Oligonucleotides containing these putative VDRE sites, as well as the positive control VDRE of the mouse Cyp24a1 promoter, were annealed and subcloned into the HindIII site upstream of the thymidine kinase promoter of the

luciferase plasmid, pTK-LUC [41]. Plasmid construction was confirmed by DNA sequencing, and plasmids containing three copies each of the respective VDRE were chosen for use in transfection experiments. Oligonucleotide sequences are available in Appendix B.

Cell culture and transfections

All cell lines were kept at 37C and 5% CO2. Culture of Min6, βTC6 and αTC1 cell lines have been described before [1]. HEK-293 cells were seeded into a 96-well plate and allowed to reach ~80% confluence. Cells in each well were transfected with 40 ng pCMX-VDR, 20 ng pCMX-RXR, 15 ng pCMX-β-Gal, and 75 ng luciferase reporter plasmid, using Lipofectamine 2000 (Invitrogen). 5-8 hours later, vehicle (DMSO) or 20 nM VitD was added at a final volume of 0.1%. 24 h after addition of ligand, cells were harvested, lysed, and analyzed for luciferase (FLUOstar OPTIMA, BMG Labtech) and β-galactosidase (PowerWave XS, BioTek) activity. Results are expressed as relative luciferase units (RLU), following correction for transfection efficiency using β-gal activity.

Mouse islet glucose stimulated insulin secretion

Islets were preincubated in DMSO as a control or 20 nM VitD for 16 hours in 11 mM glucose medium unless otherwise stated. Subsequently islets were conditioned for 1 hour at 37^{o}C in secretion assay buffer (SAB), pH 7.4, containing 114 mM NaCl, 4.7 mMKCl, 1.2 mM KH2PO4, 1.16 mM MgSO4, 2.5 mM CaCl2, 25.5 mM NaHCO3, 20 mM HEPES, 0.2% BSA and 0 mM glucose, and subsequently incubated for 60 min in

SAB containing either 5 or 17.5 mM glucose. Insulin released into the media during the 1 hour islets were incubated in low or high glucose was determined by radioimmunoassay (Millipore).

qPCR profiling

RNA was isolated from tissue samples, cultured islets or cell lines using RNA STAT-60 (Tel-Test Inc., Friendswood, TX), and 2 μg of total RNA was treated with ribonuclease-free deoxyribonuclease (Roche), and then reverse transcribed with random hexamers using SuperScript II (Invitrogen), as previously described in detail [38]. qPCR was performed using an Applied Biosystem Prism 7900HT sequence detection system (Applied Biosystems, Foster City, CA) and SYBR-green chemistry [38, 39]. Gene-specific primers were designed using D-LUX primer design software from www.invitrogen.com and validated by analysis of template titration and dissociation curves [1]. Primer sequences are available upon request. qPCRs (10 μl) contained 25 ng of reverse-transcribed RNA, each primer (150 nM), and 5 μl of 2X SYBR Green PCR master mix (Applied Biosystems). Multiple housekeeping genes were evaluated in each assay to ensure that their RNA levels were invariant under the experimental conditions of each study. Results of qPCR were evaluated by the comparative Ct method [user bulletin no. 2, PerkinElmer Life Sciences [38]] using hypoxanthine-guanine phosphoribosyl transferase (HPRT), acidic ribosomal phosphoprotein P0 (36B4) and cyclophilin as the invariant control gene.

Western analyses

Tissues and islets (300 for each group) were lysed in ice-cold cell lysis buffer (Cell Signaling) containing 1 mM PMSF and centrifuged at 10,000 x g for 10 min at 4 °C. Protein concentrations were measured using the BCA protein assay kit (Pierce).

For Klotho protein detection, proteins were size-fractionated on an 8 % denaturing SDS-polyacrylamide gel and transferred to PVDF membrane. Blots were incubated with the anti-Klotho antibody (KM2119, 1:4000) and anti-γ-Tubulin (GTU-88, 1:5000), followed by species-specific IRDye 800 CW secondary antibody (LI-COR, 1:10,000) to enable quantitative detection of Klotho using a LI-COR Odyssey Detector.

For ERK1/2 signal transduction, proteins obtained from whole-cell lysates of treated islets were size-fractionated on 10% SDS-polyacrylamide gels, transferred to PVDF membrane, and incubated with mouse anti-Phospho-Erk1/2 (Cell Signaling, #9106, 1:1000) or Rabbit anti-Erk1/2 (Cell Signaling, #9102, 1:1000), then the membranes were incubated in anti-mouse and anti-rabbit HRP-conjugated secondary antibody and the signal was detected by using Supersignal West Pico Chemiluminescent HRP substrate from Pierce (CAT#34080) and blot exposure to a Blue lite autorad film from ISC BioExpress (CAT#F-9024-8X10).

Intraperitoneal glucose tolerance test (IPGTT)

After a 16-h fast, mice were injected intraperitoneally with glucose (2 g/kg body wt). Blood glucose was measured using AlphaTrak glucose monitoring system and test strips (Abbott Laboratories. Illinois, U.S.A.) at: 0, 5, 18, 30, 60, 120 and 205 min. Plasma insulin was measured from plasma samples taken at 0 min using an enzyme-

linked immunosorbent assay kit (ALPCO Diagnostics, Salem, NH). At the end of GTT mice were analyzed for body composition by quantitative NMR [65], thereafter tissues were harvested and blood was collected for determination of calcium and phosphate levels.

Plasma calcium and phosphate analysis

Following the IPGTT, terminal blood was collected via the inferior vena cava, using a heparin-coated syringe and needle. Plasma samples were sent to the mouse metabolic phenotyping core at UT Southwestern Medical Center for plasma calcium and phosphate determination using a Vitros 250 chemistry analyzer.

In Situ Hybridization

The in situ hybridization was performed as previously described [66] but with minor modifications. Prior to hybridization, 30 μm pancreatic sections were mounted onto SuperFrost Plus slides (Fisher Scientific, Pittsburgh, PA, USA). The plasmid used for generation of sense and antisense ^{35}S-labeled Klotho riboprobes was kindly provided by Makoto Kuro-o. The probes were subjected to in vitro transcription using ^{35}S-uridine triphosphate (UTP) and T7 polymerases according to the manufacturer protocols (Promega, Madison, WI, USA). The ^{35}S-labeled probe was diluted (10^6 dpm/mL) in hybridization solution. The hybridization solution (110 μL) and a coverslip were applied to each slide, and sections were incubated overnight at 56 °C. On the following day, the coverslips were removed, and the slides were rinsed and treated with RNase A (Roche Diagnostics, Mannheim, Germany). They were then rinsed in decreasing concentrations

of SSC, dehydrated and placed in X-ray film cassettes with BMR-2 film (Kodak, Rochester, NY, USA) for 5 days. Subsequently, slides were dipped in NTB2 photographic emulsion (Kodak), dried and stored with desiccant in foil-wrapped slide boxes at 4 °C for 20 days. Slides were developed with D-19 developer (Kodak), counterstained with hematoxilin and eosin staining (H&E), dehydrated, cleared in xylene and coverslipped. H&E images were acquired on a Zeiss Axio Imager Z1 microscope with Apotome accessory using AxioCam MRm camera from Zeiss. Film images were acquired on a Zeiss Stemi 2000-C microscope using AxioCam HRc camera from Zeiss.

Glucose uptake assay

Islets were isolated from 2-3 month-old wildtype or *Klotho*$^{-/-}$ mice and allowed to recover over night (37°C, 5% CO_2). A 96-well plate (Greiner 655090) was coated with Collagen I and Poly-L-Lysine by adding 10µg/mL Collagen I and 0.1 mg/mL Poly-L-Lysine to each well and allowed to incubate at 37°C for 1 hour. The solution was removed, washed twice with PBS and allowed to air dry for 1-3 hours. Islets are dispersed by incubating them for 20 minutes in Accutase (Innovative Cell Technologies, AT104) at ambient temperature. Accutase solution is removed by aspiration after a short spin and dispersed islet cells are washed once with islet culture media. Dispersed islet cells are seeded at a 40,000 cells/well density and plate the is spun down at 30xG. Vitamin D or vehicle (DMSO) is added in the afternoon for a final concentration of 20 nM 1,25-Vitamin D3. After 16 hour incubation in 20 nM 1,25-Vitamin D_3 cells are washed with secretion assay buffer (SAB), pH 7.4, containing 114 mM NaCl, 4.7 mMKCl, 1.2 mM KH2PO4, 1.16 mM MgSO4, 2.5 mM CaCl2, 25.5 mM NaHCO3, 20

mM HEPES, 0.2% BSA and 0 mM glucose, and then incubated in 500µM 2-NBDG for 2 minutes. At the end of 2 minutes plate is moved to an ice-bucket and the 2-NBDG is washed off with ice-cold SAB buffer. 2-NBDG uptake imaging is started within 15 minutes using the BD pathway 855 Bioimaging system with FITC filter, 10x objective and 4x4 montages. After imaging cells are post-fixed with 4% Formaldehyde for 15 minutes, blocked for 1 hour at RT with PBS containing 5% Goat serum and 5% Donkey serum and then subjected to immunostaining using a guinea pig anti-Insulin primary antibody (DakoCytomation, CAT#A0564)) and anti-guinea pig TRITC secondary antibody (Jackson, CAT#706026148). Single cells that stained positive for insulin were selected for quantification of intracellular 2-NBDG signal.

Immunohistochemistry

Mice were anesthetized and perfused with 4% paraformaldehyde solution. Pancreas was excised and placed in a 4% paraformaldehyde solution at 4°C over night. Then pancreata were washed using PBS and an ethanol gradient. Pancreas was imbedded in paraffin and sent to the UT Southwestern histology core where 5 µm sections were taken at 95 µm interval and placed on glass slides. Sections were deparaffinized in Xyline, washed with ethanol and then hydrated in PBS. Blocking was done using PBS with 0.2% triton X-100 and 5% normal goat serum and 5% normal donkey serum. Immunohistochemistry using anti-GLUT-2 (Millipore, #07-1402, 1:100), anti-insulin (DakoCytomation, #A0564, 1:300), and anti-glucagon (Millipore, #AB932, 1:300) was done in blocking solution over night at 4C in a hydration chamber. Secondary antibodies, TRITC-conjugated goat anti-Guinea pig (Jackson ImmunoResearch, 1:300) and FITC-

conjugated donkey anti-Rabbit (Jackson ImmunoResearch, 1:300), were incubated for 1 hour at ambient temperature. Images were acquired on a Zeiss Axio Imager Z1 microscope with Apotome accessory using AxioCam MRm camera from Zeiss.

Statistics

All results are expressed as the means ± SEM for each treatment group. Two-tailed Student's *t*-tests were performed to compare differences between two groups. All statistical tests were performed using GraphPad Prism software (GraphPad, San Diego, CA). Significance was established at $P < 0.05$ and is represented with an asterisk (*).

3.4 Results

Klotho is expressed in endocrine pancreas.

The first step taken, to examine if Klotho has a physiological role in endocrine pancreas, was to perform a tissue distribution analysis of *Klotho* mRNA (Figure 3.5). As it had been reported that kidney and brain express Klotho [56] we used these tissues as positive controls. Of all tissues tested; only kidney, brain, islet and the two mouse beta cell lines, Min6 and βTC6 expressed Klotho. It is of note that the mouse alpha cell line αTC1 did not contain Klotho transcripts, suggesting that Klotho is solely expressed in beta cells of the islet. As we were interested in the metabolic phenotype of the *Klotho*$^{-/-}$ mice we additionally tested an array of tissues involved in metabolic homeostasis. Liver, intestine, adrenal and brown adipose tissue did not show any trace of Klotho mRNA.

However there was detectable, albeit very low quantities of Klotho mRNA present in skeletal muscle and white adipose tissue.

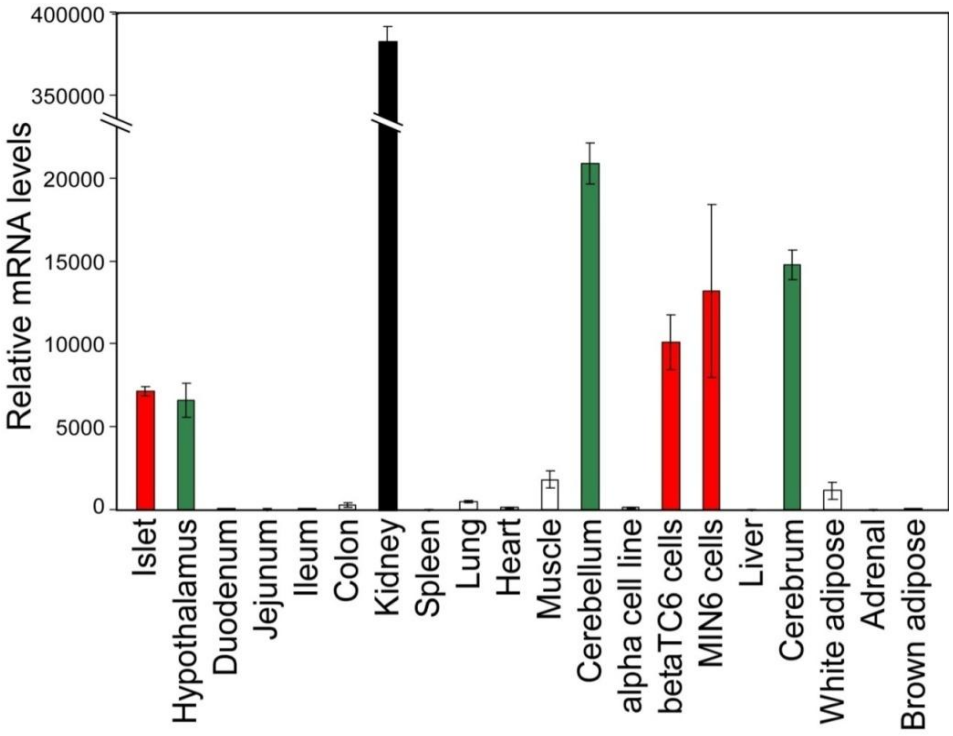

Figure 3.5. Tissue distribution of *Klotho* mRNA demonstrates that *Klotho* is expressed in mouse islets and two different β cell lines. Figure shows relative *Klotho* mRNA in an array of tissues. Kidney is labeled in black, islets and beta cell lines in red and brain region in green. All other tissues are represented in white. The alpha cell line used is alphaTC1. *Klotho* mRNA values are normalized against the housekeeping gene *cyclophilin*. All data are shown as the mean ± S.E. (n = 3).

It has been reported that *Klotho* transcripts are found in pancreas, so we perfomed *in situ* hybridization (ISH) to establish the distribution of Klotho in endocrine and/or exocrine compartments of this organ. As Figure 3.6 illustrates, *Klotho* transcripts

are only present in islets with no detectable signal in exocrine pancreas. The resolution of this teqhnique is inadequate to identify which cells of the islets are positive/negative for ISH signal. However, the central beta cell mass is clearly labeled confirming the results of our qPCR analysis.

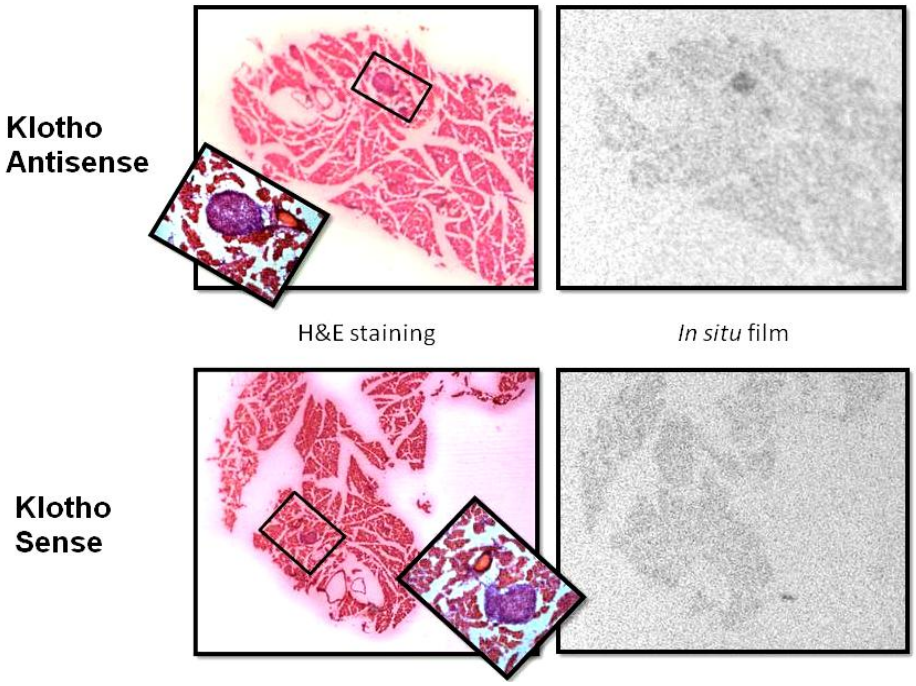

Figure 3.6. Klotho transcripts are exclusively present in endocrine pancreas. Top left figure shows H&E staining of a pancreatic section that was labeled with a Klotho ^{35}S-ISH antisense probe, one islet is present in the section (see insert and box). Top right figure shows the film exposed to the slide on the left, showing a Klotho signal at the location of the islet. Bottom left figure shows a H&E staining of a pancreatic section labeled with a Klotho ^{35}S-ISH sense probe, one islet is present in the section (see insert and box). Bottom right figure shows the film exposed to the slide on the left, showing no signal in endo- or exocrine pancreas.

The Vitamin D Receptor controls Klotho expression in islets and beta cells.

Vitamin D has been reported to upregulate Klotho in kidney [67], therefore we sought to identify if the same was true in islets and beta cells. Isolated islets from

wildtype and *Vdr*$^{-/-}$ mice were cultured in the presence of 20 nM VitD or vehicle for 16 hours and the relative quantity of Klotho mRNA was assessed using real time PCR. As seen in Figure 3.7a Klotho mRNA levels increased 5-fold when islets are treated with VitD. This upregulation is dependent on VDR as no upregulation is present in *Vdr*$^{-/-}$ islets. Next, a time-course of Klotho expression was performed in the βTC6 cell line (Figure 3.7b). VitD-dependent upregulation of Klotho is evident as early as 4 hours after ligand addition (1.5-fold), which becomes significant at 7.5 hours (2-fold), and peaks at 16 hours (3.2-fold).

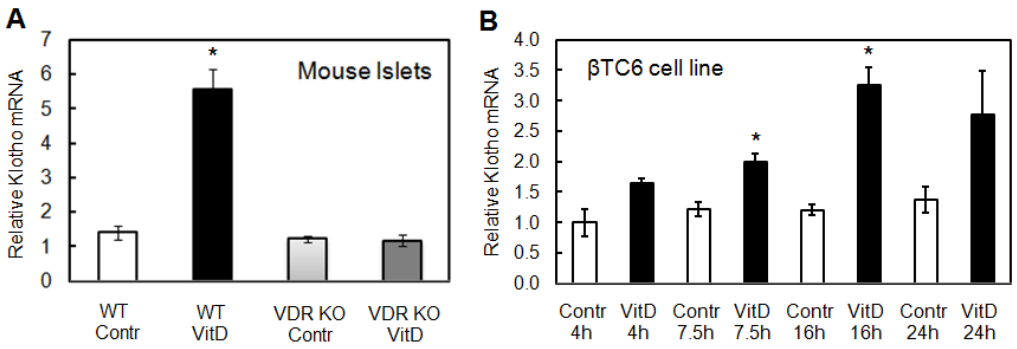

Figure 3.7. Klotho mRNA levels are increased by VitD in a VDR-dependent manner in mouse islets. A. qPCR analysis of Klotho mRNA in isolated islets from wildtype and *Vdr*$^{-/-}$ mice treated with 20 nM VitD or vehicle for 16 hours. Wildtype vehicle (white), wildtype VitD (black), *Vdr*$^{-/-}$ vehicle (light grey) and *Vdr*$^{-/-}$ VitD (dark grey). B. qPCR analysis of Klotho mRNA levels in the beta cell line βTC6 treated with 20 nM VitD (black) or vehicle (white) for 4, 7.5, 16 and 24 hours.

To confirm that the upregulation by VitD translates into increased protein abundance of Klotho, a western blot was performed. Islets isolated from wildtype and *Vdr*$^{-/-}$ mice were treated with 20 nM VitD or vehicle for 24 hours and then they were assayed for Klotho protein content using western blot (Figure 3.8). As positive- and

negative-control kidney lysates from wildtype and *Klotho*$^{-/-}$ mice were included in the western blot. The results show a 5-fold increase in Klotho protein content of wildtype islets treated with VitD and no change in *Vdr*$^{-/-}$ islets. Thsese results demonstrate that this increase is dependent on VDR transcriptional activity.

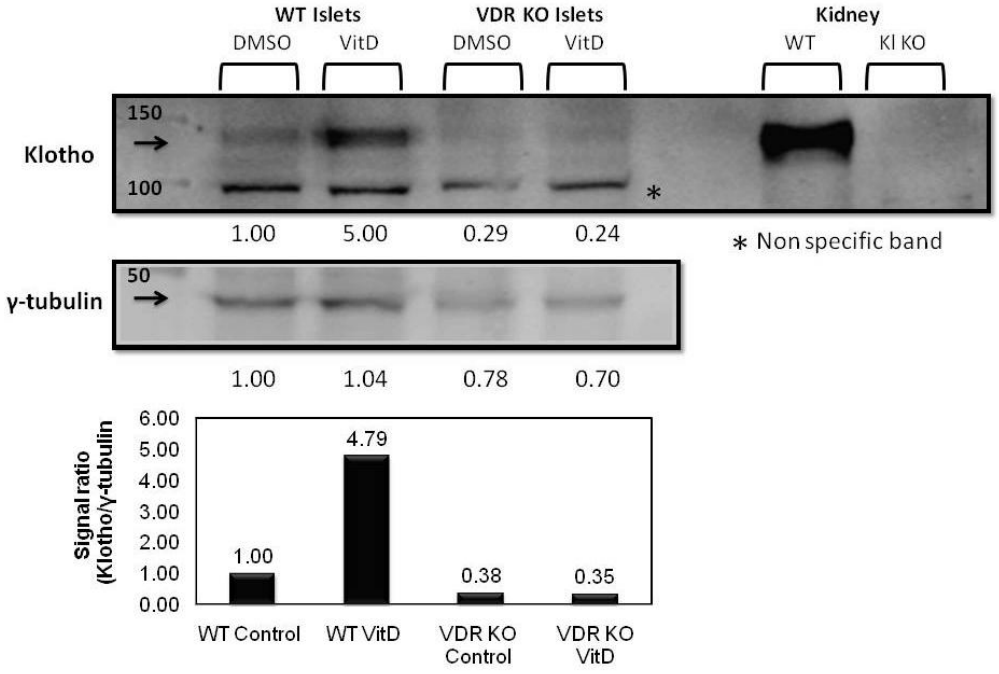

Figure 3.8 Klotho protein levels are increased by VitD in mouse islets. Isolated islets from wildtype (WT) and *Vdr*$^{-/-}$ (VDR KO) mice treated with 20 nM VitD or vehicle for 24 hours were assayed for Klotho protein by western analysis. Kidney lysates from wildtype and *Klotho*$^{-/-}$ mice were run on the same blot to provide positive and negative controls for the Klotho protein band (~130 kDa, arrow). Asterisk denotes a non-specific band. Bottom figure provides quantification of signal intensity of the Klotho bands in wildtype (WT) and *Vdr*$^{-/-}$(VDR KO) islets treated with VitD or vehicle. Signal intensity was normalized to the signal intensity of γ-tubulin using the Image J software (http://rsbweb.nih.gov/ij/).

As the upregulation of Klotho by VitD is present as early as 4 hours after ligand addition it is quite likely a direct target of VDR. Therefore an *in silico* scan of the 10 kb promoter and first intron was performed using the NHR-scan software [40]. Six putative VDREs were identified and cloned into a luciferase reporter plasmid, upstream of a

minimal Thymidine kinase promoter. Cell reporter assays were performed in HEK293 cells transfected with VDR expression plasmid, RXR expression plasmid, VDRE-Luciferase reporter plasmid and Beta-galactosidase expression plasmid. 6 hours after transfection, 100nM VitD or vehicle was added to the culture, cells were incubated for 16 hours and then luciferase and Beta-galactosidase activites were assessed in cell lysates. The results (Figure 3.9) show that the VDRE located -7335 base pairs from the transcriptional start site is nearly as competent of enhancer as the canonical VDRE (DR3 VDRE LUC). Two additional VDREs, of lesser strength (+941, +16427) are located in intron 1.

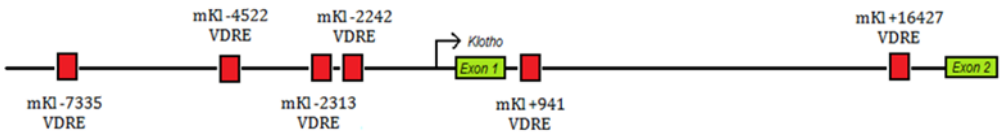

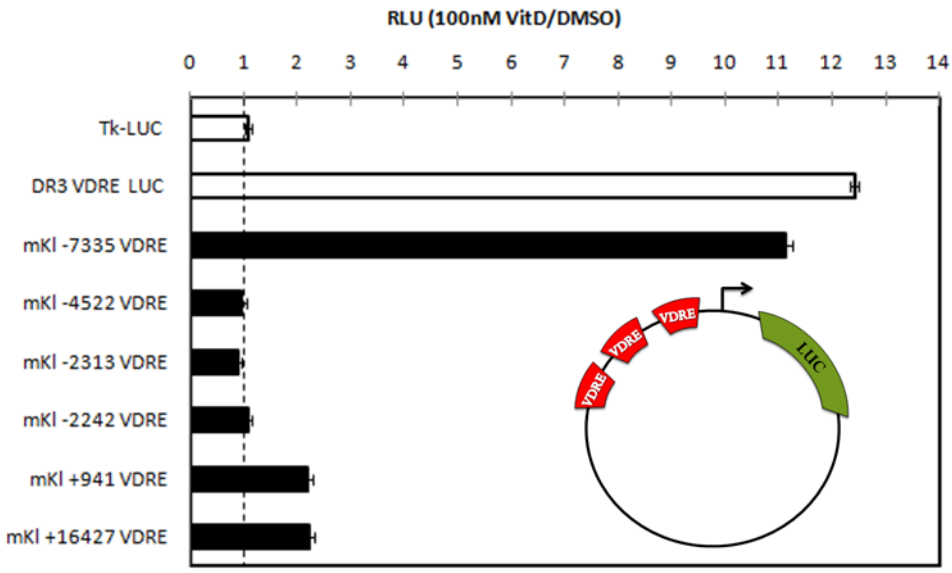

Figure 3.9 Luciferase reporter assay suggests that a potent VDRE is located in the mouse Klotho promoter. Top figure shows the location of VDREs discovered *in silico* relative to the transcriptional start site (arrow) and exon 1 and 2 (green). Bottom figure: Each luciferase reporter plasmid containes three copies of VDRE. After transfections cells were treated with 100nM VitD for 16 hours and then luciferase and beta-galactosidase (to correct for transfections efficiency) activity were assessed. Data are plotted as the Relative Luciferase Unit (RLU) of VitD to Veh treatment. Tk-LUC is a luciferase plasmid lacking VDREs, DR3 VDRE LUC is a luciferase plasmid with a canonical VDRE, the other luciferase plasmids contain VDREs found near the *Klotho* transcriptional start site.

The FGF23/Klotho/FGFR signaling pathway is present in islets

As mentioned above and exemplified with the tissue distribution in Figure 3.4, very few tissues express Klotho. Therefore, few tissues are capable of responding to FGF23 as Klotho is a coreceptor required for FGF23 signaling. Since Klotho and FGFR1 (data not shown) are expressed in islets we determined if islet FGF23 signaling could occur. Isolated wildtype mouse islets were treated with FGF23 for 20 minutes and then Erk1/2 phosphorylation was determined using western blot analysis. Erk1/2 phosphorylation has been demonstrated to be a part of the FGF23 initiated downstream

signaling pathway [68]. The results show a significant increase in Erk1/2 phosphorylation with FGF23 treatment (Figure 3.10a). When the βTC6 cell line was similarly tested for FGF23 signaling equivalent results were evident (Figure 3.10b).

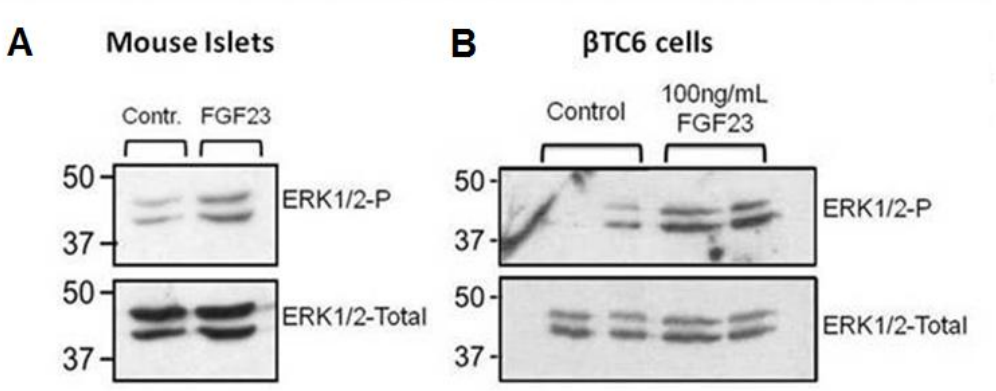

Figure 3.10. The FGF23/Klotho/FGFR1 signaling system is functional in mouse islets and the mouse insulinoma cell line βtc6. ERK1/2 phosphorylation is increased upon FGF23 treatment of isolated mouse islets (A) and βtc6 cells (B) indicating that the FGF23/Klotho/FGFR1 signaling pathway is present in islets. Islets were treated with 300 ng/mL of recombinant FGF23 for 20 minutes and βtc6 cells with 100 ng/mL FGF23 for 15 minutes.

Low-phosphate rescue-diet does not rescue the metabolic phenotype of Klotho$^{-/-}$ mice.

Klotho$^{-/-}$ mice have a shortened lifespan of merely 8 weeks, have severe calcification and only reach a bodyweight of 6-8 grams. However, if the mice are fed a rescue-diet containing low phosphate most of the phenotypes are alleviated [69]. From this we can conclude that most all phenotypes are secondary to the role of Klotho in phosphate homeostasis in the kidney. However, there have been no reports on the metabolic phenotypes of *Klotho*$^{-/-}$ mice when they are fed a rescue-diet. In order to identify what primary function Klotho has in islets, not secondary to the

hyperphosphatemia, mice were kept on a rescue-diet. First we assessed the metabolic phenotype of *Klotho*$^{-/-}$ mice and wildtype littermates, which were maintained on a rescue-diet containing 0.2% phosphate. 3 month old male mice were fasted over night and, fasting glucose and insulin was measured and an ip glucose tolerance test was performed (Figure 3.11). The results show that the *Klotho*$^{-/-}$ mice are still very glucose tolerant compared to their wildtype littermates despite keeping them on a rescue-diet. This suggests that, unlike other phenotypes, the glucose tolerant phenotype of *Klotho*$^{-/-}$ mice is not secondary to hyperphosphatemia. Using the rescue-diet; plasma calcium, bodyweight, lack of adipose tissue, hypoglycemia and hypoinsulinemia are corrected (Figure 3.11c,d,f,g,h). Plasma phosphate still tends to be slightly higher in *Klotho*$^{-/-}$ mice although it is not significant and not nearly as exaggerated as it is in *Klotho*$^{-/-}$ mice fed chow diet [56].

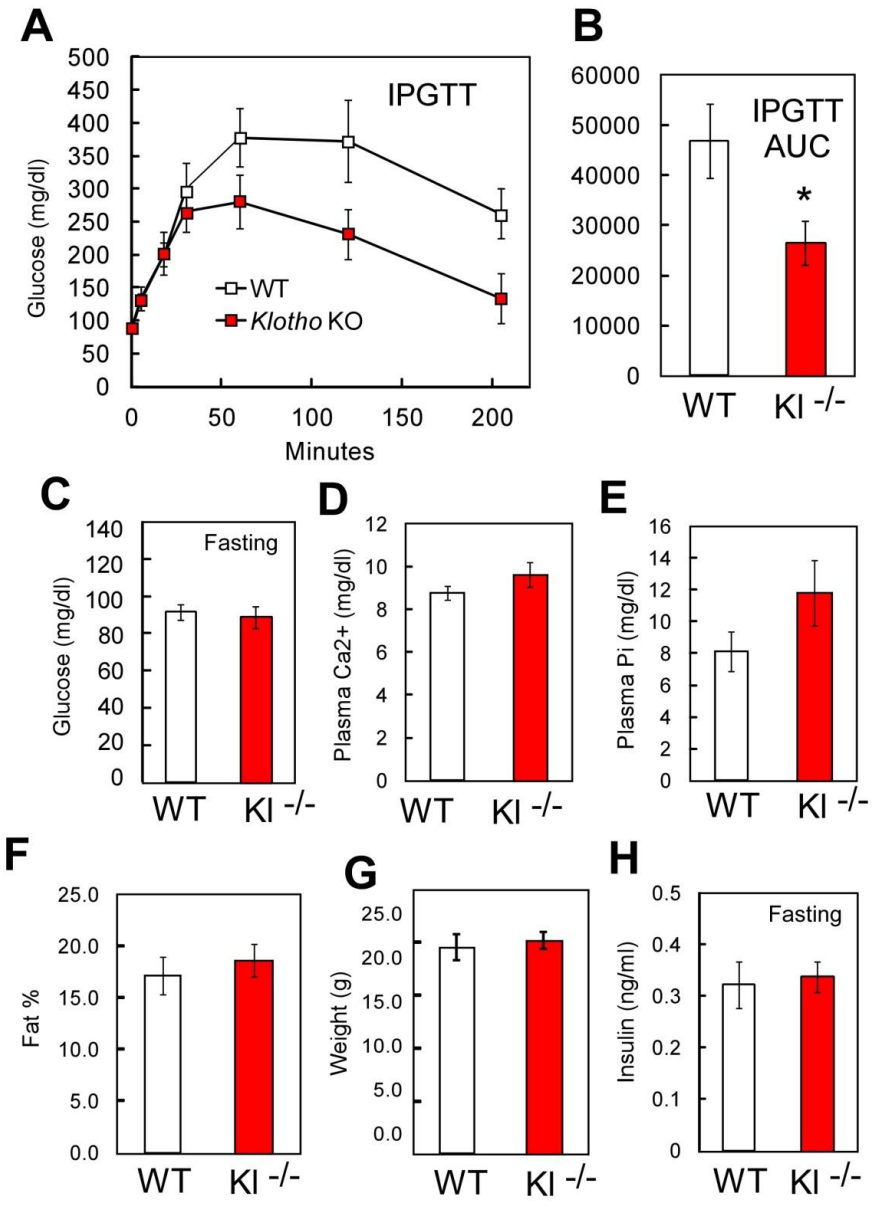

Figure 3.11. IP glucose tolerance test (IPGTT) on *Klotho*$^{-/-}$ and wildtype littermates suggests that the glucose tolerant phenotype is not secondary to hyperphosphatemia. A. IPGTT on wildtype (white squares) and *Klotho*$^{-/-}$ (red squares) 3 month old male mice maintained on a rescue-diet containing 0.2% phosphate. B. Area under the curve (AUC) for the IPGTT. C. Fasting glucose at the start of IPGTT. D. Plasma calcium after 3 hour recovery from IPGTT. E. Plasma phosphate after 3 hour recovery from IPGTT. F. %Fat mass measured with quantitative NMR. G. Bodyweight of mice used for IPGTT. H. Fasting insulin at the start of IPGTT. All data are shown as the mean ± S.E. Wildtype (n=5 white bar) and *Klotho*$^{-/-}$ (n=7 red bar). Asterisk denotes a significant difference between genotypes ($p \leq 0.05$).

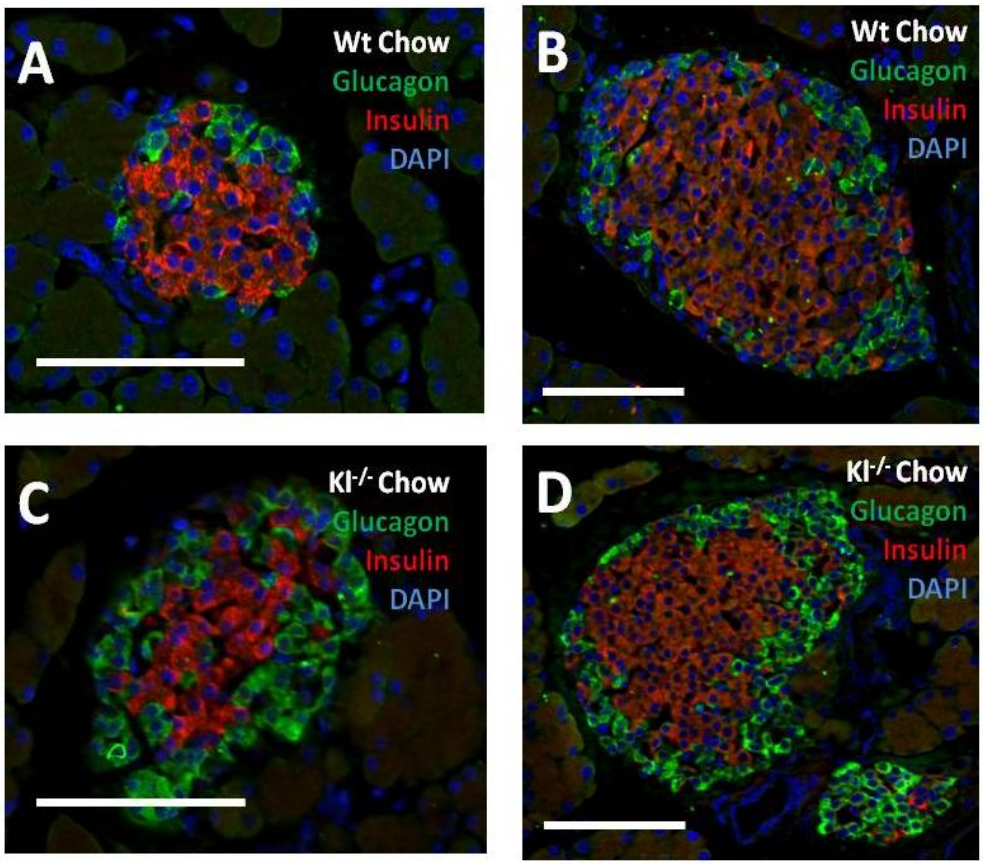

Figure 3.12. Islet structure comparison in wildtype and *Klotho*$^{-/-}$ pancreas shows a shift in alpha to beta cell ratio in *Klotho*$^{-/-}$ islets. A. Medium sized wildtype islet from a chow-fed mouse. B. Large wildtype islet from a chow-fed mouse. C. Medium sized *Klotho*$^{-/-}$ islet from a chow-fed mouse. D. Large *Klotho*$^{-/-}$ islet from a chow-fed mouse. All panels show pancreatic section from a 6 week old male mouse fed a standard rodent chow diet from weaning. Insulin is red, glucagon is green and DAPI is blue. Islets shown are a good representive of islets seen in mice from each group (n=4). White bar = 150 µm

When islet structure is examined by immunohistochemisty there is an evident increase in alpha cells in *Klotho*$^{-/-}$ islets on regular chow diet (Figure 3.12) and on a rescue-diet (Figure 3.13) compared to wildtype littermate islets. The difference is more obvious in small and medium sized islets (panels A and C), although larger islets also

show the same trend (B and D). Islet size and number is not different (data not shown) and therefore the increase in alpha cells causes a shift in the alpha/beta cell ratio.

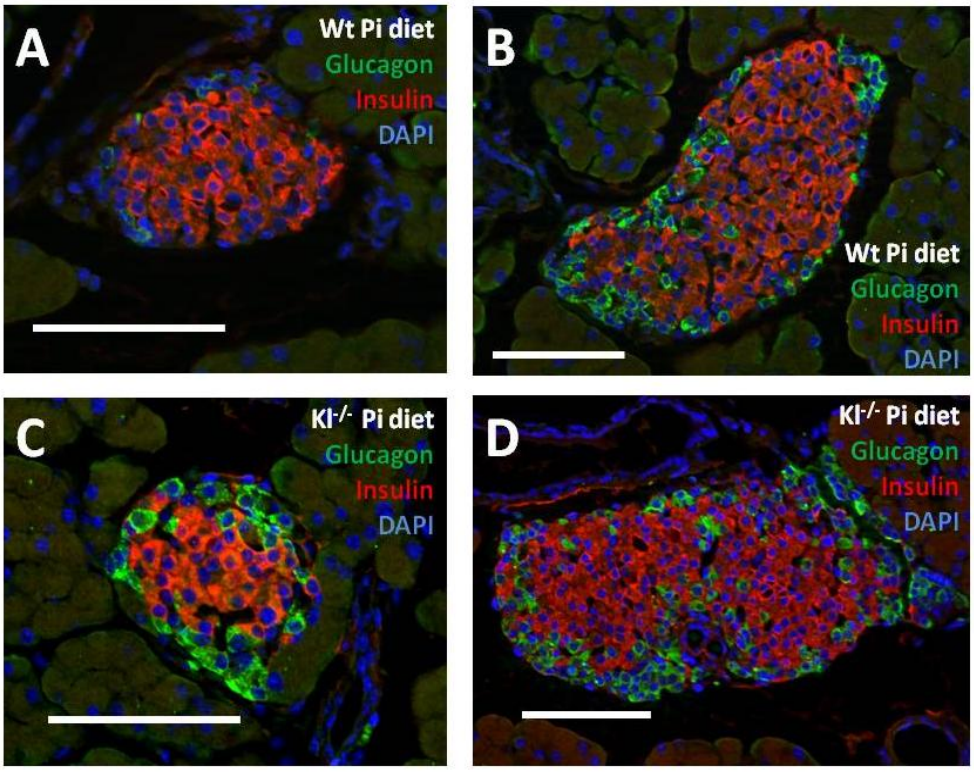

Figure 3.13. Islet structure comparison in wildtype and *Klotho*$^{-/-}$ pancreas shows a shift in alpha to beta cell ration in *Klotho*$^{-/-}$ islets. A. Medium sized wildtype islet from a rescue-diet fed mouse. B. Large wildtype islet from a rescue-diet -fed mouse. C. Medium sized *Klotho*$^{-/-}$ islet from a rescue-diet fed mouse. D. Large *Klotho*$^{-/-}$ islet from a rescue-diet fed mouse. All panels show pancreatic section from a 6 week old male mouse fed a low-phosphate rescue-diet from weaning. Insulin is red, glucagon is green and DAPI is blue. Islets shown are a good representive of islets seen in mice from each group (n=4). Low-phosphate rescue-diet (Pi diet). White bar = 150 µm

The results from the insulin and glucagon immunohistochemistry prompted us to look at fasting and fed glucagon in mice maintained on a rescue-diet. For measurement in the fed state, blood glucose measurement and blood samples for glucagon determination were taken early morning. In the fasted state mice were fasted for 16 hours overnight and

blood glucose measurement and blood samples for glucagon determination were taken early morning. The results in figure 3.14a show a significant increase in circulating plasma glucagon in the fasting state between genotypes. Additionally, there is a trend for elevated fed glucagon in the *Klotho*$^{-/-}$ mice but the results do not reach significance (p=0.07, n=4). Results show a clear impact of fasting blood glucose levels that is identical between genotypes (Figure 3.14b).

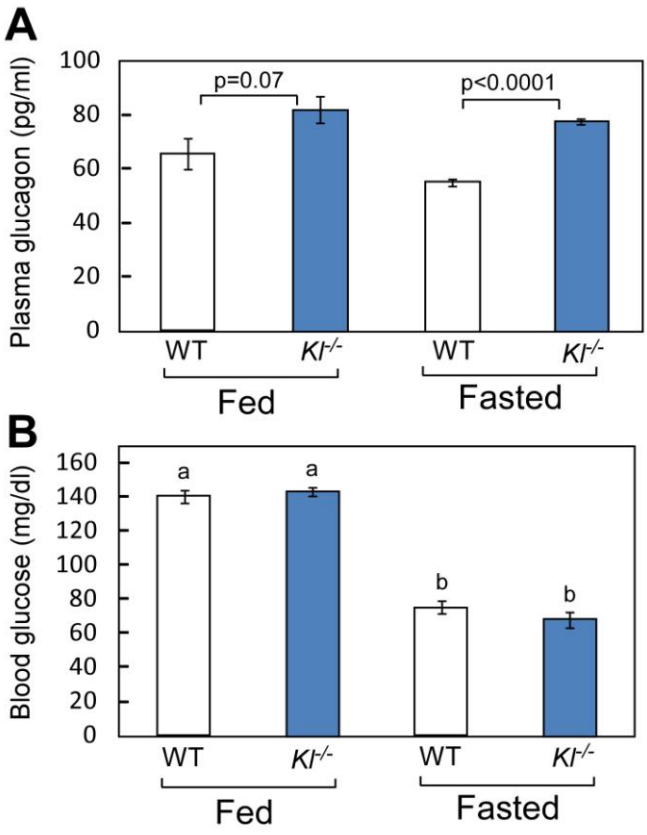

Figure 3.14. Fasting and fed glucagon is increased in *Klotho*$^{-/-}$ mice. A. Plasma glucagon measurements in wildtype (white bars) and *Klotho*$^{-/-}$ mice (blue bars) in the fed state (early morning) and after a 16 hour overnight fast. B. Blood glucose measurements in wildtype (white bars) and *Klotho*$^{-/-}$ mice (blue bars) in the fed state (early morning) and after a 16 hour overnight fast. All data are shown as the mean ± S.E. (n=4 for glucagon and n=8 for glucose). For glucagon determination two plasma samples were pooled to provide 4 samples from 8 mice.

The shift in the alpha to beta cell ratio that is observed in the *Klotho*$^{-/-}$ mice is similar to what has been described before in mice lacking glucose transporter 2 (GLUT-2) [70]. Additionally, GLUT-2 has an N-glycosylation that is identical to the one on TrpV5 and it has been shown to be very important for plama membrane localization of GLUT-2 [61]. Finally *GLUT-2*$^{-/-}$ mice have increased circulating glucagon [70], just as we saw an increase in circulating glucagon in the *Klotho*$^{-/-}$ mice (Figure 3.14). Therefore, GLUT-2 and insulin immunohistochemistry were performed on pancreatic sections from wildtype and *Klotho*$^{-/-}$ mice, fed either a chow diet or a low-phosphate rescue-diet. The results show a significant reduction of membrane-localized GLUT-2 in *Klotho*$^{-/-}$ beta cells. The same results are evident in *Klotho*$^{-/-}$ islets from mice on regular chow diet (Figure 3.15) or on a low-phosphate rescue-diet (Figure 3.16).

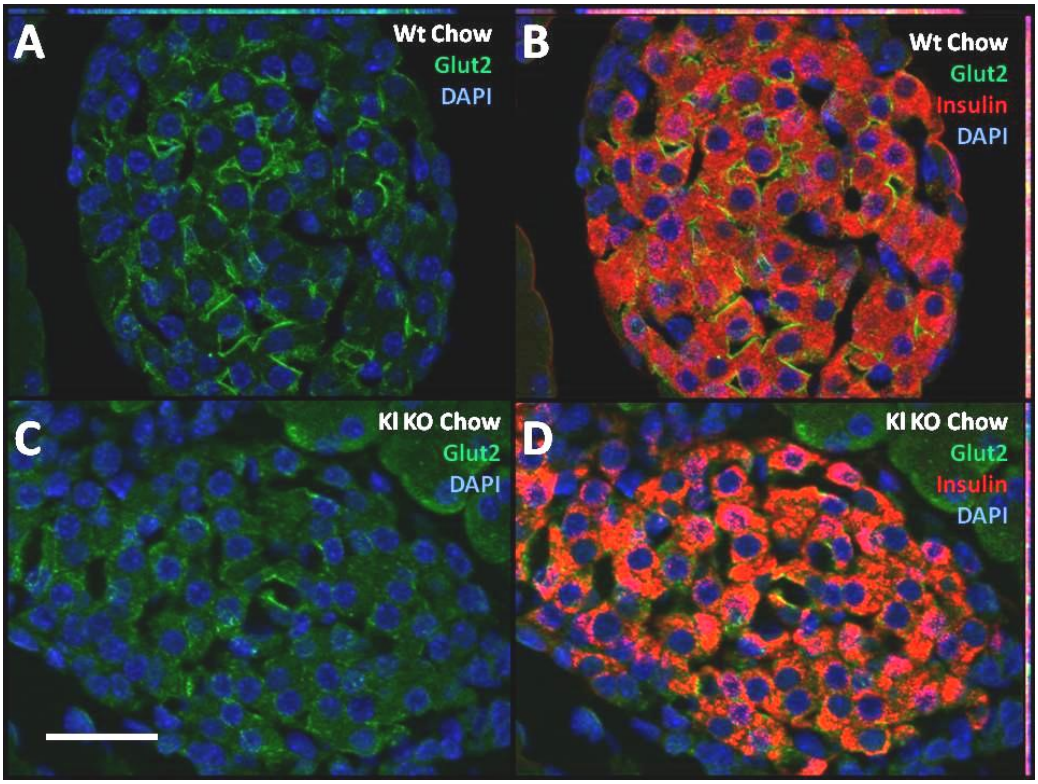

Figure 3.15 GLUT-2 membrane localization is significantly reduced in *Klotho*$^{-/-}$ islets from mice fed chow diet. A. Wildtype islet from a chow-fed mouse showing only GLUT-2 (green) and DAPI (blue) staining. B. Wildtype islet from a chow-fed mouse showing insulin (red), GLUT-2 (green) and DAPI (blue) staining. C. *Klotho*$^{-/-}$ islet from a chow-fed mouse showing only GLUT-2 (green) and DAPI (blue) staining. D. *Klotho*$^{-/-}$ islet from a chow-fed mouse showing insulin (red), GLUT-2 (green) and DAPI (blue) staining. White bar = 50 µm

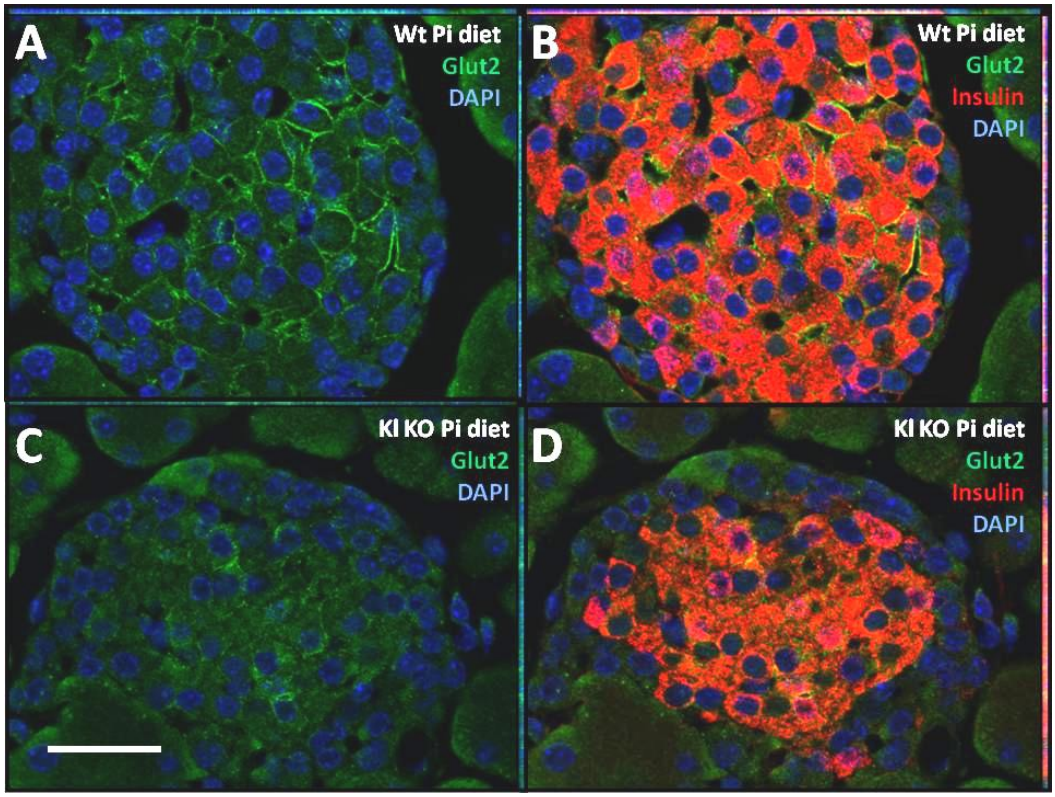

Figure 3.16. GLUT-2 membrane localization is significantly reduced in *Klotho*$^{-/-}$ islets from mice fed low-phosphate rescue-diet. A. Wildtype islet from a rescue-diet fed mouse showing only GLUT-2 (green) and DAPI (blue) staining. B. Wildtype islet from a rescue-diet fed mouse showing insulin (red), GLUT-2 (green) and DAPI (blue) staining. C. *Klotho*$^{-/-}$ islet from a rescue-diet fed mouse showing only GLUT-2 (green) and DAPI (blue) staining. D. *Klotho*$^{-/-}$ islet from a rescue-diet fed mouse showing insulin (red), GLUT-2 (green) and DAPI (blue) staining. White bar = 50 µm

The TrpV5 N-glycan processing by Klotho requires soluble Klotho, which results through enzymatic cleavage by ADAM10 and ADAM17. Additionally, the sialidase activity of soluble Klotho can only process sialic acids that are linked with a α2.6 bond to galactose in the LacNAc chain. This bond is created by ST6Gal-1and if ST6Gal-1 is not present Klotho is unable to affect TrpV5. Once the sialic acid is chewed of by Klotho the underlying LacNAc chain can bind Galectin-1 and this secures the channel at the membrane. In effort to examine if islets have all the necessary players for Klotho to work as a sialidase a tissue distribution of ST6Gal-1, Galectin-1, ADAM10 and ADAM17 was performed (Figure 3.17). Kidney was used as a reference tissue and ileum was used as a negative control as it does not have detectable levels of Klotho. Cell lines were also used in order to assess if there was a difference between alpha and beta cells. Results indicate that islets express all components of the siladase/membrane trafficking pathway described for TrpV5, at levels comparable to kidney. Of note, the αTC1 cell line which does not express Klotho (Figure 3.4), likewise lacks components of this pathway (ST6Gal1).

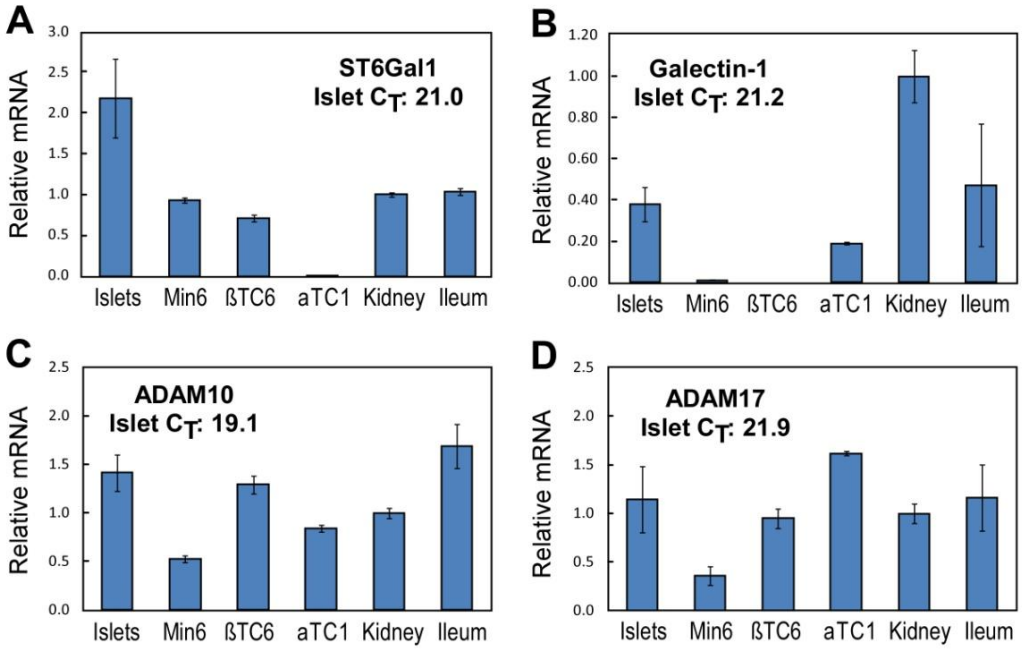

Figure 3.17. Tissue distribution analysis of genes involved in TrpV5 processing via Klotho´s sialidase activity indicates that islets have comparable levels of all transcripts compared to kidney. RNA from islets, Min6 cell line, BetaTC6 cell line, alphaTC1 cell line, kidney and Ileum was used for a real time PCR and cyclophyllin was used as the invariant housekeeping gene. All data are shown as the mean ± S.E. (n=3) A. Tissue distribution of ST6Gal1 mRNA. B. Tissue distribution of Galectin-1 mRNA. C. Tissue distribution of ADAM10 mRNA. D. Tissue distribution of ADAM17 mRNA.

As Klotho appears to be important for GLUT-2 membrane localization (Figures 3.15, 3.16) we wanted to determine if *Klotho*, *Adam10*, *Adam17*, *Galectin-1* and *St6gal1* mRNA levels were affected by different glucose concentrations. Additionally, as *Klotho* is a target gene of VDR we were also curious to see if that applied to any of the other genes involved in Klotho´s activity. Isolated islets from wildtype mice were incubated in low glucose (5 mM) or high glucose (17.5 mM), with vehicle or 20 nM VitD for 16 hours and transcript levels were determined with qPCR (Figure 3.18). The results show a clear

induction of *Klotho* transcription with VitD treatment in both high and low glucose. None of the other genes tested varied with either glucose or VitD treatment.

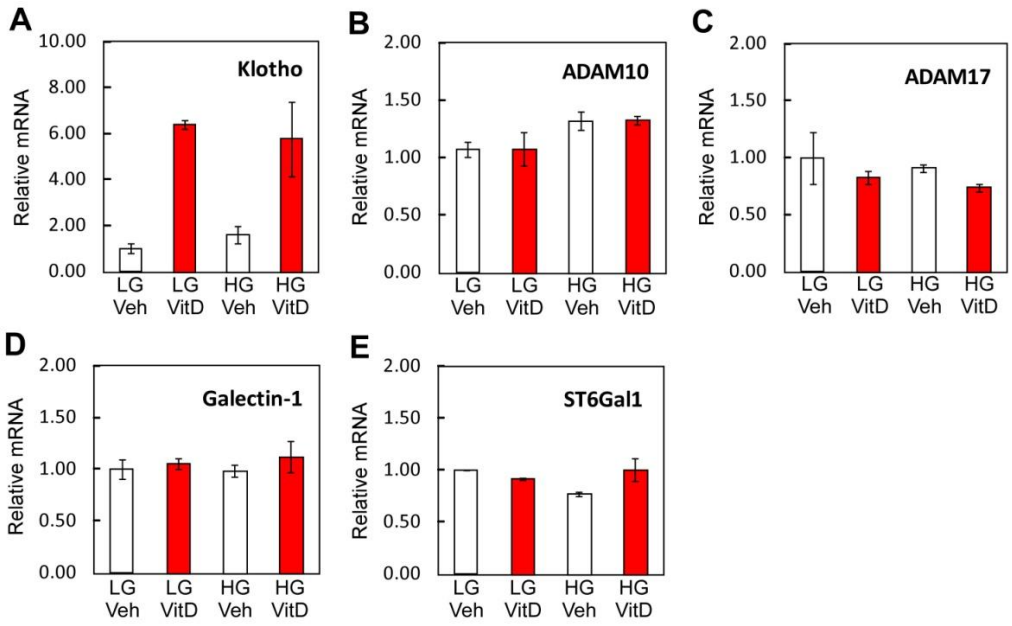

Figure 3.18. VitD treatment upregulates *Klotho* transcripts independent of glucose concentration. Figure shows relative mRNA of *Klotho* (A), *adam10* (B), *adam17* (C), *galectin-1* (D) and *st6gal1* (E) in islets treated with vehicle (white bars) or 20 nM VitD (red bars) cultured for 16 hours in 5 mM glucose (low glucose, LG) or 17.5 mM glucose (high glucose, HG). All data are shown as the mean ± S.E. (n = 2).

GLUT-2 mRNA levels are not reduced in *Klotho*$^{-/-}$ islets (data not shown), therefore the GLUT-2 changes observed in *Klotho*$^{-/-}$ islets are not because of reduced expression. Membrane localized GLUT-2 is significantly reduced in *Klotho*$^{-/-}$ mice regardless of diet and therefore, a glucose uptake into primary beta cells was assessed. Two approaches were taken: a loss-of-function approach in which wildtype and *Klotho*$^{-/-}$ beta cells were compared; and a gain-of-function approach in which recombinant Klotho

was added to the culture media overnight prior to the glucose uptake assay. A fluorescent analog of 2-deoxy glucose (2-NBDG) was used to assess glucose uptake. The assay was performed on dispersed islets using an imaging technique that allowed post fixation and insulin immunocytochemistry to select only beta cells for data analysis. The results reveal that loss of Klotho reduces glucose uptake into primary beta cells and, conversely addition of Klotho to wildtype beta cells increases glucose uptake (Figure 3.19).

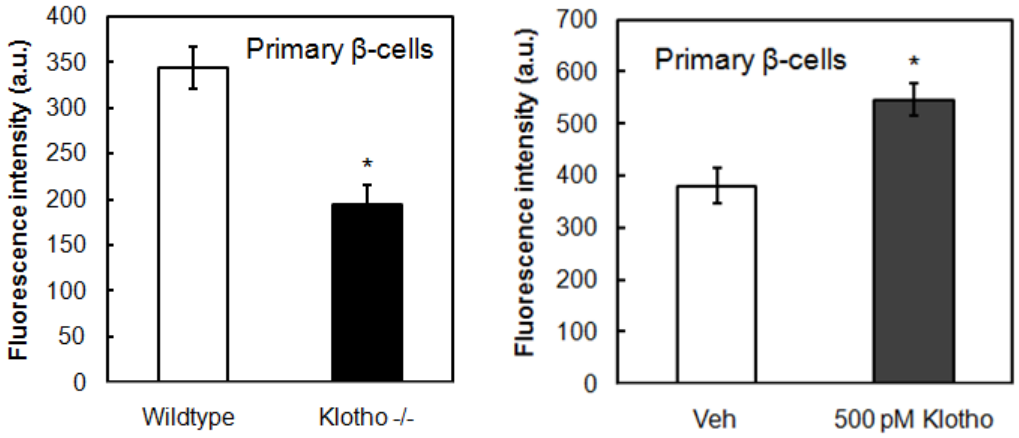

Figure 3.19. Loss of Klotho reduces 2-NBDG uptake and addition of Klotho to cell culture media increases 2-NBDG uptake. Left figure shows 2-NBDG uptake into wildtype and *Klotho*$^{-/-}$ primary beta cells from mice fed a low-phosphate rescue-diet. Right figure shows 2-NBDG uptake into wildtype primary beta cells from wildtype mice (fed standard rodent chow) treated with 500pM Klotho or vehicle for 16 hours. All data are shown as the mean ± S.E. (n = 60-140 cells).

We have clearly demonstrated that VitD increases glucose-stimulated insulin secretion (GSIS) in wildtype islets. That effect is dependent on VDR as no further induction of GSIS is seen with VitD treatment in *Vdr*$^{-/-}$ islets (chapter 2). Additionally, Klotho mRNA and protein levels are induced by VitD treatment, and Klotho levels have an impact on GLUT-2 localization. Therefore Klotho might play a role in the VitD-enhanced GSIS. Isolated wildtype and *Klotho*$^{-/-}$ islets, from mice fed a low-phosphate

rescue-diet, were cultured overnight for 16 hours in 20 nM VitD or vehicle and then a GSIS assay was performed (Figure 3.20). The results show unexpectedly that *Klotho*$^{-/-}$ islets secrete an equal amount of insulin compared to wildtype controls, despite the lack of membrane-localized GLUT-2. However, it has been reported that *GLUT-2*$^{-/-}$ islets have a defect only in the first-phase secretion (<5 min), not second-phase secretion so a perifusion experiment needs to be performed [70]. Although there is no basal difference in GSIS there is a significant difference between genotypes when islets are pretreated with VitD. These results suggest that Klotho plays a role in the VitD-enhanced GSIS.

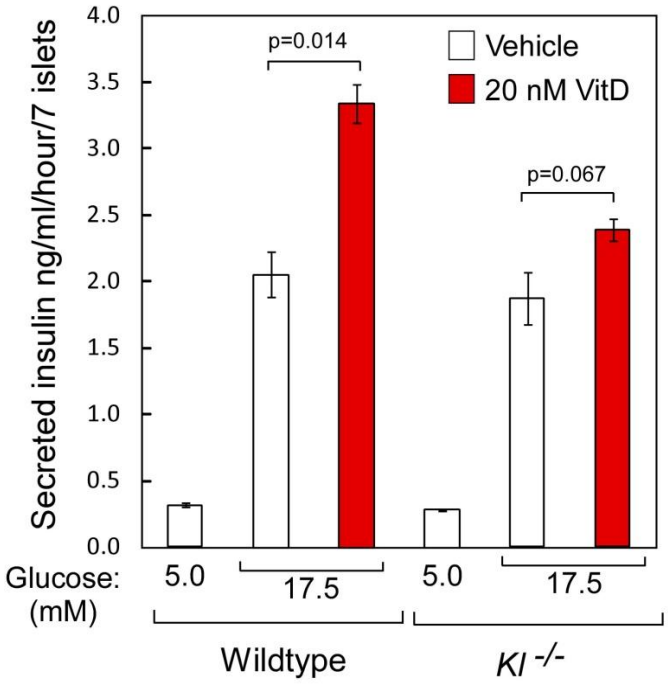

Figure 3.20. Klotho might play a role in the VitD-enhanced GSIS. Isolated islets from wildtype and Klotho$^{-/-}$ mice were incubated in 20 nM VitD for 16 hours and then a glucose stimulated insulin secretion was performed in either 5 mM or 17.5 mM glucose. All data are shown as the mean ± S.E. (n = 3).

3.5 Discussion

Klotho's role in phosphate regulation has been extensively studied [71] but its role in metabolism is poorly understood. In general Klotho is thought to inhibit insulin signaling and cause insulin resistance, however, the mechanism behind this action is not known. Our results indicate that Klotho$^{-/-}$ mice are glucose tolerant even on a low-phosphate rescue-diet, which suggests that the metabolic phenotype is not secondary to the role of Klotho in kidneys. We have identified that Klotho is present in endocrine pancreas and that it is highly upregulated by VitD at both the mRNA and protein levels. Furthermore, we have identified a strong VDRE located 7.3 kb upstream from the transcriptional start site of the mouse *Klotho* gene. Previous reports suggest that Klotho is upregulated by VitD in mice and humans [67, 72], therefore it is likely that other conserved VDREs are located in the vicinity of the *Klotho* locus.

FGF23 is an important regulator of phosphate homeostasis. We have discovered that FGF23/Klotho signaling is preserved in islets and the beta cell line βTC6. At this point it is not clear what role FGF23-activated signaling pathways perform in islets. None of the known gene changes that result from FGF23 signaling in kidney are evident in islets. However, a 36-hour treatment of islets with 100ng/ml FGF23 significantly increased expression of kappa casein (csnk) by 70% (data not shown). *Csnk* is a gene involved in binding of insoluble Calcium-Phosphate in mammary glands, therefore it might have some function in islets as plasma phosphate concentration rises.

We have identified a possible novel role of secreted Klotho in islet physiology. *Klotho*$^{-/-}$ islets have almost no GLUT-2 membrane localization. However, some membrane localization is seen so it is safe to say that Klotho is not required for the

localization but perhaps the half-life of the transporter at the membrane. *Klotho*$^{-/-}$ mice also have elevated plasma glucagon and a shifted ratio of alpha to beta cells in islets, phenotypes also observed in *GLUT-2*$^{-/-}$ mice. To support the role of Klotho in GLUT-2 membrane localization, lack of Klotho suppresses glucose uptake and addition of Klotho to islets in culture increases glucose uptake capacity. The mechanism in which Klotho regulates GLUT-2 membrane localization is likely via its sialidase activity, similar to what is seen in TrpV5 regulation (Figure 3.21). We have determined that all necessary elements for Klotho's ion channel regulation of TrpV5, such as proteases ADAM10 and ADAM17, the sialic acid translocase ST6Gal-1 and the stabilizing Galectin-1, are expressed in islets. Therefore, all the tools are present in islets for Klotho to regulate GLUT-2 in a manner similar to that described for renal TrpV5.

Lastly, we have demonstrated both that VitD increases GSIS significantly in isolated islets and that Klotho affects glucose uptake into primary beta cells. As Klotho is a target gene of VDR in islets we sought to examine if Klotho played a role in VitD-enhanced GSIS. Results suggest that Klotho has an important role in VitD-enhanced GSIS. Whether it is only though regulating GLUT-2 or if other channels are also affected by Klotho remains to be determined.

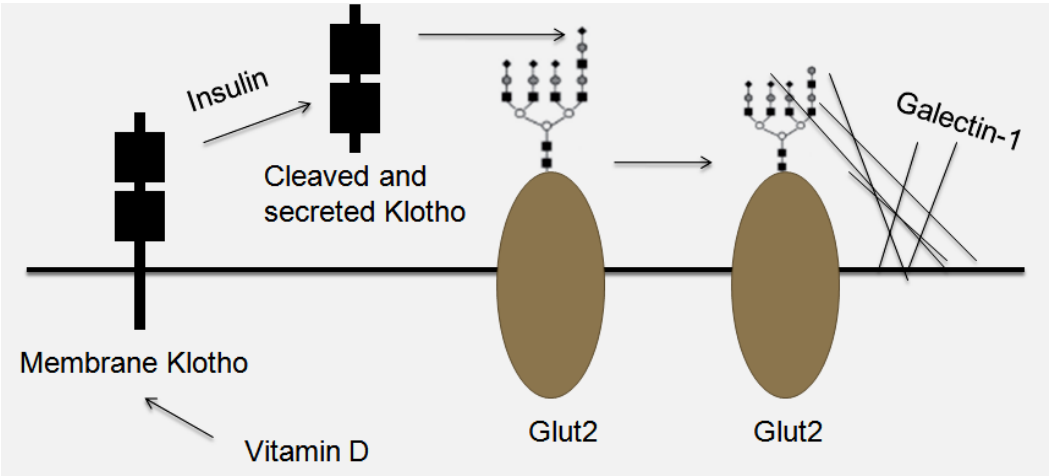

Figure 3.21. Possible mechanism for secreted Klotho in GLUT-2 membrane localization. VitD increases Klotho expression, local insulin drives cleavage of membrane bound Klotho into the extracellular space. Secreted Klotho can act in a auto- or paracrine fashion to chew of terminal sialic acids on N-glycan modification on GLUT-2. This exposes LacNAc, which binds to Galectin-1 and stabilizes GLUT-2 at the membrane.

In summary we have identified that Klotho is present in islets, it is a target gene of VDR and it plays a role in VitD-enhanced GSIS. Absence of Klotho reduces GLUT-2 membrane localization and reduces glucose uptake into beta cells. On the other hand by incubating dispersed islets with recombinant Klotho glucose uptake is exaggerated. This discovery may have implications for diabetes research and might provide a possible molecular expanation for the protective effect of Vitamin D on diabetes progression. These results might also provide a potential link between aging, reduction of GLUT-2 and accompanying beta cell dysfunction [73, 74]. As we age, Klotho levels diminish [75] and that might have a detrimental impact on GLUT-2 membrane localization and beta cell function. One possible way to minimize Klotho reduction would be to keep VitD levels optimal as we age.

CHAPTER FOUR

Vitamin D induced transcriptional changes in mouse and human islets

4.1 Abstract

The active form of vitamin D, 1,25-dihydroxyvitamin D_3 (VitD), is a ligand for the Vitamin D Receptor (VDR). VDR is a member of the Nuclear Hormone Receptor family of transcription factors that regulate gene expression. Previously, we have shown that VitD increases glucose-stimulated insulin secretion in isolated mouse and human islets. Accumulating evidence suggests that maintaining optimal serum levels of Vitamin D might delay the progression of Type 1 and Type 2 Diabetes Mellitus (T1DM, T2DM). In the case of T1DM, vitamin D appears to have positive immunomodulating effects. However, in the case of T2DM is appears to increase beta-cell function and reduce insulin resistance. Therefore, it might be a relatively inexpensive preventive measure for persons with, or at risk, for T1DM or T2DM to take Vitamin D supplements. However, despite numerous promising clinical and associational studies, not much is known about the molecular pathways activated by Vitamin D in the beta-cell. To identify molecular mechanisms linking VDR activity and islet function, we performed global gene expression profiling by microarray in mouse and human islets. These studies identified multiple genes that can be connected to T1DM and T2DM by a direct or an indirect manner (Amigo2, Gadd45a, Nedd9, PRG-3, H2-Bl, Gpc6, Gdf10, Slitrk1, Stx18, Sytl2, Tmem27, Arrb2, Kl, Dok5, Ak5, Cacna2d3, TacR3 and Csnk). Furthermore as the samples used for both mouse and human arrays were treated with the same concentration of VitD and for the same length of time, we were able to do a comparative analysis. We

identified 13 commonly regulated genes in mouse and human islets due to VitD treatment. One of them, transforming growth factor beta 1 (Tgfb1), has a strong connection to diabetes and beta-cell function and might have implications for both T1D and T2D. This is the first detailed report on VitD-regulated gene expression in mouse and human islets describing multiple genes that might play a role in VitD-enhanced insulin secretion and beta-cell function.

4.2 Introduction

Vitamin D is a fat-soluble vitamin that is naturally present in fatty fish but it is also added to many milk and cereal products. In addition, Vitamin D can be obtained from the sun and tanning beds when the skin is exposed to ultraviolet radiation. Vitamin D is converted to the active metabolite 1,25-dihydrxoyvitamin D (VitD) after undergoing hydroxylation steps in the liver and kidney. The active form, VitD, is a ligand for the Vitamin D Receptor (VDR, NR1I1), which is a member of the Nuclear Hormone Receptor superfamily (NHR) of transcription factors. We have previously shown that VDR is very highly expressed in mouse and human islets. Furthermore, we have demonstrated that activation of VDR by VitD leads to enhanced glucose-stimulated insulin secretion in isolated mouse and human islets.

Accumulating evidence suggests that maintaining optimal serum levels of VitD might delay progression of all forms of Diabetes Mellitus. Studies in human subjects with type 1 diabetes (T1DM) and adult onset latent autoimmune diabetes (LADA) suggest that VitD can prevent beta-cell destruction [1-4]. Studies in non-obese diabetic (NOD) mice have supported that notion and have suggested VitD’s positive actions are especially

potent if it is given at an early age [5-7]. Studies on VitD-deficient NOD mice show similar results, as VitD deficiency, especially at an early age increases the incidence of T1DM [8]. This effect of VitD on T1DM and LADA is most likely driven by its immunomodulatory actions. The progression of both T1DM and LADA involves infiltration of the pancreas with dendritic cells, macrophages, T cells and B cells [9]. There is still not much known on how VitD affects the autoimmune processes in T1DM and LADA: however; evidence suggests that it might be mediated by reduction in interferon and interleukin secretion [10], suppression of dendritic cell maturation [11], and enhancement of suppressor T cell function [12].

The immunomodulatory role of VDR might also play a role in T2DM as inflammation has been connected to increased insulin resistance [13]. Moreover, VitD is thought to affect T2DM by improving beta-cell function and insulin secretion. Numerous observational studies suggest that people with low VitD status have an increased risk of developing T2DM [14-16]. Additionally, there are several randomized trials of VitD that suggest people with glucose intolerance or T2DM may benefit from VitD supplementation [17-19].

In addition, several VDR gene polymorphisms have been associated with T1DM [20-23] and T2DM [24]. Alterations in the VDR gene may affect all forms of diabetes progression not only through its presence and function in beta-cells but also through its presence in other tissues. With all the positive reports connecting VitD status to diabetes and more importantly no reports of adverse effects, it seems plausible that VitD supplementation could be a relatively inexpensive preventive measure for persons at risk

for diabetes. However despite multiple promising clinical studies and associational studies, not much is known about how VitD might improve beta-cell function.

To identify molecular mechanisms linking VDR activity to increased insulin secretion and islet function, we performed global gene expression profiling by microarray in mouse and human islets. Because the samples used for both mouse and human arrays were treated with the same concentration of VitD and for the same length of time, we extended these analyses by doing a comparison aseessment to identify commonly regulated genes in mouse and human islets.

4.3 Materials and methods

Materials

1,25-dihydroxyvitamin D_3 (>99.0 % by HPLC) was purchased from Sigma-Aldrich, and was resuspended in tissue-culture grade DMSO. This VDR ligand is referred to as "VitD" hereafter in this manuscript. (CAT#N13195). Collagenase P (CAT#11213857001) for islet isolation was obtained from Roche. Oligonucleotides were obtained from Integrated DNA Technologies. Real-time PCR reagents were purchased from Applied Biosystems.

Animals

All tissues and islets were obtained from 3-5 month-old, male A129/SvJ mice. Mice were maintained in a temperature-controlled room (23 ± 1 C) with 12-h light (0700 h–1900 h), 12-h dark cycle and *ad libitum* access to water, a standard rodent diet (Teklad Diet 7001 or Harlan Teklad Premier Laboratory Diet no. 2016), and housed with sanitized wood-

chip bedding (Sani-Chips, P.J. Murphy Forest Products, Montville, NJ). Tissues were harvested and islets were isolated in the morning with mice in the fed state. All experiments were performed with the approval of the Institutional Animal Care and Use Committee of the University of Texas Southwestern Medical Center, which assures that all animal use adheres to federal regulations as published in the Animal Welfare Act, the Guide for the Care and Use of Laboratory Animals (Guide), the Public Health Service Policy, and the US Government Principles Regarding the Care and Use of Animals (http://www.utsouthwestern.edu/utsw/cda/ dept41600/files/54634.html).

Mouse Islet Microarray

Isolated mouse islets from 3 month old wildtype and *Vdr*$^{-/-}$ male mice were cultured over night in RPMI medium containing 11 mM glucose and 10% FBS. Islets (200/well) were then cultured for 16h in the presence of 20 nM Vit D or vehicle (DMSO, final concentration 0.1% v/v) with triplicate biologic samples prepared for each condition. Total RNA was isolated and microarray analysis was performed using the Mouse Illumina 6-beadchip V2 array platform. Mixed model analysis of variance was performed using Partek® software, version 6.3 Copyright © 2011 Partek Inc., St. Louis, MO, USA, with fold change cut-off between wildtype vehicle-treated and VitD-treated at ≥ 1.5 and $p \leq 0.1$. Additionally, genes showing a change of $p \leq 0.1$ between vehicle and VitD treated *Vdr*$^{-/-}$ islets were excluded from analysis.

Human Islet Microarray

Human pancreatic islets were obtained from a cadaveric donor (49 year old Caucasian male, islet purity at 90%) and immediately placed in RPMI medium containing 11 mM glucose and 10% FBS. Islets (200/well) were then cultured for 16h in the presence of 20 nM Vit D or vehicle (DMSO, final concentration 0.1% v/v) with duplicate biologic samples prepared for each condition. Total RNA was isolated and microarray analysis was performed using the Human Affymetrix U133 Plus 2.0 array platform. Comparative gene expression was done using GeneSifter (Seattle, WA) software with fold change cut-off at ≥ 1.5 and $p \leq 0.1$. Downstream pathway analysis was performed using Ingenuity Pathway Analysis (Redwood City, CA).

Islet isolation

The islet isolation method used has been described before [1]. Briefly, the mouse pancreas was perfused and digested with Collagenase P (Roche, Indianapolis, IN). Islets were then isolated using Ficoll gradient centrifugation and hand selection under a stereomicroscope for transfer to RPMI 1640 medium (11.1 mM glucose) supplemented with 10% (vol/vol) heat-inactivated fetal bovine serum (FBS), 100 IU/ml penicillin, and 100 μg/ml streptomycin (Invitrogen, Carlsbad, CA). Islets were allowed to recover overnight (37°C, 5% CO_2) and the following day exposed to 20 nM VitD (or DMSO) for 16 hours before harvesting for RNA isolation.

qPCR profiling

RNA was isolated from cultured islets using RNA STAT-60 (Tel-Test Inc., Friendswood, TX), and 2 μg of total RNA was treated with ribonuclease-free deoxyribonuclease (Roche), and then reverse transcribed to cDNA with random hexamers using SuperScript II (Invitrogen), as previously described in detail [38]. qPCR was performed using an Applied Biosystem Prism 7900HT sequence detection system (Applied Biosystems, Foster City, CA) and SYBR-green chemistry [38, 39]. Gene-specific primers were designed using D-LUX primer design software (www.invitrogen.com) and validated by analysis of template titration and dissociation curves [1]. Primer sequences are available in Appendix B. qPCRs (10 μl) contained 25 ng of cDNA, each primer (150 nM), and 5 μl of 2X SYBR Green PCR master mix (Applied Biosystems). Multiple housekeeping genes were evaluated in each assay to ensure that their RNA levels were invariant under the experimental conditions of each study. Results of qPCR were evaluated by the comparative Ct method [user bulletin no. 2, PerkinElmer Life Sciences [38]] using hypoxanthine-guanine phosphoribosyl transferase (HPRT), acidic ribosomal phosphoprotein P0 (36B4) and cyclophilin as the invariant control genes.

Statistics

All results are expressed as the means ± SEM for each treatment group. Two-tailed Student's *t*-tests were performed to compare differences between two groups. 1-way and 2-way ANOVA, with Bonferroni's multiple comparisons post test were used to compare samples in experiments with 3 or more groups. All statistical tests were

performed using GraphPad Prism software (GraphPad, San Diego, CA). Significance was established at $P < 0.05$ and is represented with an asterisk (*).

4.4 Results

Mouse islet microarray analysis identified multiple genes that can be connected to diabetes. In hope to identify molecular mechanisms linking VDR activity to increased insulin secretion, we performed global gene expression profiling by microarray in mouse islets. Figure 4.1 shows microarray results from wildtype and *Vdr*$^{-/-}$ mouse islets treated with Vit D. Wildtype and *Vdr*$^{-/-}$ mouse islets were treated with 20 nM Vit D or vehicle (DMSO) for 16 hours. Triplicate biologic samples were prepared for each condition. Total RNA was isolated and analyzed using the Illumina Mouse-6 V2 BeadChip microarray platform. The VitD-regulated genes that were related to islet function and insulin secretion were confirmed by qPCR in independent samples (Figure 4.2). These genes were grouped into four categories.

Category 1 contains genes involved in survival, proliferation and migration (Slitrk1, Nedd9, Gpc6, Amigo2, KIAA1199, Gdf10, Gadd45a, H2-Bl and PRG-3). SLIT and NTRK-like family, member 1 (Slitrk1) partakes in neurite outgrowth, neural circuity and norepinephrine secretion [94, 95]. Neural precursor cell expressed, developmentally down-regulated gene 9 (Nedd9) plays a role in cell differentiation, neurite outgrowth, cell proliferation and cell migration [96-98]. Glypican 6 (Gpc6) is a heparan sulfate proteoglycan and the glypican family has been implicated in the control of cell growth and division [99]. Adhesion molecule with Ig-like domain 2 (Amigo2) promotes neurite outgrowth, inhibits apoptosis and promotes neuronal survival [100, 101]. KIAA1199 has

been implicated in TGF-Beta [102] and Wnt signaling [103]. Growth differentiation factor 10 (Gdf10) is a member of the TGF-Beta superfamily and is highly related to bone morphogenetic protein-3. Members of this family affect growth and proliferation [104]. Growth arrest and DNA-damage-inducible, alpha (Gadd45a) is a stress responder and the closely related Gadd45b has been shown to improve beta cell survival in response to cytokines [105]. Blastocyst MHC (H2-Bl) has been implicated in protection of fetal trophoblasts from maternal NK cells and evasion of some tumor cells from NK cell attack [106]. Finally, Plasticity-related gene 3 (PRG-3 also known as Lppr1) is an integral membrane protein involved in neural development and neurite outgrowth and is a susceptibility gene for T2DM [107, 108].

Category 2 contains genes involved in vesicle transport (Tmem27, Stx18 and Sytl2). Transmembrane protein 27 (Tmem27) has been shown enhance SNARE mediated insulin secretion [109-111] and enhance beta cell proliferation [110, 112]. Syntaxin 18 (Stx18), encodes for an endoplasmic reticulum and golgi transport protein that is also a susceptibility gene for T2DM [108, 113, 114]. Lastly, Synaptotagmin-like 2 (Sytl2) is an exocytic sensor for Ca^{2+} signaling systems that has been shown to enhance secretion in multiple cell systems [115-117].

Category 3 contains genes involved in insulin signaling (Dok5, Arrb2 and Kl). Docking protein 5 (Dok5) is a susceptibility gene for T2DM and is a component of the insulin signaling pathway [118, 119]. Arrestin, beta 2 (Arrb2) is involved in GPCR signaling and insulin signaling [120, 121]. Klotho (Kl) is involved in ion channel localization and its secretion is enhanced by insulin [58, 60]. The role of Klotho in islet function is considered in detail in chapter 3.

Category 4 contains genes involved in calcium mobilization and/or associated with diabetes (Tacr3, Cacna2d3, Ak5 and Csnk). Tachykinin receptor 3 (TacR3) is a g-protein couple receptor that is associated with G proteins that activate a phosphatidylinositol-calcium second messenger system[122]. Calcium channel, voltage-dependent a2/d3 subunit (Cacna2d3) is a susceptibility gene for T2DM and its expression is upregulated in the presence of IGF-1 [108, 123]. Adenylate kinase 5 (AK5) has been shown to regulate K-ATP channel activity and is a susceptibility gene for T2DM [108, 124]. Finally there is Casein kappa (Csnk), a susceptibility gene for T2DM, for which the only function described to date is that of a chaperone for otherwise insoluble CaP in breast milk [125, 126].

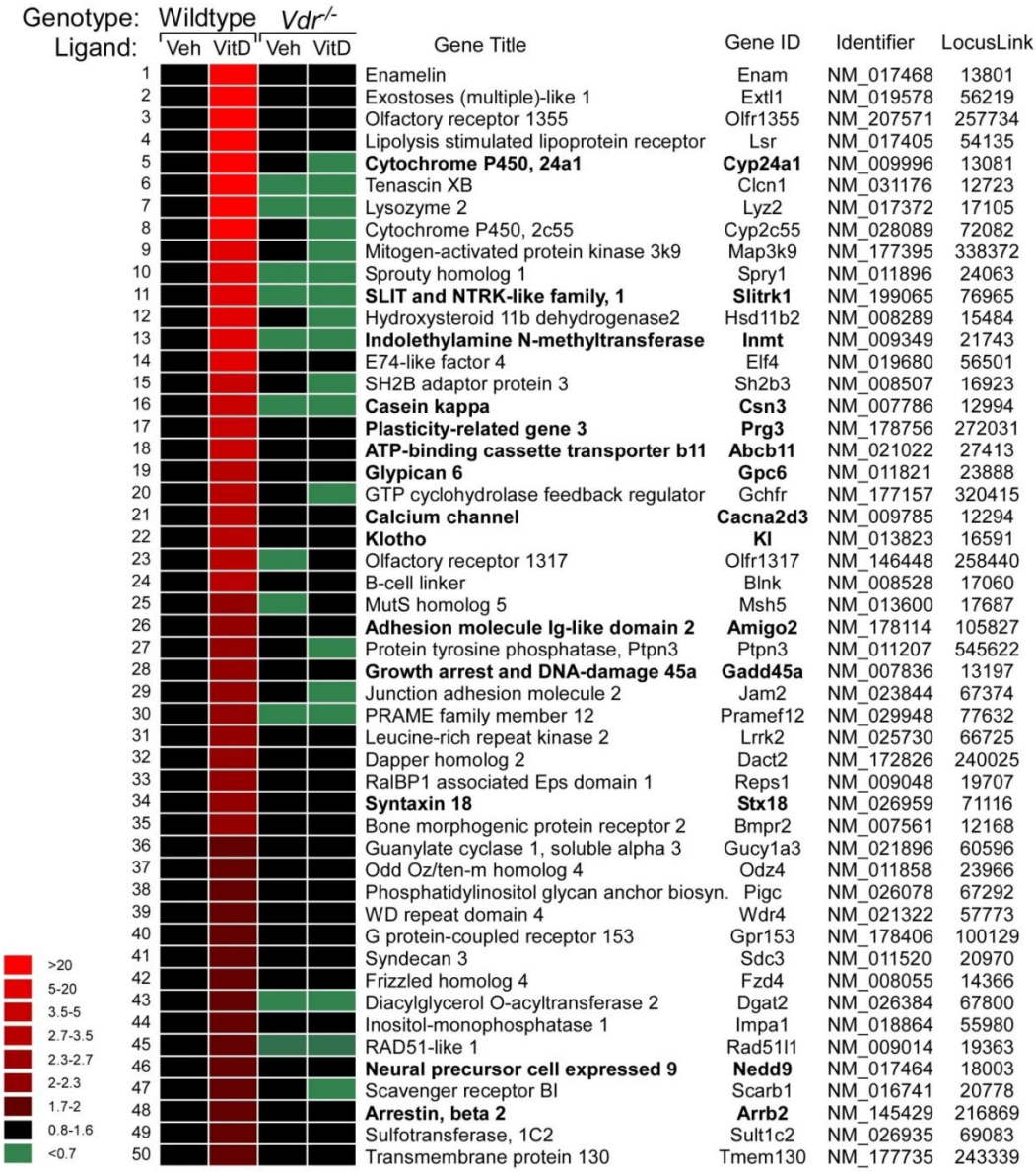

Figure 4.1. Microarray results from wildtype and *Vdr*$^{-/-}$ mouse islets treated with Vit D. Wildtype and *Vdr*$^{-/-}$ mouse islets were treated with 20 nM Vit D or vehicle (DMSO) for 16 hours. Triplicate biologic samples were prepared for each condition. Total RNA was isolated and analyzed using the Illumina Mouse-6 V2 BeadChip microarray platform. Genes in bold have been validated by qPCR

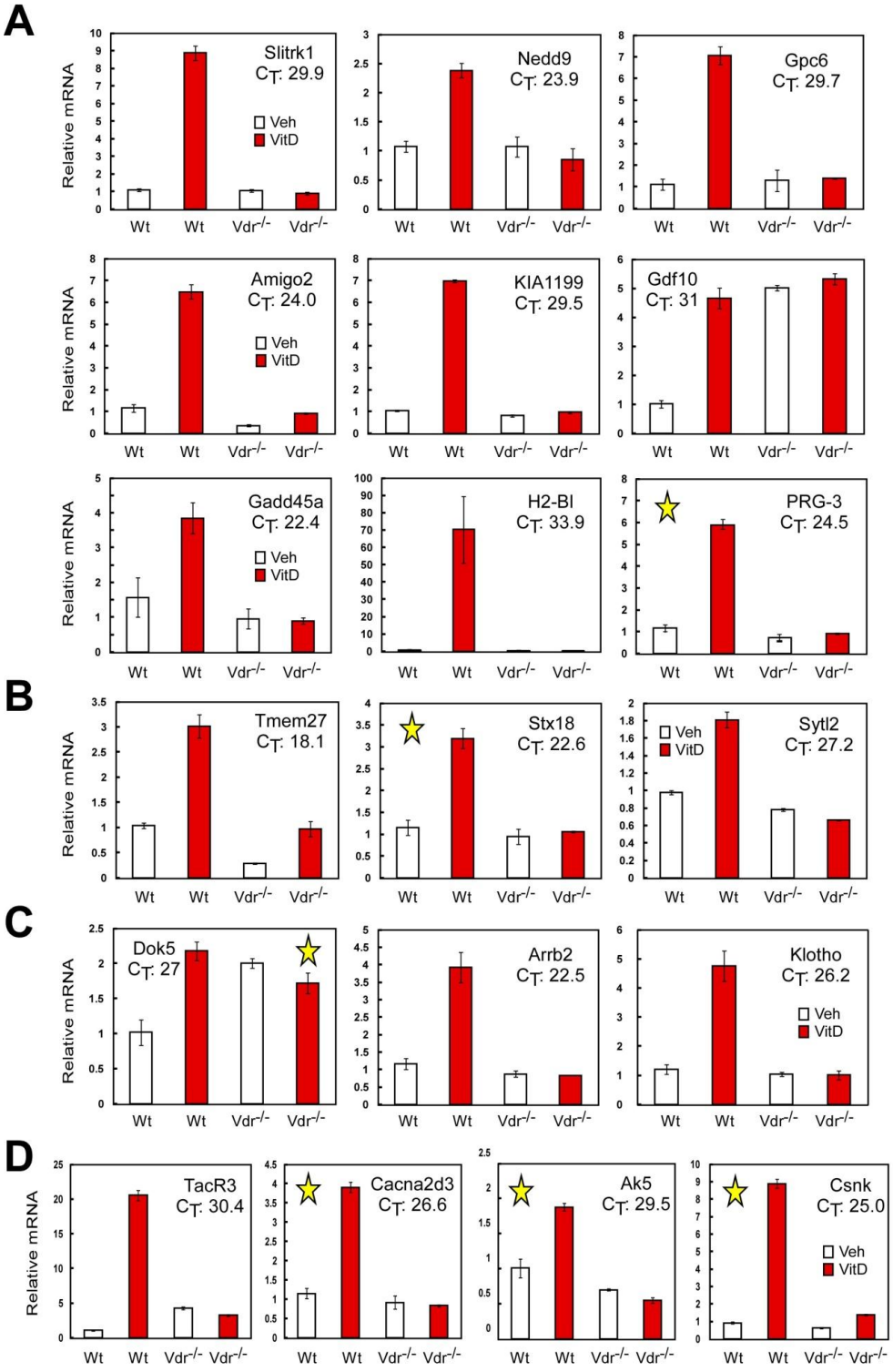
A
Slitrk1
CT: 29.9
Veh
VitD
Nedd9
CT: 23.9
Gpc6
CT: 29.7
Amigo2
CT: 24.0
KIA1199
CT: 29.5
Gdf10
CT: 31
Gadd45a
CT: 22.4
H2-Bl
CT: 33.9
PRG-3
CT: 24.5
B
Tmem27
CT: 18.1
Stx18
CT: 22.6
Sytl2
CT: 27.2
C
Dok5
CT: 27
Arrb2
CT: 22.5
Klotho
CT: 26.2
D
TacR3
CT: 30.4
Cacna2d3
CT: 26.6
Ak5
CT: 29.5
Csnk
CT: 25.0
Relative mRNA
Wt
Wt
Vdr-/-
Vdr-/-

Figure 4.2. qPCR validation of selected target genes identified by microarray using RNA from wildtype and *Vdr*$^{-/-}$ mouse islets treated with Vit D. A. Group 1, genes involved in survival, proliferation and migration. B. Group 2, genes involved in vesicle transport. C. Group 3, genes involved in insulin signaling. D. Group 4, genes involved in and calcium mobilization and/or associated with diabetes. Genes labeled with a star have been connected to Diabetes via Genome-wide association studies.

To find possible genes connecting VitD to diabetes and insulin secretion we expanded our search by performing a pathway analysis using Ingenuity Pathway Analysis software. That search identified 86 upregulated genes and 40 down-regulated genes that have a direct or indirect connection to T1DM and T2DM (Table 4.1).

Table 4.1. IPA analysis - Genes connected to diabetes from mouse islet microarray

Symbol	Entrez Gene Name	p-value	Fold Change	Entrez Gene ID
CSN3	**casein kappa**	6.9E-02	3.28	12994
LPPR1	lipid phosphate phosphatase-related protein type 1	2.3E-03	2.68	272031
ADCY2	adenylate cyclase 2 (brain)	5.2E-02	2.12	210044
TUBE1	tubulin, epsilon 1	3.9E-02	2.09	71924
UNC45B	unc-45 homolog B (C. elegans)	5.5E-02	2.07	217012
FBN1	fibrillin 1	7.4E-02	2.07	14118
CHRNA5	cholinergic receptor, nicotinic, alpha 5	1.8E-02	2.07	110835
FAM38B	family with sequence similarity 38, member B	2.3E-02	2.04	667742
KIF26B	kinesin family member 26B	1.1E-02	1.95	269152
GRIN2B	glutamate receptor, ionotropic, N-methyl D-aspartate 2B	4.0E-03	1.94	14812
RXFP2	relaxin/insulin-like family peptide receptor 2	4.8E-02	1.93	140498
SEZ6L	seizure related 6 homolog (mouse)-like	1.2E-02	1.90	56747
CSGALNACT1	chondroitin sulfate N-acetylgalactosaminyltransferase 1	6.3E-02	1.89	234356
PTGS1	prostaglandin-endoperoxide synthase 1	8.4E-03	1.89	19224
EDNRA	endothelin receptor type A	4.8E-02	1.87	13617
KLF11	Kruppel-like factor 11	6.3E-02	1.87	194655
ODZ4	odz, odd Oz/ten-m homolog 4 (Drosophila)	1.7E-03	1.84	23966
ESR1	estrogen receptor 1	2.6E-02	1.81	13982
ADAMTS18	ADAM metallopeptidase with thrombospondin motif, 18	2.8E-03	1.81	208936

SLC24A3	solute carrier family 24, member 3	3.9E-02	1.81	94249
DSCAM	Down syndrome cell adhesion molecule	1.2E-02	1.80	13508
COL23A1	collagen, type XXIII, alpha 1	1.1E-02	1.79	237759
F13A1	coagulation factor XIII, A1 polypeptide	1.4E-02	1.78	74145
ITGBL1	integrin, beta-like 1 (with EGF-like repeat domains)	2.1E-02	1.78	223272
DERL1	Der1-like domain family, member 1	2.1E-03	1.77	67819
MYLK2	myosin light chain kinase 2	7.0E-02	1.77	228785
STX18	**syntaxin 18**	6.9E-02	1.77	71116
PXDN	peroxidasin homolog (Drosophila)	4.7E-03	1.75	69675
ANO4	anoctamin 4	1.6E-02	1.74	320091
CACNA2D3	**calcium channel, voltage-dependent, alpha 2/delta subunit 3**	8.9E-02	1.73	12294
KALRN	kalirin, RhoGEF kinase	2.0E-03	1.73	545156
COL4A1	collagen, type IV, alpha 1	1.6E-02	1.72	12826
RBL1	retinoblastoma-like 1 (p107)	2.2E-02	1.72	19650
BLNK	B-cell linker	6.6E-03	1.71	17060
C10orf18	chromosome 10 open reading frame 18	2.5E-02	1.70	105203
EPHA3	EPH receptor A3	9.7E-02	1.70	13837
MMP16	matrix metallopeptidase 16 (membrane-inserted)	5.5E-02	1.68	17389
TGFBR2	transforming growth factor, beta receptor II (70/80kDa)	8.8E-02	1.67	21813
SULF1	sulfatase 1	9.6E-02	1.67	240725
ADAM23	ADAM metallopeptidase domain 23	3.1E-02	1.67	23792
VAV3	vav 3 guanine nucleotide exchange factor	4.7E-02	1.66	57257
SYK	spleen tyrosine kinase	4.0E-02	1.66	20963
LDB2	LIM domain binding 2	9.6E-02	1.66	16826
CNDP1	carnosine dipeptidase 1 (metallopeptidase M20 family)	4.9E-03	1.65	338403
CTNNA2	catenin (cadherin-associated protein), alpha 2	4.7E-02	1.65	12386
RYR2	ryanodine receptor 2 (cardiac)	6.5E-02	1.65	20191
C10orf128	chromosome 10 open reading frame 128	6.1E-02	1.64	69069
LPPR5	lipid phosphate phosphatase-related protein type 5	1.4E-02	1.63	75769
LAMC2	laminin, gamma 2	9.9E-02	1.63	16782
BDNF	brain-derived neurotrophic factor	9.5E-03	1.62	12064
NCF2	neutrophil cytosolic factor 2	3.3E-02	1.62	17970
SORL1	sortilin-related receptor, L(DLR class) A repeats containing	2.7E-02	1.61	20660
DGAT2	diacylglycerol O-acyltransferase 2	8.2E-02	1.60	67800
NOX4	NADPH oxidase 4	6.4E-02	1.60	50490

WISP1	WNT1 inducible signaling pathway protein 1	1.6E-02	1.60	22402
GBE1	glucan (1,4-alpha-), branching enzyme 1	1.0E-02	1.59	74185
VCAN	Versican	5.5E-02	1.59	13003
ICA1	islet cell autoantigen 1, 69kDa	5.6E-02	1.59	15893
SEMA3E	sema domain, immunoglobulin domain (Ig), secreted,3E	7.3E-02	1.59	20349
COL24A1	collagen, type XXIV, alpha 1	2.7E-02	1.58	71355
NPHP4	nephronophthisis 4	9.1E-02	1.57	260305
LASS6	LAG1 homolog, ceramide synthase 6	3.6E-02	1.56	241447
AK5	**adenylate kinase 5**	8.9E-02	1.56	229949
PTPRE	protein tyrosine phosphatase, receptor type, E	5.6E-02	1.56	19267
LHFP	lipoma HMGIC fusion partner	5.2E-02	1.55	108927
TNXB	tenascin XB	3.1E-02	1.55	81877
PCDH7	protocadherin 7	7.7E-02	1.54	54216
AKT2	v-akt murine thymoma viral oncogene homolog 2	2.3E-02	1.54	11652
GNA14	guanine nucleotide binding protein (G protein), alpha 14	8.6E-02	1.54	14675
HDAC9	histone deacetylase 9	7.5E-02	1.53	79221
MPP7	MAGUK p55 subfamily member 7	8.7E-02	1.53	75739
FUT9	fucosyltransferase 9 (alpha (1,3) fucosyltransferase)	6.1E-03	1.53	14348
ARHGAP42	Rho GTPase activating protein 42	2.9E-02	1.53	71544
MYLK	myosin light chain kinase	6.7E-02	1.52	107589
CLIC5	chloride intracellular channel 5	2.9E-02	1.52	224796
CD40LG	CD40 ligand	3.0E-02	1.52	21947
FN1	fibronectin 1	7.2E-02	1.52	14268
MTOR	mechanistic target of rapamycin (serine/threonine kinase)	7.6E-03	1.51	56717
SKA1	spindle and kinetochore associated complex subunit 1	2.0E-02	1.51	66468
CRMP1	collapsin response mediator protein 1	2.3E-02	1.51	12933
EDNRB	endothelin receptor type B	8.7E-02	1.51	13618
DCLK1	doublecortin-like kinase 1	6.1E-02	1.51	13175
MS4A7	membrane-spanning 4-domains, subfamily A, member 7	7.2E-02	1.51	109225
ACE	angiotensin I converting enzyme (peptidyl-dipeptidase A) 1	6.9E-02	1.50	11421
HNMT	histamine N-methyltransferase	3.4E-02	1.50	140483
IRS2	insulin receptor substrate 2	1.6E-03	1.50	384783
ACAA2	acetyl-CoA acyltransferase 2	3.0E-02	-1.50	52538
TRIM10	tripartite motif containing 10	6.8E-02	-1.50	19824
IRS1	insulin receptor substrate 1	8.2E-03	-1.51	16367
CNTN4	contactin 4	2.0E-02	-1.51	269784
PSMB9	proteasome subunit, beta type, 9	3.9E-02	-1.52	16912

EFCAB2	EF-hand calcium binding domain 2	4.6E-02	-1.53	68226
DYSF	dysferlin, limb girdle muscular dystrophy 2B	6.2E-02	-1.54	26903
IQCH	IQ motif containing H	3.7E-02	-1.54	78250
MTUS1	microtubule associated tumor suppressor 1	1.6E-02	-1.55	102103
SPTLC2	serine palmitoyltransferase, long chain base subunit 2	5.8E-02	-1.55	20773
FAM19A4	family with sequence similarity 19, member A4	6.3E-02	-1.55	320701
LATS2	LATS, large tumor suppressor, homolog 2 (Drosophila)	4.3E-02	-1.55	50523
EXT2	exostosin 2	8.8E-02	-1.56	14043
EYA4	eyes absent homolog 4 (Drosophila)	5.4E-02	-1.56	14051
TGFA	transforming growth factor, alpha	4.0E-02	-1.57	21802
CTIF	CBP80/20-dependent translation initiation factor	3.9E-02	-1.58	269037
FANCA	Fanconi anemia, complementation group A	7.8E-03	-1.59	14087
ELOVL7	ELOVL fatty acid elongase 7	1.2E-02	-1.59	74559
STRN	striatin, calmodulin binding protein	5.2E-02	-1.59	268980
UCP3	uncoupling protein 3 (mitochondrial, proton carrier)	5.6E-02	-1.61	22229
ATP8A2	ATPase, aminophospholipid transporter, class I, type 8A, member 2	5.5E-02	-1.62	50769
HAPLN1	hyaluronan and proteoglycan link protein 1	6.5E-02	-1.62	12950
GLRA3	glycine receptor, alpha 3	3.0E-02	-1.66	110304
CPB1	carboxypeptidase B1 (tissue)	9.7E-02	-1.67	76703
PPP3R1	protein phosphatase 3, regulatory subunit B, alpha	6.4E-02	-1.70	19058
ANKFN1	ankyrin-repeat and fibronectin type III domain containing 1	3.5E-02	-1.71	382543
BCL2	B-cell CLL/lymphoma 2	2.9E-02	-1.72	12043
DCC	deleted in colorectal carcinoma	5.7E-02	-1.75	13176
ADRA1A	adrenergic, alpha-1A-, receptor	1.4E-02	-1.77	11549
KCNK7	potassium channel, subfamily K, member 7	3.6E-02	-1.79	16530
C18orf1	chromosome 18 open reading frame 1	2.0E-02	-1.80	52662
PDE6A	phosphodiesterase 6A, cGMP-specific, rod, alpha	2.3E-02	-1.83	225600
CRYBB1	crystallin, beta B1	8.7E-03	-1.87	12960
GPR98	G protein-coupled receptor 98	2.5E-02	-1.88	110789
HTR3B	5-hydroxytryptamine (serotonin) receptor 3B	4.8E-02	-1.88	57014
SSTR2	somatostatin receptor 2	3.9E-02	-1.96	20606
PTF1A	pancreas specific transcription factor, 1a	9.9E-02	-2.04	19213
ADAM32	ADAM metallopeptidase domain 32	6.0E-02	-2.10	353188
NIPSNAP3A	nipsnap homolog 3A (C. elegans)	3.3E-02	-2.13	66536
CD96	CD96 molecule	2.3E-03	-2.28	84544

*Genes represented by bold lettering have been verified by pPCR in mouse islets.

Human islet microarray analysis identified genes that can be connected to diabetes.

To identify similarly upregulated genes in mouse and human islet that could link VDR activity to increased insulin secretion, we performed global gene expression profiling by microarray in human islets. Human pancreatic islets were obtained from a cadaveric donor and were cultured for 16 hours in the presence of 20 nM VitD or vehicle (DMSO) with duplicate biologic samples prepared for each condition. The well known VitD target gene Cytochrome P450, family 24, subfamily A, polypeptide 1 (Cyp24a1) showed the highest upregulation, thereby confirming the efficacy of our VitD treatment. 90 of the most highly upregulated genes from the microarray are listed in Table 4.2. There, cacna1e (CaV2.3) is identified as the 44th most highly upregulated gene in human islets, discussions regarding the role of CaV2.3 in islets is located in chapter 2. To find possible candidates for the VitD-enhanced insulin secretion we performed an *in silico* analysis using Ingenuity Pathway Analysis software. That search identified 68 upregulated genes and 79 down-regulated genes that have a direct or indirect connection to T1D and T2DM (Table 4.3).

Table 4.2. Microarray results from human islets treated with VitD.

	Stats	ratio	Gene Identifier	Gene ID
1	0.0002	149.94	NM_000782	CYP24A1
2	0.0005	24.79	NM_000776	CYP3A
3	0.0000	23.25	AL359584	BXDC5
4	0.0026	22.38	BF941046	EFHB
5	0.0002	20.03	BC034633	CLK4
6	0.0002	18.82	AF189251	TAPT1
7	0.0170	17.30	BC038840	NAALAD2
8	0.0128	16.98	AW205659	CMAH
9	0.0068	14.42	AL556703	CP
10	0.0020	14.36	AW665184	LOC283484
11	0.0046	13.86	NM_018557	LRP1B
12	0.0035	13.85	M21121	CCL5
13	0.0031	12.93	NM_005295	GPR22
14	0.0203	12.83	AL832635	VWA3B
15	0.0438	12.63	AI928218	ATP1B3
16	0.0135	12.44	BC036786	CDH7
17	0.0240	12.35	BC036592	GABRB2
18	0.0208	12.16	BE467321	SIN3A
19	0.0448	11.58	BC038806	PHLDB2
20	0.0054	11.12	AK058122	CCDC67
21	0.0079	10.30	NM_014211	GABRP
22	0.0202	10.20	NM_002886	RAP2B
23	0.0289	10.11	AI699994	PMP2
24	0.0017	9.88	NM_021955	GNGT1
25	0.0204	9.75	AF047190	SARDH
26	0.0053	9.63	AF388367	CLRN1OS
27	0.0003	8.84	AL832631	SLC9A11
28	0.0147	8.59	AI809341	PTPRC
29	0.0125	8.56	NM_007347	AP4E1
30	0.0064	8.31	AF494535	PPP1R1C
31	0.0057	8.28	AF318328	AVIL
32	0.0374	8.26	NM_001464	ADAM2
33	0.0039	8.26	NM_014659	HSPPD2A
34	0.0046	8.24	K03206	PRB1
35	0.0451	8.24	AB028977	SV2C
36	0.0089	8.01	AA779495	PTPRA
37	0.0017	7.87	NM_001446	FABP7
38	0.0179	7.86	AY063454	D21S2090E
39	0.0092	7.81	NM_001566	INPP4A
40	0.0407	7.81	NM_139319	SLC17A8
41	0.0441	7.72	AA193477	NUB1
42	0.0349	7.55	AI817264	SP6
43	0.0100	7.38	NM_003446	ZNF157
44	0.0059	7.21	R15004	CACNA1E
45	0.0031	7.21	AK094684	FLJ16686
46	0.0251	7.21	AA772306	SPTBN1
47	0.0042	7.08	NM_000515	GH1
48	0.0118	7.02	BF574523	TTN
49	0.0015	7.01	NM_018063	HELLS
50	0.0448	6.95	M61872	ZNF92
51	0.0104	6.81	NM_013959	NRG1
52	0.0244	6.81	AK096159	PGM5P1
53	0.0394	6.76	AF429305	RMST
54	0.0151	6.71	NM_002559	P2RX3
55	0.0023	6.68	AF288209	B3GNT2
56	0.0035	6.65	AF276292	KIR2DL4
57	0.0067	6.63	AJ296272	LHX9
58	0.0065	6.46	NM_006790	MYOT
59	0.0453	6.45	H20055	GRIA4
60	0.0213	6.41	AL136754	ARMC2
61	0.0039	6.39	BG334196	EHBP1L1
62	0.0077	6.37	AA974579	FAM70B
63	0.0093	6.34	NM_000660	TGFB1
64	0.0314	6.28	AF284435	IL1RAPL1
65	0.0019	6.24	BC028414	TBC1D26
66	0.0116	6.21	AA503373	TCEA3
67	0.0094	6.17	NM_000579	CCR5
68	0.0303	6.09	BC013753	ACSM5
69	0.0338	5.92	AB000277	DLGAP1
70	0.0131	5.80	AI809779	C10orf79
71	0.0228	5.79	AA524895	CCDC74B
72	0.0167	5.78	NM_014433	RTDR1
73	0.0036	5.68	M17263	C8G
74	0.0072	5.64	NM_012144	DNAI1
75	0.0425	5.61	AI417992	EIF3M
76	0.0062	5.59	NM_005031	FXYD1
77	0.0199	5.56	AF319439	FCRL2
78	0.0459	5.52	BC000513	CHRNA3
79	0.0180	5.51	X02162	APOA1
80	0.0369	5.50	AF166327	NOX1
81	0.0037	5.50	AL565812	PTN
82	0.0387	5.47	AL161984	FRMD7
83	0.0234	5.46	NM_000330	RS1
84	0.0004	5.45	AI917627	SLC19A1
85	0.0485	5.39	NM_001882	CRHBP
86	0.0224	5.36	BC031223	MPZL3
87	0.0004	5.33	X90579	CYP3A5
88	0.0035	5.30	X63575	ATP2B2
89	0.0414	5.28	BC017828	ART1
90	0.0461	5.25	BG413572	MAGIX

Table 4.3. IPA analysis - Genes connected to diabetes from human islet microarray

Symbol	Entrez Gene Name	Fold Change	p-value	Entrez Gene ID
CLK4	CDC-like kinase 4	19.4	1.9E-04	57396
NAALAD2	N-acetylated alpha-linked acidic dipeptidase 2	17.05	1.8E-02	10003
CP	ceruloplasmin (ferroxidase)	14.41	6.1E-03	1356
LRP1B	low density lipoprotein receptor-related protein 1B	13.49	4.3E-03	53353
CDH7	cadherin 7, type 2	12.78	1.3E-02	1005
VWA3B	von Willebrand factor A domain containing 3B	12.7	2.2E-02	200403
GABRB2	gamma-aminobutyric acid (GABA) A receptor, beta 2	12.26	2.3E-02	2561
PHLDB2	pleckstrin homology-like domain, family B, member 2	11.58	4.3E-02	90102
GABRP	gamma-aminobutyric acid (GABA) A receptor, pi	10.44	7.2E-03	2568
SARDH	sarcosine dehydrogenase	9.71	1.9E-02	1757
AP4E1	adaptor-related protein complex 4, epsilon 1 subunit	8.45	1.1E-02	23431
SPTBN1	spectrin, beta, non-erythrocytic 1	7.19	2.4E-02	6711
CACNA1E	**calcium channel, voltage-dependent, R type, alpha 1E subunit**	7.17	6.9E-03	777
GH1	growth hormone 1	7.02	3.9E-03	2688
GRIA4	glutamate receptor, ionotrophic, AMPA 4	6.46	4.7E-02	2893
TGFB1	**transforming growth factor, beta 1**	6.24	9.5E-03	7040
CD44	CD44 molecule (Indian blood group)	6.2	1.4E-02	960
AKNAD1	AKNA domain containing 1	6.13	6.7E-04	254268
GNAS	GNAS complex locus	6.12	6.2E-02	2778
IGF1	insulin-like growth factor 1 (somatomedin C)	5.99	4.8E-02	3479
DLGAP1	discs, large (Drosophila) homolog-associated protein 1	5.93	3.5E-02	9229
DNAI1	dynein, axonemal, intermediate chain 1	5.62	7.1E-03	27019
APOA1	apolipoprotein A-I	5.57	1.6E-02	335
CHRNA3	cholinergic receptor, nicotinic, alpha 3	5.39	4.9E-02	1136
AOC3	amine oxidase, copper containing 3	5.14	3.6E-02	8639
EPHA5	EPH receptor A5	5.05	2.8E-03	2044
CSF1	colony stimulating factor 1 (macrophage)	4.84	7.0E-03	1435
MTOR	mechanistic target of rapamycin	4.83	2.8E-02	2475
CCDC40	coiled-coil domain containing 40	4.82	1.6E-02	55036
GRIK1	glutamate receptor, ionotropic, kainate 1	4.73	2.8E-02	2897
WDR93	WD repeat domain 93	4.66	5.7E-02	56964
CCDC11	coiled-coil domain containing 11	4.57	4.2E-02	220136
F11	coagulation factor XI	4.53	1.3E-02	2160

CC2D2A	coiled-coil and C2 domain containing 2A	4.52	4.0E-02	57545
NEK6	NIMA (never in mitosis gene a)-related kinase 6	4.43	4.5E-03	10783
IL22	interleukin 22	4.3	2.8E-03	50616
DPCR1	diffuse panbronchiolitis critical region 1	4.19	3.4E-02	135656
C14orf166B	chromosome 14 open reading frame 166B	3.92	3.6E-03	145497
SLC24A4	solute carrier family 24, member 4	3.9	2.0E-02	123041
SORCS3	sortilin-related VPS10 domain containing receptor 3	3.88	4.8E-02	22986
PON1	paraoxonase 1	3.86	5.3E-02	5444
AUTS2	autism susceptibility candidate 2	3.84	2.4E-02	26053
KCNT2	potassium channel, subfamily T, member 2	3.75	6.7E-02	343450
IL2RA	interleukin 2 receptor, alpha	3.48	4.4E-02	3559
SMARCA4	SWI/SNF related, matrix associated, actin dependent regulator of chromatin, subfamily a, member 4	3.47	4.5E-02	6597
CA9	carbonic anhydrase IX	3.41	1.8E-02	768
LOC339505	hypothetical LOC339505	3.38	6.5E-02	339505
CAND2	cullin-associated and neddylation-dissociated 2	3.27	1.2E-02	23066
SPAG6	sperm associated antigen 6	3.17	1.7E-03	9576
UBE2Z	ubiquitin-conjugating enzyme E2Z	3.1	3.8E-02	65264
ATPBD4	ATP binding domain 4	3.03	3.5E-02	89978
EBF3	early B-cell factor 3	2.97	5.2E-02	253738
SYNE2	spectrin repeat containing, nuclear envelope 2	2.92	2.2E-02	23224
LSAMP	limbic system-associated membrane protein	2.64	4.8E-02	4045
FLJ43663	hypothetical LOC378805	2.63	5.0E-02	378805
SLC38A10	solute carrier family 38, member 10	2.42	7.0E-02	124565
PREX2	phosphatidylinositol-3,4,5-trisphosphate-dependent Rac exchange factor 2	2.39	1.2E-02	80243
MOBKL2B	MOB1, Mps One Binder kinase activator-like 2B	2.29	6.8E-02	79817
CUX2	cut-like homeobox 2	2.24	6.8E-02	23316
ZZEF1	zinc finger, ZZ-type with EF-hand domain 1	2.16	3.2E-02	23140
HTR2C	5-hydroxytryptamine (serotonin) receptor 2C	2.12	2.2E-02	3358
ADAMTSL1	ADAMTS-like 1	2.09	1.7E-02	92949
GAD2	glutamate decarboxylase 2	2.09	1.9E-02	2572
PYROXD2	pyridine nucleotide-disulphide oxidoreductase domain 2	2.08	1.8E-02	84795
C2	complement component 2	2.07	7.9E-03	717
GATS	GATS, stromal antigen 3 opposite strand	2.04	2.8E-02	352954
HLA-DQB2	major histocompatibility complex, class II, DQ beta 2	2.03	5.3E-02	3120
UBQLNL	ubiquilin-like	2.03	2.4E-02	143630

ANO2	anoctamin 2	-2.01	4.2E-03	57101
CTNS	cystinosin, lysosomal cystine transporter	-2.11	1.2E-02	1497
NRP2	neuropilin 2	-2.16	5.6E-02	8828
CLASP2	cytoplasmic linker associated protein 2	-2.21	3.0E-02	23122
TBRG4	transforming growth factor beta regulator 4	-2.21	4.9E-02	9238
CALB1	calbindin 1, 28kDa	-2.26	6.5E-02	793
DOCK9	dedicator of cytokinesis 9	-2.27	5.8E-02	23348
MAST2	microtubule associated serine/threonine kinase 2	-2.28	2.4E-02	23139
MS4A14	membrane-spanning 4-domains, subfamily A, member 14	-2.3	2.4E-02	84689
ZFP57	zinc finger protein 57 homolog (mouse)	-2.31	4.1E-02	346171
CIT	citron (rho-interacting, serine/threonine kinase 21)	-2.33	7.3E-04	11113
GABRD	gamma-aminobutyric acid (GABA) A receptor, delta	-2.39	7.9E-04	2563
GHRHR	growth hormone releasing hormone receptor	-2.42	1.1E-02	2692
GPR133	G protein-coupled receptor 133	-2.5	5.1E-03	283383
MAST4	microtubule associated serine/threonine kinase family member 4	-2.5	3.1E-02	375449
PPP2R2C	protein phosphatase 2, regulatory subunit B, gamma	-2.51	6.0E-02	5522
NOD2	nucleotide-binding oligomerization domain containing 2	-2.6	5.6E-02	64127
ENPP1	ectonucleotide pyrophosphatase/phosphodiesterase 1	-2.61	4.7E-02	5167
C1orf21	chromosome 1 open reading frame 21	-2.62	6.6E-02	81563
CNTNAP4	contactin associated protein-like 4	-2.64	4.8E-02	85445
FRMD4A	FERM domain containing 4A	-2.66	1.1E-02	55691
ATP2C2	ATPase, Ca++ transporting, type 2C, member 2	-2.68	6.4E-02	9914
LASS3	LAG1 homolog, ceramide synthase 3	-2.72	2.7E-03	204219
DSCAM	Down syndrome cell adhesion molecule	-2.73	1.4E-02	1826
SRGAP1	SLIT-ROBO Rho GTPase activating protein 1	-2.75	4.1E-03	57522
ZNHIT6	zinc finger, HIT-type containing 6	-2.77	5.3E-02	54680
FGFR2	fibroblast growth factor receptor 2	-2.8	3.5E-03	2263
FAM19A2	family with sequence similarity 19, member A2	-2.82	4.9E-02	338811
GRID1	glutamate receptor, ionotropic, delta 1	-2.86	4.5E-02	2894
PAX5	paired box 5	-2.89	1.2E-02	5079
MGC34774	ribosomal protein L13a pseudogene 17	-2.9	2.0E-02	399670
ERC1	ELKS/RAB6-interacting/CAST family member 1	-3.1	9.5E-03	23085
TACR1	tachykinin receptor 1	-3.14	1.1E-02	6869
SFTA3	surfactant associated 3	-3.3	1.5E-02	253970
HERC4	hect domain and RLD 4	-3.33	1.0E-02	26091
SCN7A	sodium channel, voltage-gated, type VII, alpha	-3.37	1.9E-03	6332

IGHG1	immunoglobulin heavy constant gamma 1	-3.46	6.5E-02	3500
PTPN22	protein tyrosine phosphatase, non-receptor type 22	-3.63	4.4E-02	26191
TMF1	TATA element modulatory factor 1	-3.67	3.9E-03	7110
IL21R	interleukin 21 receptor	-3.8	4.2E-02	50615
PITPNC1	phosphatidylinositol transfer protein, cytoplasmic 1	-3.85	1.3E-02	26207
MASP1	mannan-binding lectin serine peptidase 1	-3.97	2.9E-02	5648
SLC6A2	solute carrier family 6, member 2	-4.02	4.2E-02	6530
ANKFY1	ankyrin repeat and FYVE domain containing 1	-4.04	4.0E-02	51479
KSR1	kinase suppressor of ras 1	-4.06	3.6E-02	8844
CNTRL	Centriolin	-4.07	6.7E-02	11064
DOC2A	double C2-like domains, alpha	-4.07	6.0E-02	8448
NFYA	nuclear transcription factor Y, alpha	-4.16	5.9E-02	4800
PTHLH	parathyroid hormone-like hormone	-4.2	3.4E-02	5744
PPP3CC	protein phosphatase 3, catalytic subunit, gamma isozyme	-4.33	5.8E-02	5533
CHD5	chromodomain helicase DNA binding protein 5	-4.34	3.3E-02	26038
CHRM4	cholinergic receptor, muscarinic 4	-4.34	3.9E-02	1132
NCOA7	nuclear receptor coactivator 7	-4.35	2.4E-02	135112
CHRM3	cholinergic receptor, muscarinic 3	-4.46	1.3E-03	1131
BNC2	basonuclin 2	-4.53	3.9E-02	54796
ZNF804B	zinc finger protein 804B	-4.59	5.6E-02	219578
TNXB	tenascin XB	-4.72	9.1E-05	7148
YPEL2	yippee-like 2 (Drosophila)	-5.03	6.6E-02	388403
TGM2	transglutaminase 2	-5.26	4.7E-02	7052
VASH2	vasohibin 2	-5.31	5.8E-02	79805
CCDC13	coiled-coil domain containing 13	-5.32	8.1E-03	152206
GRIN2C	glutamate receptor, ionotropic, N-methyl D-aspartate 2C	-5.52	5.6E-03	2905
PTPN11	protein tyrosine phosphatase, non-receptor type 11	-5.59	4.2E-02	5781
EPOR	erythropoietin receptor	-5.61	1.0E-02	2057
E2F2	E2F transcription factor 2	-5.98	4.4E-02	1870
ZKSCAN3	zinc finger with KRAB and SCAN domains 3	-6.97	2.4E-02	80317
KCNK1	potassium channel, subfamily K, member 1	-7.51	2.4E-02	3775
TTLL5	tubulin tyrosine ligase-like family, member 5	-7.55	4.9E-02	23093
HEATR1	HEAT repeat containing 1	-8	3.4E-02	55127
CD96	CD96 molecule	-8.26	6.7E-02	10225
YPEL4	yippee-like 4 (Drosophila)	-8.35	3.5E-02	219539
PPP1R12B	protein phosphatase 1, regulatory (inhibitor) subunit 12B	-9.3	7.0E-03	4660
ESR2	estrogen receptor 2 (ER beta)	-9.43	2.1E-03	2100

PLD5	phospholipase D family, member 5	-9.6	3.9E-02	200150
ITGBL1	integrin, beta-like 1 (with EGF-like repeat domains)	-10.46	2.7E-02	9358
CCDC85A	coiled-coil domain containing 85A	-11.56	1.7E-02	114800
CLIC5	chloride intracellular channel 5	-11.62	1.6E-02	53405
LOC400550	hypothetical LOC400550	-12.46	5.5E-02	400550
C11orf58	chromosome 11 open reading frame 58	-15.49	5.8E-02	10944

*Genes represented by bold lettering have been verified by pPCR in mouse islets.

13 genes are commonly regulated by VitD in mouse and human islets.

As our experimental design was identical between the mouse and the human islets that were utilized for the microarray analysis we had a unique opportunity to compare the results from both arrays to find commonly regulated genes. The IPA software has a comparison feature that enables this type of analysis, even between species, to find commonly regulated genes. The comparison between the mouse and human array revealed 13 VitD-regulated genes, 8 were upregulated and 5 were downregulated (Table 4.4). Unsurprisingly, Cyp24a1 was at the top of the list for co-regulated genes.

Further analysis of the 13 commonly regulated genes revealed that 2 of them have a connection to diabetes (TGFB1 and CD96). Transforming growth factor beta 1 (Tgfb1) was upregulated by VitD in both mouse and human microarray (table 4.4). Furthermore, upregulation of Tgfb1 was confirmed by qPCR in mouse islets (Figure 4.3). VitD upregulates Tgfb1 approximately 2-fold in wildtype islets but shows no effect in *Vdr*$^{-/-}$ islets, however, its transcript level is basally higher in *Vdr*$^{-/-}$ islets. Tgfb1 regulates proliferation, differentiation, adhesion, migration, and many other cellular functions. Additionally, a certain Tgfb1 allele has been associated with type 2 diabetes [127]. The

other diabetes-associated gene is CD96, which was down-regulated in human and mouse islets (table 4.4). A single nucleotide polymorphism in CD96 has been associated with type 2 diabetes [126]. CD96 might also be of interest to T1DM as CD96 is primarily expressed in T-cells and may play a role in interactions of activated T and NK cells during the late phase of the immune response [128].

Table 4.4 – VitD regulated genes common to both human and mouse microarray

Symbol	Human			Mouse		
	Fold Change	p-value	Entrez Gene ID	Fold Change	p-value	Entrez Gene ID
CYP24A1	146.79	0.000	1591	42.29	0.026	13081
TAL1	7.43	0.000	6886	1.57	0.020	21349
TGFB1	**6.23**	**0.009**	**7040**	**2.28**	**0.054**	**21803**
CYP2C18	4.57	0.003	1562	3.13	0.003	72082
TLX3	4.01	0.009	30012	1.68	0.011	27140
SDC3	3.51	0.022	9672	1.73	0.009	20970
TTLL10	2.78	0.059	254173	1.56	0.006	330010
FGA	2.12	0.031	2243	2.90	0.070	14161
KLK7	-2.88	0.067	5650	-1.57	0.091	23993
UBE3A	-3.99	0.056	7337	-1.52	0.069	22215
PHACTR1	-6.04	0.003	221692	-1.54	0.050	218194
CD96	**-8.26**	**0.067**	**10225**	**-2.28**	**0.002**	**84544**
NEK1	-11.86	0.015	4750	-1.75	0.017	18004

Genes in bold have been previously identified as having a connection to diabetes

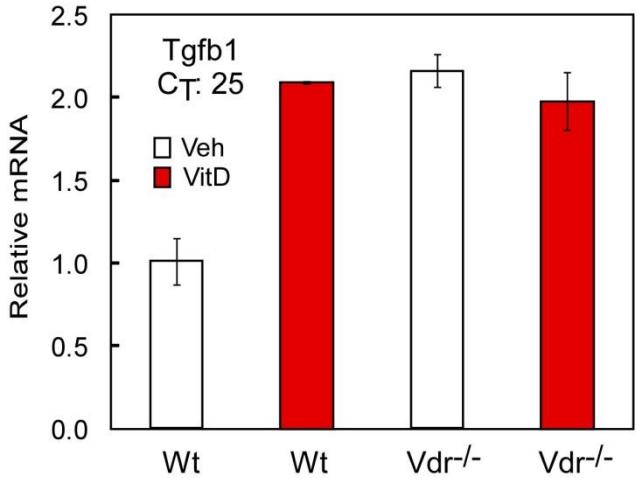

Figure 4.3. Validation of vitamin D induced upregulation of Tgfb1 suggested by mouse and human microarray. qPCR results from wildtype and *Vdr*$^{-/-}$ islets, cultured in 11 mM glucose and treated with 20 nM Vit D or vehicle (DMSO) for 16 hours.

4.5 Discussion

We performed microarray analyses in mouse and human islets to find VitD-regulated genes that might be related to T1DM and T2DM. The experimental design employed for the mouse islet studies assured that all regulated genes were VDR-dependent (not altered in islets from *Vdr*$^{-/-}$ mice). However, with a VitD treatment period of 16 hours in length, we may be observing both direct VDR target genes (for which VDR binds enhancer elements to directly regulate the transcription of that gene) that show altered expression quickly, and secondary targets that occur later by an indirect manner. In this report we have primarily focused on genes that have been associated with insulin secretion and beta cell function, as our previous studies have revealed that VitD/VDR can enhance glucose-stimulated insulin secretion. However genes with reported functions in other molecular pathways, which could impact islet biology, were also identified. Some of the most

highly upregulated genes in the human and mouse microarray are genes of currently unknown function. Further studies are needed to determine their significance.

Genes that can be connected to insulin secretion were more abundant in the mouse microarray compared to the human microarray. However, even though these genes are not upregulated by VitD in human islets they are still of interest to diabetes research. All genes connecting VitD-treatment to improved beta cell function might prove to be potential drug targets to treat diabetes. The genes identified in the mouse microarray, and validated by qPCR in mouse islets, can be segregated into several groups; first, genes involved in survival, proliferation and migration; second, genes involved in vesicle transport; third, genes involved in insulin signaling and finally, genes involved in calcium mobilization and/or associated with diabetes. Potential roles of all validated genes are represented in figure 4.4.

Group 1 contains genes involved in survival, proliferation and migration. Many of them have been shown to affect neurite extension and the differentiation and survival of neurons (Slitrk1 [94, 95], Nedd9 [96-98], Amigo2 [100, 101], and PRG-3 [41]). This is a recurring theme in beta cell biology, as key transcription factors (e.g. NeuroD1, [129]) and even neurotransmitter signaling systems (e.g. serotonin, [130]) commonly considered as neural regulatory pathways are being recognized for their important roles in beta cell function. Genes identified here could also be involved in neural innervation mechanisms essential for proper islet development *in vivo* [131, 132]. Nedd9, might also have a role in insulin secretion, as it has been shown to be involved in reorganization of the actin skeleton [98], and actin rearrangement is an important component of insulin secretion [133]. Other genes in group 1 have been implicated in growth factor signaling (Gpc6,

Gdf10 and Tgfb1). Gpc6 is a heparan sulfate proteoglycan that regulates growth factor receptors and therefore can affect cellular response to extracellular stimuli [99]. Gdf10, by similarity to morphogenetic protein-3 (Bmp3), might be involved in an autocrine system to affect growth and differentiation of islet cells [104]. The role of another growth factor, Tgfb1, is discussed below. Gadd45a and KIAA1199 are upregulated in response to stress and seem to have growth haltering effect on cells. These genes work as tumor suppressors and might be involved in cell repair or apoptosis of damaged cells [134-136]. Additionally, a close relative of Gadd45a has been shown to improve survival of beta cells in response to cytokine treatment [105]. The last gene in group 1 is H2-Bl, this gene shows a very impressive 70-fold upregulation in response to VitD-treatment. H2-Bl might be of special interest to T1DM as it aids in the evasion of cells from natural killer T cell attack [106].

Group 2 contains genes involved in vesicle transport (Tmem27, Stx18 and Sytl2) Transmembrane protein 27 (Tmem27) has been shown to enhance SNARE-mediated insulin secretion [109-111], enhance beta cell proliferation [110, 112] and it is transcriptionally upregulated when beta cells are incubated in high glucose [137]. Syntaxin 18 (Stx18), plays a role in organization of the endoplasmic reticulum (ER), participates in post-Golgi transport and is a susceptibility gene for T2DM [108, 113, 114]. Recently, Stx18 was identified, among other proteins, to be required for constitutive secretion in mammalian cells [138], making it a very strong candidate for insulin secretion. Last in the category is Synaptotagmin-like 2 (Sytl2), which is an exocytic sensor for Ca^{2+} signaling systems that has been shown to enhance secretion in multiple cell systems [115-117]. However, it is unlikely that Sytl2 is an effector in insulin

secretion, as it has been reported to be expressed selectively in alpha cells. The same report showed a reduction in glucagon secretion when Sytl2 was over-expressed in an alpha cell line [115]. Therefore the VitD-induced increase in Sytl2 transcription might negatively affect glucagon secretion.

Group 3 contains genes involved in insulin signaling (Dok5, Arrb2 and Kl). Docking protein 5 (Dok5) and Arrestin, beta 2 (Arrb2) have been shown to augment the insulin signaling pathway [118-121]. Beta cells express all components of the insulin receptor-signaling pathway and are capable of responding to secreted insulin in an autocrine and paracrine manner. This insulin signaling capability has proven to be an important component in beta cell function, expansion and survival [139-142]. Klotho (Kl) is a type 1 transmembrane protein that is cleaved from the membrane, a process that is enhanced by insulin. The secreted Klotho can then affect ion channel localization [58, 60]. Additionally, our data (reviewed in chapter 3) suggests that Klotho might have an important role in the beta cell by affecting membrane localization of Glucose transporter 2 (GLUT-2).

Group 4 contains genes involved in calcium mobilization and/or associated with diabetes (Tacr3, Cacna2d3, Ak5 and Csnk). Tachykinin receptor 3 (TacR3) is a G-protein couple receptor that is associated with G-proteins that activate a phosphatidylinositol-calcium second messenger system [122]. TacR3 is a receptor for the neuropeptide neurokinin B, which can affect both endocrine and exocrine secretion [143]. Calcium channel, voltage-dependent a2/d3 subunit (Cacna2d3) is a susceptibility gene for T2DM and its expression is upregulated in the presence of IGF-1 [108, 123]. Cacna2d3 is a regulatory subunit that controls trafficking and activity of voltage-gated calcium

channels, which are critical to insulin secretion. Adenylate kinase 5 (AK5) activity impacts the ATP/ADP ratio and has been shown to regulate K-ATP channel activity, additionally, it is a susceptibility gene for T2DM [108, 124]. K-ATP channels play a critical role in insulin secretion as their closure, in response to an increase in the ATP/ADP ratio, is necessary for depolarization and activation of voltage-gated calcium channels (Figure 4.4). Finally there is Casein kappa (Csnk), a susceptibility gene for T2DM that acts as a chaperone for otherwise insoluble calcium-phosphate in breast milk [125, 126, 144]. Furthermore it might also play a role in stabilizing proteins from unfolding and aggregating [78]. The presence of Csnk in islet is intriguing as it has only been reported to have a function in lactating mammary glands. Csnk has been reported to bind to insulin and might therefore possibly act in the beta cell as an insulin chaperone [144]. However, it might also play a role in controlling the intracellular concentration of free calcium and phosphate.

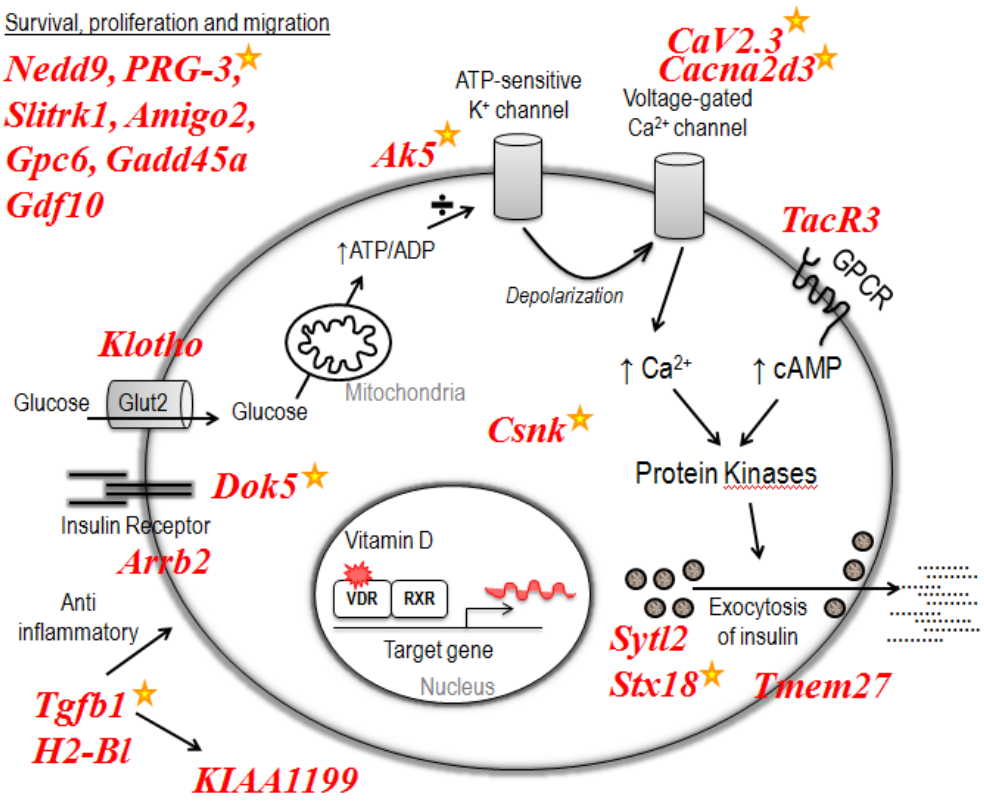

Figure 4.4. Suggested role of qPCR validated genes found in mouse and human microarray. See text for details. Genes labeled with a star have been associated with diabetes in genome wide studies.

As experimental design was identical between the mouse and the human islets that were utilized for the microarray analysis we had a unique opportunity to compare the results from both arrays to identify commonly regulated genes. The most intriguing co-regulated gene is Tgfb1, which exhibited VitD-dependent upregulation in both mouse and human islet microarrays and was confirmed by qPCR in mouse iselts. Tgfb1 upregulation might have implications for both T1DM and T2DM. A certain Tgfb1 allele has been associated with type 2 diabetes [127] and there are multiple reports showing that Tgfb1

prevents progression of diabetes in NOD mice [145-147]. Additionally, Tgfb1 transgenic mice have improved beta cell function and regeneration capacity [148].

Another co-regulated gene, cacna1e (CaV2.3), was identified when a few selected human array genes were tested by qPCR in mouse islets. Cacna1e was not identified in the mouse microarray but it has been repeatedly validated in mouse islets by qPCR. This shows that there might still be other conserved VitD target genes in islets that we have missed in our analysis. CaV2.3 is another good candidate for the VitD-enhanced GSIS as it has been implicated in insulin secretion and is a susceptibility gene for T2DM [50-52, 108].

In summary this is the first detailed report on VitD-regulated gene expression in mouse and human islets identifying multiple genes with interesting links to insulin secretion and improved beta cell function. Further research is needed to fully understand to what extent each individual gene contributes beta cell function. Another, perhaps more likely scenario is a multi-gene effect, where VDR turns on transcription of an array of genes that concomitantly affect beta cell function. Finally, we hope that this report will excite further research on the role of VDR in the endocrine pancreas as a component of VitD effects in T1DM and T2DM.

CHAPTER FIVE

Conclusions and Recommendations for future studies

5.1 Vitamin D-induced GSIS and calcium influx studies

Conclusions and implications

My dissertation research has clearly demonstrated that VDR is highly expressed in islets. Furthermore, it is present at nRNA levels comparable to kidney and small intestine, suggesting that VDR has an important function in islets. Even tissues that have been reported to respond to VitD, for example liver [149], white adipose tissue [150] and muscle [151], contain miniscule amounts of VDR mRNA compared to islets. Another interesting observation is that VDR levels themselves, are induced by high glucose in islets, suggesting an increased need for VDR action once glucose level rises.

Most importantly, my studies provide the first report that describes VitD-enhanced GSIS. I have discovered that preincubation of isolated mouse and human islets with VitD leads to enhanced glucose-stimulated insulin secretion (GSIS). This response is VDR-dependent, as no VitD-mediated change in GSIS is observed in islets obtained from *Vdr*-null mice. Of great significance is the increase in insulin secretion observed at 0.2 nM, which is a physiological concentration of VitD. However, must of my studies are performed using 20 nM VitD (a level commonly used in cell culture systems), which is non-toxic as no VitD-effect was observed in GSIS samples exposed to low glucose and no effect was observed in $Vdr^{-/-}$ islets. In line with the VitD-protective role in islets, we observed a reduction in low-glucose stress-induced insulin secretion in human islets.

Furthermore we reproduced the VDR-enhanced GSIS by using a 2nd VDR ligand, LCA, further supporting the role of VDR in insulin secretion.

Results from our studies suggest that VitD does not affect GSIS by enhancing *insulin* gene expression, nor does it change glucose uptake into primary beta cells. VitD does however increase glucose-stimulated calcium uptake, suggesting that VitD affects transcription of genes involved in calcium flux into the beta cell.

These findings tie well with the multiple epidemiological studies have implicated Vitamin D deficiency in the development of T2DM. However no reports have described any mechanism(s) linking VitD status with pancreatic islet function. Therefore, my studies focused on the role of Vitamin D and VDR in islet biology.

To identify molecular mechanisms linking VDR activity to increased insulin secretion and increased glucose-stimulated calcium uptake, we took an unbiased microarray approach using human islets treated with VitD. The microarray revealed multiple genes involved in calcium transport and signaling. One of these genes is the R-type voltage-gated calcium channel, CaV2.3, which has previously been reported to be linked to insulin secretion and Type 2 Diabetes. We confirmed its upregulation by qPCR in mouse islets, suggesting that CaV2.3 is a target gene in mouse and human islets. To support that, we identified a strong VDR binding element within intron 7 of the Cav2.3 gene that is conserved in mouse and man. Another voltage gated calcium channel subunit was identified to be transcriptionally upregulated in mouse islets; that gene is *cacna2d3*, an auxiliary subunit that has been reported to affect activity and membrane localization of multiple voltage gated calcium channels.

In summary, our findings support a role for vitamin D signaling in the transcriptional regulation of voltage gated calcium channels and calcium uptake, which enhance glucose-stimulated insulin secretion by beta cells of the endocrine pancreas. The results from my dissertation work are especially valuable to the field because this is the first report suggesting a mechanism that links VitD status to insulin secretion.

Recommendations for future studies

Future studies should include further examination of the increased glucose-induced calcium influx observed after VitD pretreatment of primary beta cells. In particularly employment of clamp studies, to identify the characteristics of the calcium current, and calcium imaging studies, that can exploit the plethora of calcium channel inhibitors available.

Additional mouse models, including global or beta cell selective *CaV2.3*$^{-/-}$ mice to use for islet isolation would be immensely valuable. By using islets from *CaV2.3*$^{-/-}$ mice and wildtype littermates, one could determine how much of the VitD-enhanced GSIS is caused by *CaV2.3* upregulation. Furthermore, beta cell selective *Vdr*$^{-/-}$ mice would allow us to evaluate the contribution of VDR effects in islets or/and whole-animal glucose balance.

Finally, to compliment the reporter assays identifying both conserved and unique VDREs in CaV2.3, chromatin immunoprecipitation studies (ChIP), preferably in mouse and human islets would be valuable. Indeed, with technologic advancements in Chip-Seq, a glocal assessment of VDR binding in islets/beta cells would be very informative, and would complement the microarray analysis already performed.

5.2 Klotho as a target gene of VDR in islets

Conclusions

In addition to *CaV2.3,* we identified a second VDR target gene in islets. This gene is *Klotho,* a key regulator of phosphate homeostasis. Glucose tolerance studies in *Klotho*$^{-/-}$ mice fed a low-phosphate rescue-diet suggest that Klotho's role in metabolism in not entirely dependent on its effect on phosphate homeostasis. However, there might be some connection between islet function and phosphate regulation as islets are able to respond to FGF23 treatment. As Klotho's presence is required for FGF23 signaling it can be concluded that Klotho is sufficiently abundant in islets to be physiologically relevant. Plasma FGF23 levels are elevated under conditions of hyperphosphatemia. Therefore, we suggest that FGF23 signaling has a role in islet biology under conditions of elevated phosphate.

We have established that klotho mRNA and protein are strongly upregulated by VitD pretreatment. A likely candidate mediating that upregulation is a strong VDRE located 7.3 kb upstream from the transcriptional start site. By analysis of islets from *Klotho*$^{-/-}$ mice, we observed an increased number of glucagon positive alpha cells resulting in a shift of the alpha-to-beta cell ratio. This phenotype is independent of phosphate as the same results are obtained in mice on low-phosphate rescue-diet and control diet. Another phenotype we noted in *Klotho*$^{-/-}$ mice is elevated plasma glucagon, under both fed and fasting conditions. These phenotypes, the elevated alpha-to-beta cell ratio and elevated plasma glucagon, are similar to the phenotypes of *GLUT-2*$^{-/-}$ mice. Therefore, pancreatic sections from *Klotho*$^{-/-}$ and wildtype mice were co-stained with anti-insulin and anti-GLUT-2 antibody. These experiments revealed a vast reduction in

membrane localization of GLUT-2 in *Klotho*$^{-/-}$ mice. As N-glycosylation is an important regulator of GLUT-2 membrane localization we suggest that the sialidase activity of Klotho may modulate the half-life of GLUT-2 at the plasma membrane. Glucose uptake studies support that notion; as *Klotho*$^{-/-}$ beta cell glucose uptake is much reduced compared to wildtype beta cells and conversely incubation of wildtype beta cells with recombinant secreted Klotho increases glucose uptake considerably.

Lastly GSIS experiments using *Klotho*$^{-/-}$ and wildtype islets, pretreated with VitD, suggest that Klotho might have a role in the clearly established VitD-enhanced GSIS.

Recommendations for future studies

My dissertation research clearly establishes a role for Klotho in beta cell biology and warrant the production of a mouse strain with a beta cell selective deletion of Klotho. The advantages to a model like that are great: as they would likely have a normal life span; they would be larger; there would be no need for rescue diet; and contribution of islet-localized Klotho to glucose homeostasis could be determined.

To connect sialidase activity of Klotho to GLUT-2 membrane localization several experiments are needed. First of all glycan analysis of GLUT-2 is required both before and after Klotho treatment. Secondly, injection of recombinant Klotho into the bloodstream of *Klotho*$^{-/-}$ mice would establish if secreted Klotho is enough to re-acquire GLUT-2 membrane localization or if beta cell located Klotho is also necessary. Lastly, as there is a connection between Klotho and VitD-enhanced GSIS, one might inject VitD

into *Klotho*$^{-/-}$ and wildtype mice and observe if VitD increases GLUT-2 membrane localization in a Klotho dependent manner.

As for the FGF23/Klotho axis present in islets, we recommend performing studies *in vitro* at first using isolated islets. Here an unbiased approach might be taken by performing microarray or proteomic analysis on islets cultured under control or hyperphosphatemic conditions, cultured with or without FGF23. Results from these studies would then guide future directions.

5.3 Other VDR regulated genes in endocrine pancreas

Conclusions

To identify molecular mechanisms linking VDR activity to increased insulin secretion and increased glucose-stimulated calcium uptake, we performed global gene expression profiling by microarray in mouse and human islets. These studies identified multiple genes associated with islet function, survival and insulin secretion. Some unique to either mouse or human islets but also some that were co-regulated in mouse and human islets. The results provide a needed mechanistic aevaluation, which complements the current clinical and observational reports that exist, regarding potential roles for Vitamin D in the progression of Diabetes. In addition, our identification of numerous Vitamin-D regulated genes of the human and mouse islet can form the basis for future hypothesis-driven research efforts to identify novel therapeutic targets to affect insulin secretion and beta cell function.

Recommendations for future studies

Follow up studies on any of the identified genes would provide important information on the function VitD has in beta cell biology. Of all the genes identified, *Tgfb1* might be the most relevant to diabetes research (in addition to *CaV2.3)*. With many tools available, such as recombinant Tgfb1, *Tgfb1*$^{-/-}$ mice and mouse strains lacking Tgfb1 receptors, elucidating the role(s) of Tgfb1 in VitD mediated enhancement of beta cell function is well justified.

Another consideration is the variable respond observed in human islets treated with VitD (islets available to researchers are often those not adequate for transplantation). This might be a result of islet quality at the time of the experiment, donors might be pre-diabetic (a condition often overseen) or the donors might have been VitD insufficient. However, it might also reflect differences between the genetically diverse human beings. A side by side comparison of islets from multiple donors undergoing both microarray analysis and GSIS studies after VitD or vehicle treatment might further elucidate what genes are important in the VitD-enhanced GSIS.

APPENDIX A

Bile acid effects on mouse islet biology

A.1 Abstract

Bile acids are detergent-like molecules exclusively produced in hepatocytes and secreted as a major component of bile to facilitate the absorption of lipids. For decades it has been recognized that certain cells respond to ectopic bile acids by altering intracellular signal transduction (via cAMP and calcium) and transcription (target genes include bile acid transporters and enzymes of bile acid synthesis). With the discovery of a nuclear bile acid sensor, the farnesoid X receptor (FXR, NR1H4), and a G protein-coupled receptor, TGR5 (also called MBAR, GPBAR1) that bind selected bile acids, the mechanisms that allow bile acids to serve as signaling molecules are being defined. By using *Fxr*$^{-/-}$ mice and *Tgr5*$^{-/-}$ mice, in conjunction with high-affinity, specific, synthetic agonists for each receptor, we have started to elucidate the roles of these receptors in endocrine islets. Our results suggest that these receptors, both responsive to bile acids in this context, have divergent roles in beta cell biology. Activation of FXR increases the expression of genes involved in cell cycle regulation and immune response, whereas activation of TGR5 enhances glucose-stimulated insulin secretion. Initial *in vivo* studies have shown that, bile acid-deficient *Cyp27a1*$^{-/-}$ mice have significantly reduced circulating levels of insulin and glucagon when compared to wild-type littermates. These results suggest that bile acids may regulate beta cell function in multiple ways and are thus of interest for diabetes research.

A.2 Introduction

Bile acids are detergent-like molecules exclusively produced in hepatocytes and secreted as a major component of bile to facilitate the absorption of dietary lipids. The primary bile acids, chenodeoxycholic acid (CDCA) and cholic acid (CA) are converted by gut flora to the secondary bile acids, lithocholic acid (LCA) and deoxycholic acid (DCA), respectively, see Figure A.1. The majority of bile acids are modified by their conjugation to an amino acid (taurine or glycine), which increases their solubility, but limits their membrane permeability. Conjugated bile acids thus require dedicated transport proteins to facilitate their movement into and out of cells. The major bile acid transporters are the sodium-taurocholate cotransporter polypeptide (NTCP, SLC10A1) and bile salt efflux pump (BSEP, ABCB11) of the hepatocyte, and the ileal bile acid transporter (IBAT, SLC10A2) and organic solute transporters (OSTα/β,) of the enterocyte.

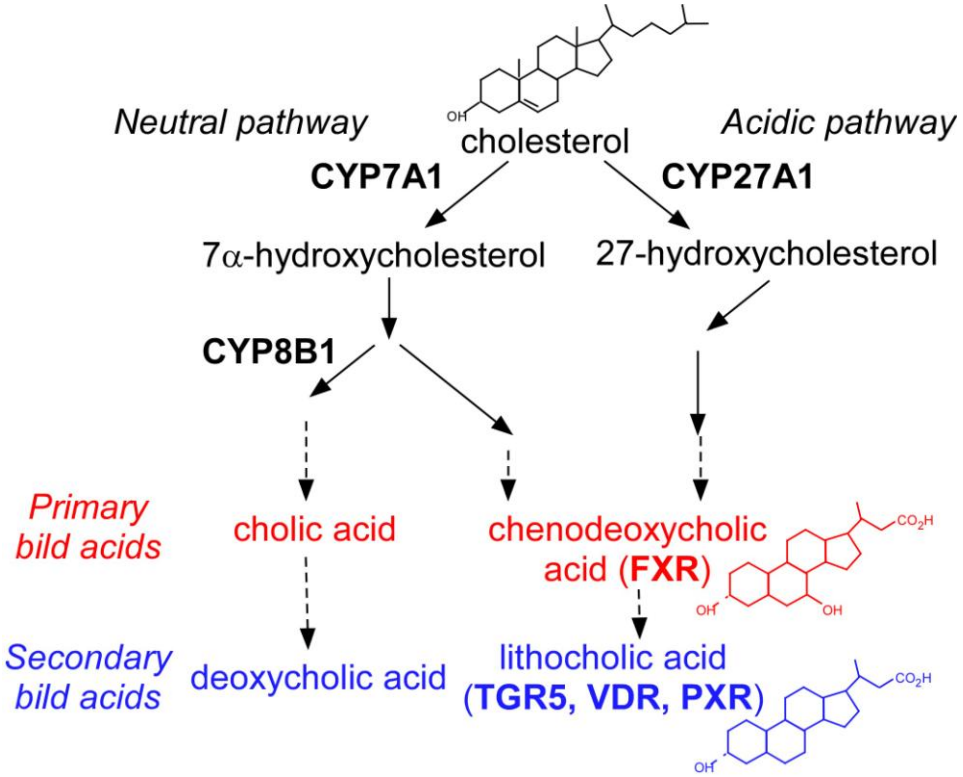

Figure A.1. Major pathways for synthesis of primary (from liver) and secondary (modified by gut flora) bile acids. Only selected enzymes and substrates/products are illustrated. Provided in parentheses are receptors that are bound and activated by selected bile acids. Abbreviations include: CYP7A1, cholesterol 7α-hydroxylase; CYP27A1, sterol 27-hydroxylase; CYP8B1, sterol 12α-hydroxylase; FXR, farnesoid X receptor, TGR5, bile acid G protein-coupled receptor; VDR, vitamin D receptor; and PXR, pregnane X receptor. See text for further details.

The conversion of cholesterol to bile acids occurs in hepatocytes and involves at least fifteen different enzymes (reviewed in [152]). There are two bile acid biosynthetic pathways: the classic (neutral) pathway initiated by the rate-limiting enzyme cholesterol 7α-hydroxylase, CYP7A1; and the alternative (acidic) pathway in which the mitochondrial sterol 27-hydroxylase, CYP27A1, is the first enzyme (Figure A.1). The expression of CYP7A1 is dramatically repressed by bile acids via a transcriptional mechanism. In addition, CYP8B1, an enzyme of the neutral pathway that catalyzes 12-

hydroxylation to alter the ratio of cholic and chenodeoxycholic acids, is similarly repressed by bile acids. Elucidating the molecular mechanism(s) linking bile acids and transcriptional repression of CYP7A1 and CYP8B1 led to the identification and characterization of FXR as a nuclear bile acid sensor [153-155].

The Farnesoid X Receptor

FXR is a member of the nuclear hormone receptor superfamily of ligand-activated transcription factors. It was originally named the farnesoid X receptor, when it was discovered that high-dose derivatives of farnesol could elicit FXR-mediated transcription in cell culture assays [156]. More recently however, three groups simultaneously identified FXR as a nuclear bile acid receptor [153-155]. The work presented in these three reports confirmed that: bile acids demonstrate high-affinity binding to the carboxy-terminal portion (ligand-binding domain) of FXR; FXR functions as an obligate heterodimer with the retinoid X receptor (RXR); the RXR/FXR heterodimer binds DNA sequences consisting of 2 hexanucleotides positioned tail-to-tail with one intervening base (IR1 motif, also called an FXRE); and dietary conditions that alter the bile acid pool size and composition in mice result in FXR-dependent changes in the expression of CYP7A1 and CYP8B1 in liver, and the ileal bile acid binding protein (IBABP) in intestine (See Figure A.2).

Using a variety of advanced technologies, additional FXR target genes and pathways have been identified in mouse liver and intestine. Using microarray analyses, FGF15 (called FGF19 in humans) was identified as a novel FXR target gene in the distal small intestine [157]. FGF15 was further characterized as a novel endocrine factor that

binds an FGF receptor on hepatocytes to ultimately limit bile acid synthesis. Again, using microarray, additional target genes in intestine identified bile acids/FXR as antibacterial agents in the gut [158]. Bile acids have been reported to regulate hepatocyte proliferation in regenerating liver in an FXR-dependent manner [159]. With the advent of chromatin-immunoprecipitation-sequencing methodologies, two groups have further identified hundreds of genes in mouse liver and intestine that appear to contain FXR-binding sites [160, 161]. Further work on these novel targets will reveal the biological significance of these FXR-regulated gene products.

Despite the wealth of information on FXR actions in liver and intestine, very little information is yet reported on possible roles of this nuclear hormone receptor in the endocrine pancreas. FXR RNA was first reported present in both mouse and human islets by our group in 2008 (Figure A.2 and [1]). Since that time, a single report suggests that a synthetic FXR agonist may increase glucose-stimulated insulin secretion in mouse islets, although unfortunately *Fxr*$^{-/-}$ islets were not included as a negative control [162]. An additional report suggests that FXR agonists may protect human islets from palmitate-induced lipotoxicity [163]. Finally, in microarray analyses performed on islet RNA isolated during various stages of pregnancy in wild-type mice, FXR mRNA levels were found to decline during stages associated with increased islet cell mass [164]. Thus additional studies are warranted to define the role of FXR in the endocrine pancreas.

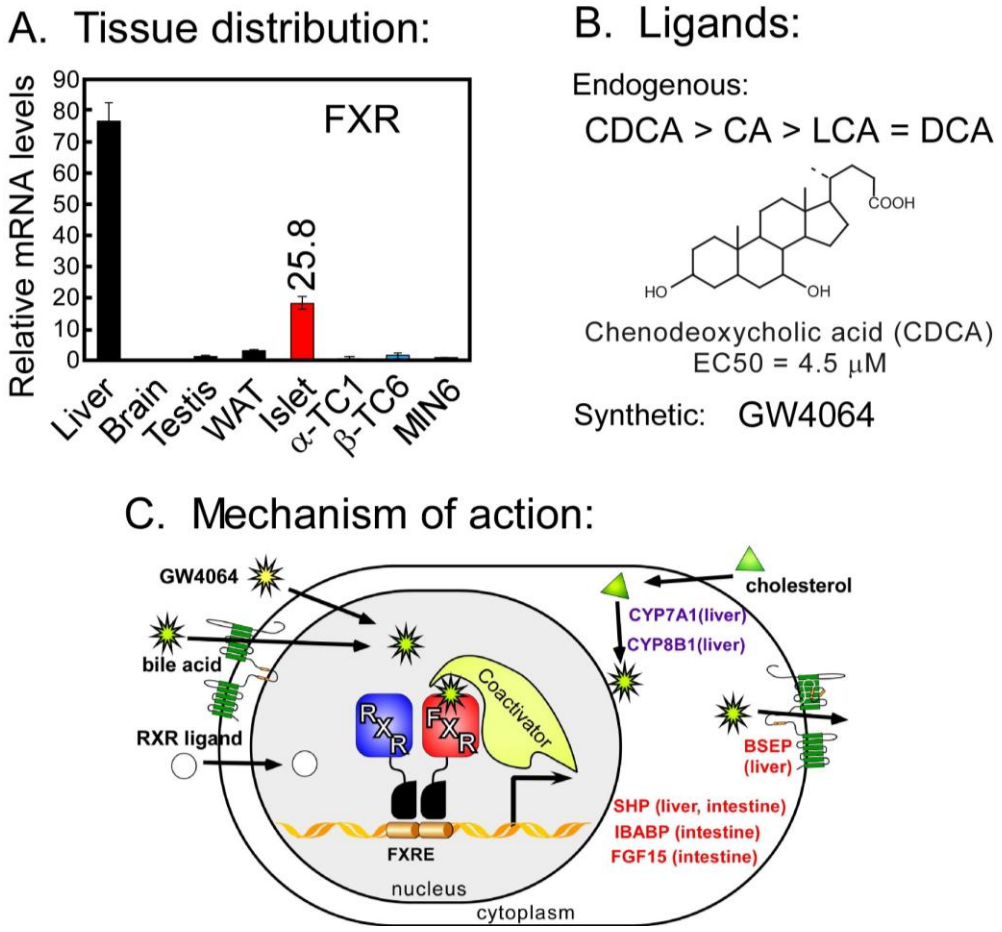

Figure A.2. The farnesoid X receptor. A. FXR is expressed in mouse islet. RNA was measured in various tissues and cell lines by qPCR, standardized against cyclophilin, and expressed relative to ileum (at 100%). Values are means ± SEM, n=3. The cycle number at threshold, C_T, for islets is provided. B. Chenodeoxycholic acid (CDCA) is the most potent bile acid ligand. C. FXR functions as a ligand-activated transcription factor. Selected target genes that are increased (in red) or decreased (purple) are indicated on the right. Abbreviations: BSEP, bile salt efflux pump; SHP, short heterodimer partner. Also refer to Figure A.1.

TGR5, a bile acid activated G protein-coupled receptor

TGR5, was first identified as a receptor for bile acids during cell-based chemical library screening [165, 166]. More recently, additional TGR5 ligands have been described including natural products such as oleanolic acid (from olive tree leaves [167]), the neurosteroid allopregnanolone [168], and several synthetic agonists [169, 170]. TGR5 is coupled to GαS, thus upon ligand binding, activates adenylate cyclase to generate cAMP (See Figure A.3).

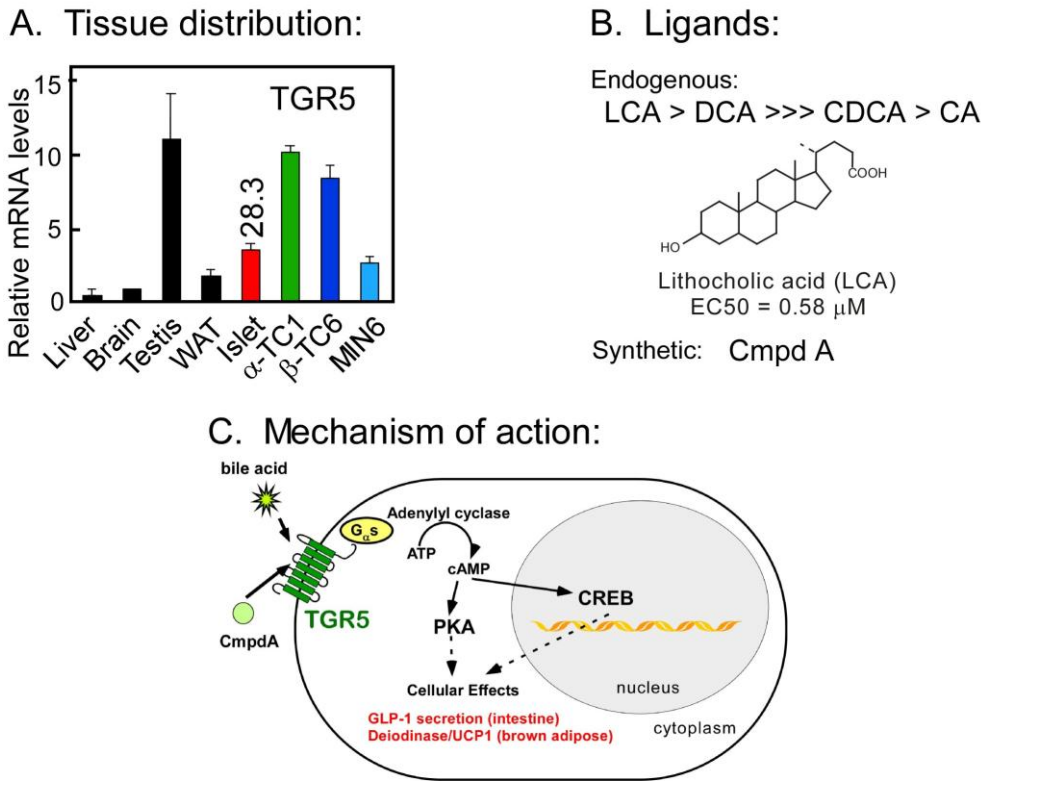

Figure A.3. TGR5. A. TGR5 is expressed in mouse islet. RNA was measured in various tissues and cell lines by qPCR, standardized against cyclophilin, and expressed relative to gall bladder (at 100%). Values are means ± SEM, n=3. The cycle number at threshold, C_T, for islets is provided. B. Lithocholic acid (LCA) is the most potent bile acid ligand. Cmpd A is a synthetic TGR5 ligand we are testing. C. TGR5 activation results in elevated cytosolic cAMP. Selected biologic functions are provided in red text. Abbreviations: PKA, protein kinase A; CREB, cAMP-responsive element binding protein.

TGR5 is most highly expressed in the gall bladder, brown adipose tissue, and muscle. TGR5 has been shown to affect energy metabolism, its activation increases energy expenditure and attenuates diet-induced obesity [171]. Recently it was shown that TGR5 signaling enhances intestinal glucagon-like peptide-1 (GLP-1) release [172, 173]. GLP-1 is well known for its positive effects on islet function and enhanced glucose tolerance [174]. There are no reports to date describing the presence and action of TGR5 in the endocrine pancreas.

Recent progress in bile acid research suggests that bile acids are important signaling molecules that affect glucose and energy homeostasis (reviewed in [175]). FXR agonists improve hyperglycemia and hyperlipidemia in diabetic mice, and *Fxr*$^{-/-}$ mice exhibit insulin resistance and an impaired response to oral glucose [175-177]. There are several physiologic conditions that exhibit elevated serum bile acids: serum bile acid levels increase 3-5 fold immediately after food consumption [178] [179]; plasma bile acid levels increase dramatically following gastric bypass surgery [180]; and the use of bile acid sequestrants (e.g. cholestyramine) in mice results in a decreased bile acid pool size but a 10-fold increase in serum lithocholic acid levels [181]. Interestingly, all of these conditions are associated with enhanced glycemic control suggesting a possible link between elevated serum bile acid levels and glucose/insulin response. In addition, as FXR and TGR5 agonists are in various stages of preclinical and clinical testing as therapeutic agents, it is of interest to determine, and thus anticipate, how these drugs may affect the endocrine pancreas.

Thus our goal was to define the roles of bile acids and bile acid receptors in the function of the endocrine pancreas. We have used a variety of techniques to interrogate

bile acid effects on isolated islets, made use of mouse models that either lack bile acid receptors or are bile acid deficient (*Fxr*$^{-/-}$, *Tgr5*$^{-/-}$, *Cyp27*$^{-/-}$), and have taken advantage of a wide range of endogenous and synthetic ligands to determine whether FXR and/or TGR5 are tractable drug targets to affect islet function.

A.3 Materials and methods

Animals

All tissues and islets were obtained from 3-5-month-old mice. Mice were maintained in a temperature-controlled room (23 ± 1 C) with 12-h light (0700 h–1900 h), 12-h dark cycle, *ad libitum* access to water and a standard rodent diet (Teklad diet 7001), and housed with sanitized wood-chip bedding (Sani-Chips, P.J. Murphy Forest Products, Montville, NJ). Tissues were harvested and islets were isolated in the morning with mice in the fed state. All experiments were performed with the approval of the Institutional Animal Care and Use Committee of the University of Texas Southwestern Medical Center, which assures that all animal use adheres to federal regulations as published in the Animal Welfare Act, the Guide for the Care and Use of Laboratory Animals (Guide), the Public Health Service Policy, and the US Government Principles Regarding the Care and Use of Animals (http://www.utsouthwestern.edu/utsw/cda/ dept41600/files/54634. html).

Islet isolation

The islet isolation method used has been previously described [1]. Briefly, the mouse pancreas was perfused and digested with Collagenase P (Roche, Indianapolis, IN).

Islets were then isolated using Ficoll gradient centrifugation and hand selection under a stereomicroscope for transfer to RPMI 1640 medium (11.1 mM glucose) supplemented with 10% (vol/vol) heat-inactivated fetal bovine serum (FBS), 100 IU/ml penicillin, and 100 μg/ml streptomycin (Invitrogen, Carlsbad, CA). Islets were allowed to recover by overnight incubation (37°C, 5% CO_2) with mild shaking to avoid attachment to culture plates. Either islet RNA was isolated the next morning (for tissue distribution analyses), or islets were treated with ligands and a second overnight, 16-hour incubation was performed prior to RNA isolation or functional assay.

Microarray

Mouse pancreatic islets from wild-type and *Fxr*-knockout mice (all on a C57Bl/6 strain background) were isolated and cultured overnight in RPMI medium containing 11 mM glucose and 10% FBS. The following day, islets (200/well) were then cultured for 16h in the presence of the synthetic FXR agonist GW4046 (1 μM) or vehicle (DMSO) with triplicate biologic samples prepared for each condition. Total RNA was isolated and microarray analysis was performed by the UT Southwestern Microarray Core Facility using the Mouse Illumina 6-beadchip V2 array platform. Comparative gene expression was done using GeneSifter software with fold change cut-off at ≥2.0.

Mouse islet glucose-stimulated insulin secretion

Islets were conditioned for 1 hour at 37^{o}C in secretion assay buffer (SAB), pH 7.4, containing 114 mM NaCl, 4.7 mMKCl, 1.2 mM KH2PO4, 1.16 mM MgSO4, 2.5 mM CaCl2, 25.5 mM NaHCO3, 20 mM HEPES, 0.2% BSA and 0 mM glucose, then

incubated for 60 min in SAB containing either low glucose (5 mM) or high glucose (17.5 mM) glucose. Culture media were obtained and islets collected to measure insulin content by radioimmunoassay (Ultrasensitive rat RIA, Millipore).

To activate FXR, islets were exposed to the synthetic ligand GW4064 (1 μM [182]), chenodeoxycholic acid (CDCA, 10 μM), or tauro-chenodeoxycholic acid (TCDCA, 10 μM) for 16 hours prior to initiating the GSIS assay. FXR ligands were not included in the SAB buffers, as it was presumed that transcriptional targets and their biological effects would persist during this final 2 hours of the GSIS assay. To activate TGR5, ligands such as Cmpd A (400 nM or 2 μM), α- and β-allopregnanolone (30μM) or bile acids (10 μM) were introduced only during the final one-hour SAB+glucose incubation of the GSIS assay, as was GLP-1 a positive control for GPCR-augmented GSIS.

qPCR profiling

RNA was isolated from tissue samples, cultured islets or cell lines using RNA STAT-60 (Tel-Test Inc., Friendswood, TX), and 2 μg of total RNA was treated with ribonuclease-free deoxyribonuclease (Roche), and then reverse transcribed with random hexamers using SuperScript II (Invitrogen), as previously described in detail [38]. qPCR was performed using an Applied Biosystems Prism 7900HT sequence detection system (Applied Biosystems, Foster City, CA) and SYBR-green chemistry [38, 39]. Gene-specific primers were designed using D-LUX primer design software (www.invitrogen.com) and validated by analysis of template titration and dissociation

curves [1]. Primer sequences are provided in a supplementary table. qPCRs (10 μl) contained 25 ng of reverse-transcribed RNA, each primer (150 nM), and 5 μl of 2X SYBR Green PCR master mix (Applied Biosystems). Multiple housekeeping genes were evaluated in each assay to ensure that their RNA levels were invariant under the experimental conditions of each study. Results of qPCR were evaluated by the comparative Ct method [user bulletin no. 2, PerkinElmer Life Sciences [38]] using hypoxanthine-guanine phosphoribosyl transferase (HPRT), acidic ribosomal phosphoprotein P0 (36B4) and cyclophilin as the invariant control gene, as appropriate.

Statistics

Values shown reflect the mean ± SEM, n = 3-4 samples. Two-tailed Student's *t*test was performed to compare difference between two groups using the GraphPad software. For multiple groups, a one-way ANOVA was performed with post-hoc analysis. Significance was established at $P < 0.05$.

Results

FXR activation does not affect glucose- stimulated insulin secretion

Islets from wild-type and *Fxr*$^{-/-}$ mice were pretreated with the FXR-specific agonist GW4046, and a glucose-stimulated insulin secretion assay was performed. There was no difference in glucose-stimulated insulin secretion between wild-type islets and those obtained from mice lacking FXR (Figure A.4). Pretreatment of islets with GW4064 had no effect on insulin secretion under either low-glucose or high-glucose conditions.

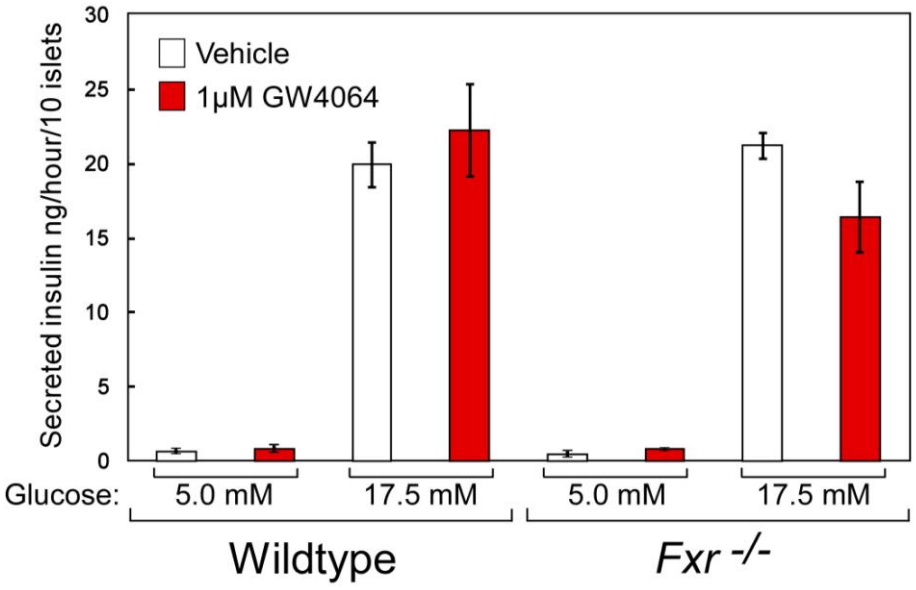

Figure A.4. FXR and GSIS. Islets from wildtype or *Fxr*$^{-/-}$ mice were preincubated for 16 hours with the FXR agonist GW4064 (1 μM, red bars or vehicle (DMSO, 0.1% v/v, white bars), then insulin secretion over 1 hour was measured under low-glucose (5 mM) or high-glucose (17.5) conditions. Robust high-glucose stimulated insulin secretion is evident, but no significant differences are evident due to genotype or drug treatment.

To confirm and extend these findings, wild-type and *Fxr*$^{-/-}$ islets were exposed to GW4064 or vehicle for 16 hours, then harvested to measure RNA levels of hormones and hormone-processing enzymes (Figure A.5). The mouse genotypes were confirmed by the

absence of FXR mRNA in islets from *Fxr*$^{-/-}$ mice. The relative expression of islet FXR mRNA was consistent with other experiments (C_T=25.4 in Figure A.5 compared to experiments of Figure A.2, Figure A.6), and in agreement with studies reported for other tissues exhibited no autoregulation by FXR agonist. The heterogenous RNA transcript for insulin (a sensitive readout of insulin expression, [1]), glucagon, and somatostatin mRNA levels were unaffected by GW4064 treatment, and did not differ among genotypes. Likewise FXR status did not affect the mRNA levels of the proprotein convertases PC1/3 and PC2, which are essential for processing mature hormone proteins.

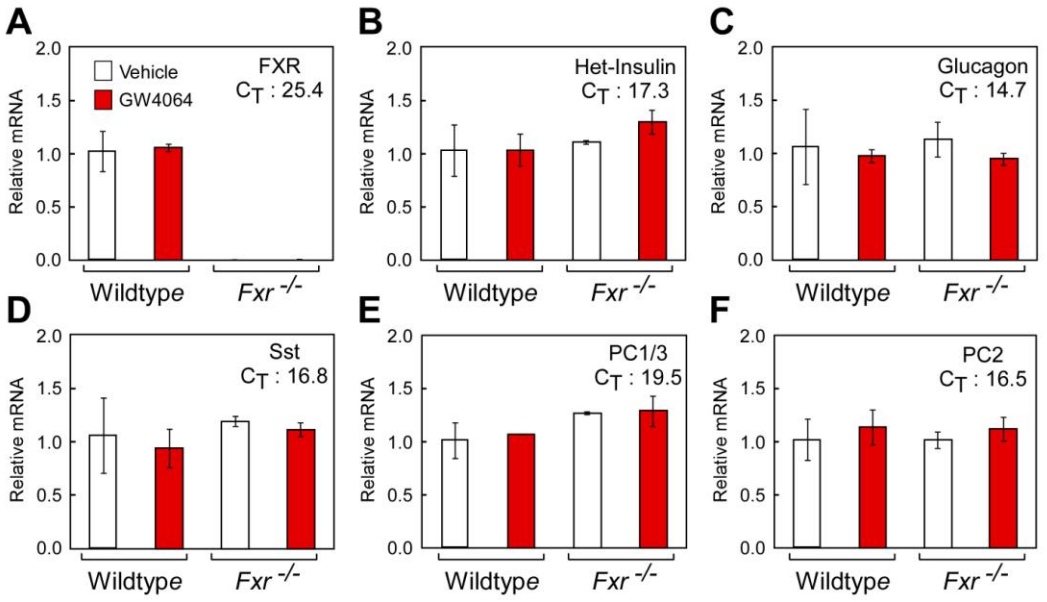

Figure A.5. FXR status does not affect expression of key hormones or their processing enzymes in mouse islets. Wild-type and *Fxr*$^{-/-}$ islets were isolated and cultured in RPMI containing 10% FBS (at 11 mM glucose). Vehicle (DMSO, at a final concentration of 0.1%, v/v) and GW4064 (1 μM) were applied to islets for 16h, then RNA was isolated. Genotype, and candidate gene expression changes were examined by qPCR. C_T values for each gene are provided for the vehicle-treated wild-type to allow an appreciation of RNA quantity (C_T =20, cyclophilin; 40, no-template control).

Genome-wide identification of FXR-regulated genes in the mouse islet.

Despite the fact that FXR activity does not appear to affect glucose-stimulated insulin secretion, there may be alternative roles of this nuclear receptor in the pancreatic islet. Therefore an unbiased microarray approach was taken; we isolated islets from wild-type and *Fxr*-knockout mice, treated the islets with 1 μM GW4046 or vehicle (DMSO) for 16 hour and isolated RNA for a microarray analysis. The array analysis revealed 213 genes that were altered by GW4064 in wild-type, but not $Fxr^{-/-}$, islets. The top 50 upregulated genes are listed in table A.1. Selected genes were measured again by qPCR using independent samples to confirm the microarray results (Figure A.6).

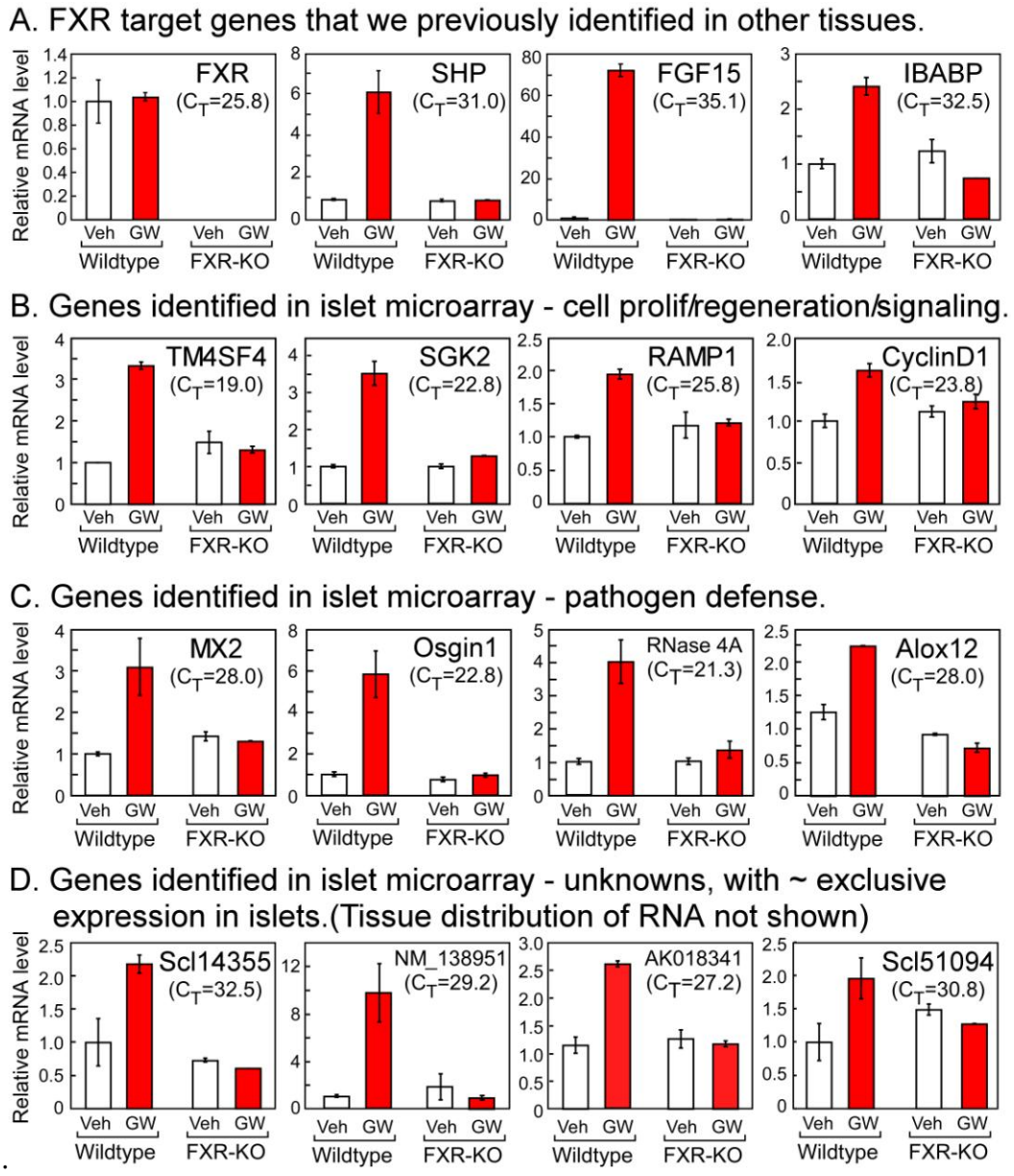

Figure A.6. FXR-dependent gene expression changes in the mouse islet. Wildtype and *Fxr*$^{-/-}$ islets were isolated and cultured in RPMI containing 10% FBS (at 11 mM glucose). Vehicle (DMSO) and GW4064 (1 μM, red) were applied to islets for 16h, then RNA was isolated. Genotype (A), and candidate gene expression changes were confirmed in panels **B-D**. C_T values for each gene are provided for the vehicle-treated wild-type to allow an appreciation of RNA quantity (C_T =20, cyclophilin; 13, insulin; 40, no-template control).

Among genes found in the microarray and confirmed by qPCR are SHP, FGF15, and IBABP, previously identified as FXR target genes in intestine (Figure A. 2 and [153, 157]). This reveals that functional FXR is present in the islet, and that the chosen time and dose of GW4064 used in this and previous studies were appropriate to activate FXR. In addition, familiar and novel FXR target genes involved in pathogen defense were found [158]. FXR targets with possible roles in cell proliferation and tissue regeneration were identified, and target genes of unknown function (but almost exclusive expression in islet, data not shown) were revealed by this microarray analysis.

Mouse islets do not respond to physiologic concentrations of conjugated bile acids.

Experiments to this point took advantage of the high-potency, receptor-specific FXR agonist GW4064. Therefore, we tested the ability of bile acids, and particularly a conjugated bile acid, at physiologically relevant concentrations to determine whether FXR may play a role in linking bile acid metabolism with islet biology. As our microarray and qPCR results revealed that FGF15 mRNA levels were a sensitive readout of FXR activation, we used this measure to assess bile acid/FXR action in wild-type islets (Figure A.7).

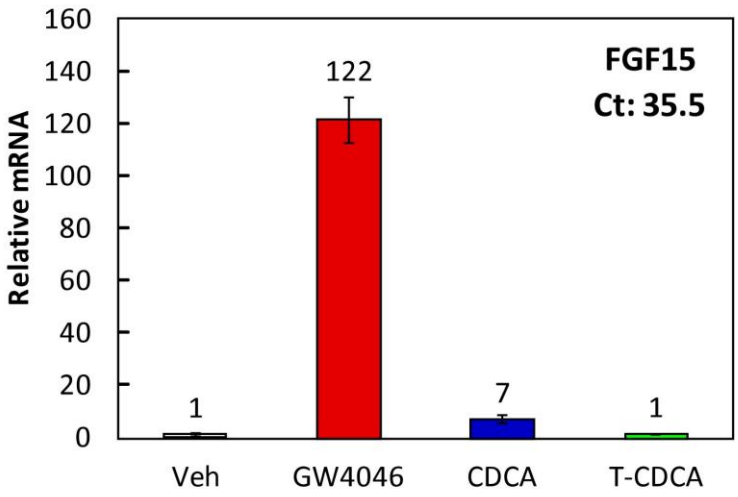

Figure A.7. FGF15 expression in response to various FXR ligands. Wildtype islets were isolated and cultured in RPMI containing 10% FBS (at 11 mM glucose). Vehicle (DMSO, at a final concentration of 0.1%), GW4064 (1 μM), and CDCA/tauro-CDCA (10 μM) were applied to islets for 16h, then RNA was isolated and expression of FGF15 was determined by qPCR. Fold-change values are provided above each bar.

As seen previously, the FXR target gene FGF15 showed robust upregulation (>100-fold increase in mRNA levels) following islet incubation with GW4064. However, far less response was observed following islet incubation with the unconjugated CDCA (7-fold), and none observed with the conjugated tauro-CDCA. This is consistent with our failure to detect significant mRNA levels for the known bile acid transport proteins, NTCP, IBAT, BSEP, and OSTα/β in mouse islets (qPCR C_T values > 33) which are required for translocation of conjugated bile acids across the plasma membrane of cells. These results suggest that under normal physiologic states, circulating serum bile acids are unlikely to be present at sufficient concentrations to elicit

FXR signaling in islets. Islet FXR physiology would thus be of greater relevance as therapeutic synthetic FXR drugs are tested.

TGR5 activation enhances glucose- stimulated insulin secretion

To further evaluate the role of bile acids in islet function we used a variety of bile acids and synthetic TGR5 agonists and tested their effect on glucose-stimulated insulin secretion. Wild-type mouse islets were incubated with ligand only during the 1-hour GSIS, except in the case of GW4046, where the incubation period was 16 hours pre-GSIS. Therefore, all ligands except for GW4046 were tested in an acute setting, appropriate for a G protein-coupled receptor such as TGR5. TGR5 agonists (shown in blue, Figure A.7) enhanced glucose-stimulated insulin secretion. The bile acid, lithocholic acid, increased glucose-stimulated insulin secretion by ~50% and the experimental synthetic agonist, Cmpd A when applied at 2 μM (albeit not at 400 nM) increased GSIS by almost 2-fold. Included in this analysis was GLP-1, an agonist of the GLP-1 receptor previously shown to enhance GSIS, as a positive control. Again, it should be noted that FXR activation by GW4064 had no effect on GSIS in mouse islets.

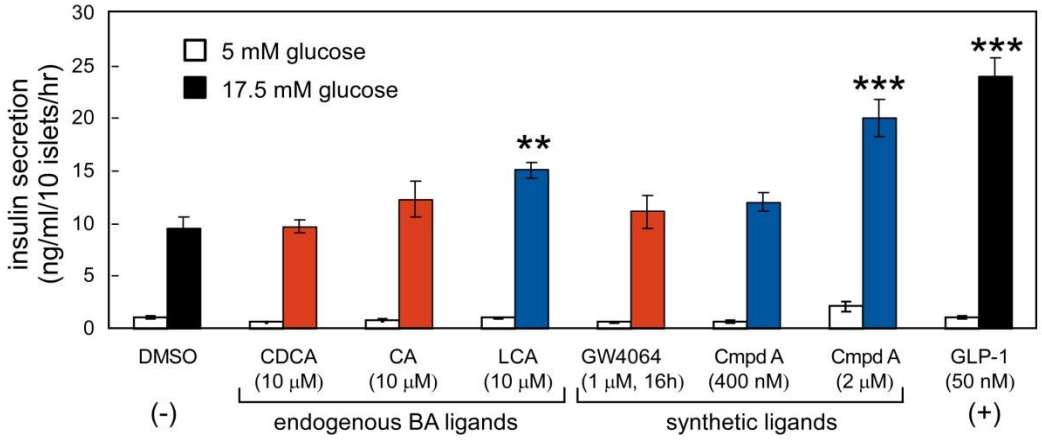

Figure A.7. Bile-acid-receptor ligands and GSIS. Insulin secretion during a 1 hr exposure to low (5 mM) or high (17.5 mM) glucose was determined for wild-type mouse islets co-treated with a variety of bile acid receptor ligands. All ligands, except GW4064, were provided during the one-hour glucose exposure period. Islets were pre-exposed to GW4064 for 16h to allow sufficient time for increased transcription /translation of FXR target genes. FXR ligands (red), TGR5 ligands (blue). Means ± SEM (n=4 wells). ** $p<0.01$, *** $p<0.0001$. vs. DMSO high-glucose group.

The results in figure A.7 suggest that TGR5 has an effect on glucose-stimulated insulin secretion. To further characterize this action of TGR5 we evaluated transcription of the three known bile acid receptors in islets (TGR5, FXR and VDR) in *Tgr5*-knockout islets and transcription of insulin and GLP1R (figure B.8). Results confirm the absence of TGR5 in knockout islets, but show no compensatory effect of TGR5 loss on the mRNA abundance of FXR or VDR. The levels of mature insulin transcript are not changed in *Tgr5*-knockout islets but the heterogeneous insulin transcript was significantly reduced. This transcript is very transient in nature and reflects newly generated transcripts and thus the transcriptional activity of insulin. The reduction in heterogeneous insulin transcripts suggests that insulin transcriptional activity is reduced in *tgr5*-knockout islets. There was also a reduction in GLP1R mRNA levels in $Tgr5^{-/-}$ islets. GLP1R is the receptor for the incretin hormone GLP-1, and TGR5 has been shown to control secretion of GLP-1 by

intestinal enteroendocrine cells. These findings suggest that TGR5 may also regulate islet responsivity to GLP-1, but further work will be required to fully define this relationship.

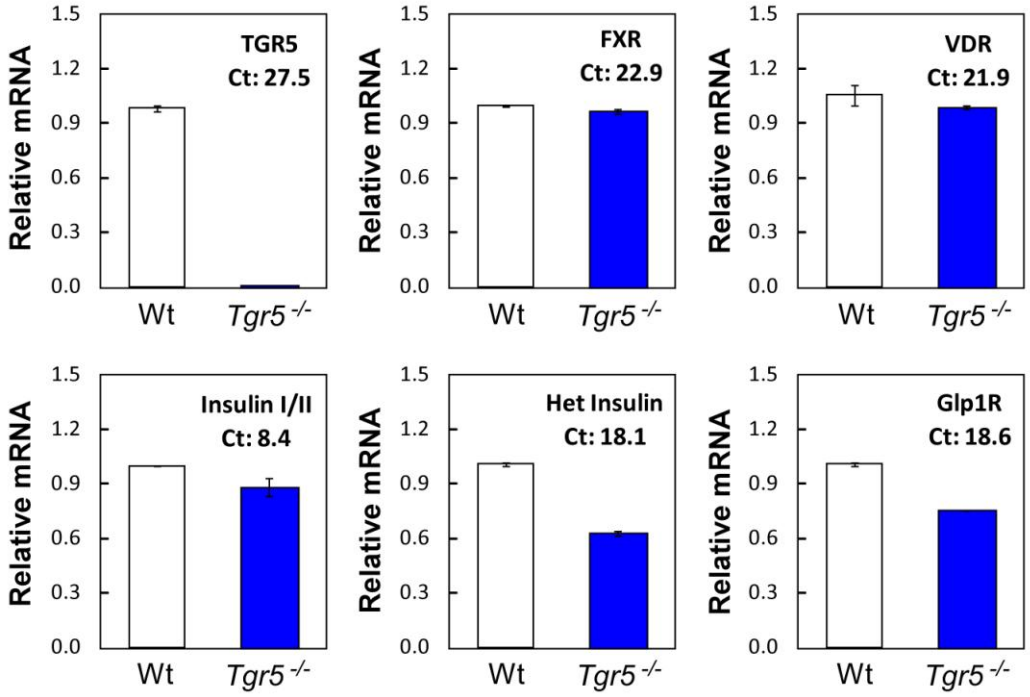

Figure A.8. Gene expression changes in islets of mice lacking TGR5. Islets were cultured at 11 mM glucose, and RNA extracted for analysis by qPCR. Genotype was confirmed by the absence of TGR5 mRNA in islet from knockout mice (TGR5 KO, blue bar). No significant changes in mRNA levels were observed for alternative bile acid receptors, FXR and VDR, or mature insulin transcripts (Insulin I/II). However, significant reductions in mRNA levels were observed for the heterogenous insulin transcript (Het Insulin) and the GLP1 receptor in *Tgr5*-null islets. Values depict mean ± SEM, n=4.

Recently the neurosteroid allopregnanolone was shown to activate TGR5 signaling in neurons [168]. In a glucose-stimulated insulin secretion assay both the alpha form (3α-hydroxy-5α-pregnan-20-one) and the beta form (3α-hydroxy-5β-pregnan-20-one) of this neurosteroid show a trend towards enhanced GSIS in wild-type islets but not in *Tgr5*-knockout islets (Figure A.9). In fact, GSIS tends to be reduced with the

compounds when islets are lacking TGR5. This suggests that in the absence of TGR5-activated signaling pathways, these neurosteroids might be unfavorable to beta cell function.

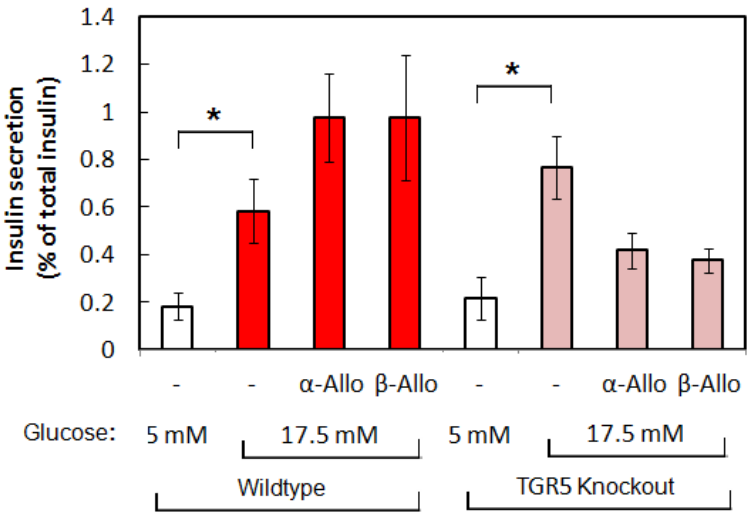

Figure A.9. Allopregnanolone induced GSIS. Insulin secretion during a 1 hr exposure to low (5 mM) or high (17.5 mM) glucose was determined for wild-type and TGR5-knockout mouse islets co-treated with 3α-hydroxy-5α-pregnan-20-one (α-Allo) and 3α-hydroxy-5β-pregnan-20-one (β-Allo). Ligands were provided during the one-hour glucose exposure period. Means ± SEM (n=3 wells). Asterisk denotes a significant difference of $p<0.05$

Our RNA analysis of Figure A.8 suggests that the basal transcript level of GLP1R is reduced in *Tgr5*-knockout islets. Therefore, we tested whether GLP-1-enhanced GSIS was affected in *Tgr5*$^{-/-}$ islets (Figure A.10). With the one-hour exposure of islets to 50 nM GLP-1, there was no difference in the enhanced GSIS observed between wild-type and *Tgr5*$^{-/-}$ islets. This suggests that TGR5 protein levels may not be sufficiently reduced to cause a functional change in GLP-1 action, or that dose or kinetic effects of GLP-1 were not evident in this one-hour static incubation.

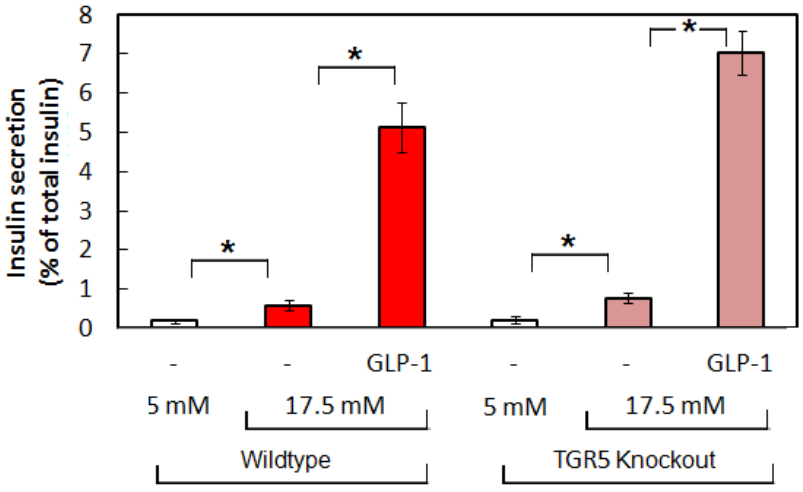

Figure A.10. GLP-1 induced GSIS in wild-type and TGR5-knockout islets. Insulin secretion during a 1 hr exposure to low (5 mM) or high (17.5 mM) glucose was determined for wild-type and TGR5-knockout mouse islets co-treated with vehicle or 50 nM GLP-1. GLP-1was provided during the one-hour glucose exposure period. Means ± SEM (n=3 wells). Asterisk denotes a significant difference of $p<0.05$

Bile acid-deficient (CYP27$^{-/-}$) mice have lower circulating insulin and glucagon levels.

We have determined that both FXR and TGR5 receptors are abundant in islets and their activation results in genetic regulation (FXR) and enhanced glucose-stimulated insulin secretion (TGR5). As an initial *in vivo* approach to evaluate the effects of bile acids on functions of the endocrine pancreas, we used the *CYP27*$^{-/-}$ mouse strain. Mice lacking CYP27A1 have a bile acid pool size of about 10% that observed in wild-type mice, and would be expected to have reduced serum levels of bile acids. This analysis was a piggyback study in conjunction with testing diosgenin as a cholesterol-lowering drug, so these data are also presented to increase the number of observations. We obtained plasma samples for glucose and hormone measurements as preliminary data and

found that the "bile-acid deficient" mice had significantly lower circulating insulin and glucagon in the fed state (Figure A.11), despite apparent euglycemia.

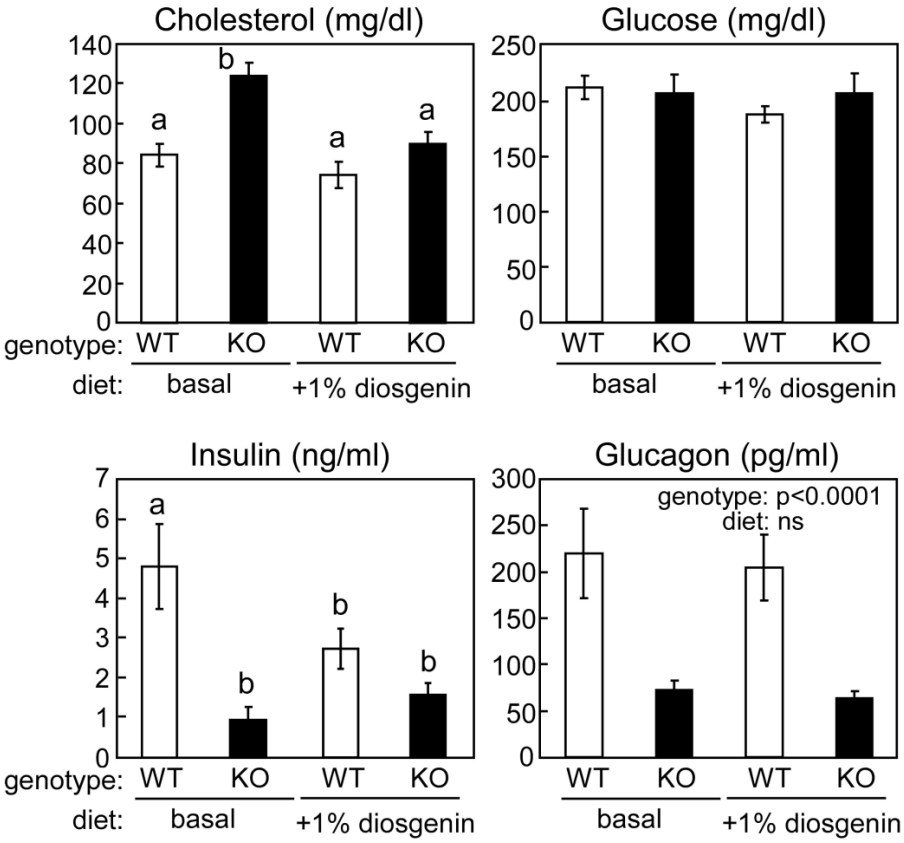

Fig. A.11. Plasma measures of glucose balance in *Cyp27*$^{-/-}$ mice. Female wild-type (WT) and *Cyp27*$^{-/-}$ (KO) mice were fed a low-fat rodent chow ±1% diosgenin (a hypocholesterolemic agent that works by an unknown mechanism) for 2 weeks. At lights-on (in a post-prandial state), plasma was collected in the presence of 250 KIU aprotonin/ml to preserve glucagon. Total cholesterol (by gas chromatography), glucose (PGO enzyme-based colorimetric method, Sigma), insulin and glucagon (RIA, Linco) levels were determined. Values represent the mean and SEM of 6 mice/group, and 2-way ANOVA was performed. If a significant interaction was observed between factors (genotype and diet, as in **A** and **C**), a one-way ANOVA was used to identify significant differences designated by different letters ($p<0.05$). For glucagon (**D**), a statistical effect was observed only by genotype.

These results compelled us to examine the glucose tolerance in wild-type versus *Cyp27a1* knockout mice. An intraperitoneal glucose tolerance test was performed on wild-type and *Cyp27a1*$^{-/-}$ mice, then they were allowed to recover for a week on a regular chow. The mice were then placed on a bile acid rescue-diet containing cholic acid. Results from the IPGTT suggest that the glucose tolerance is not significantly different between genotypes (figure A.12). The only discernable difference is the fasting blood glucose, where the *Cyp27a1* null mice exhibit a nearly significant increased fasting blood glucose ($p=0.06$) on regular chow diet. This difference was gone on the rescue-diet, suggesting that decreased bile acid pool size might have an effect on fasting blood glucose. The interpretation of these results may be further complicated because these mice are on a mixed-strain background, which adds variability in analyses of glucose homeostasis (back-crossing to C57Bl/6 is underway).

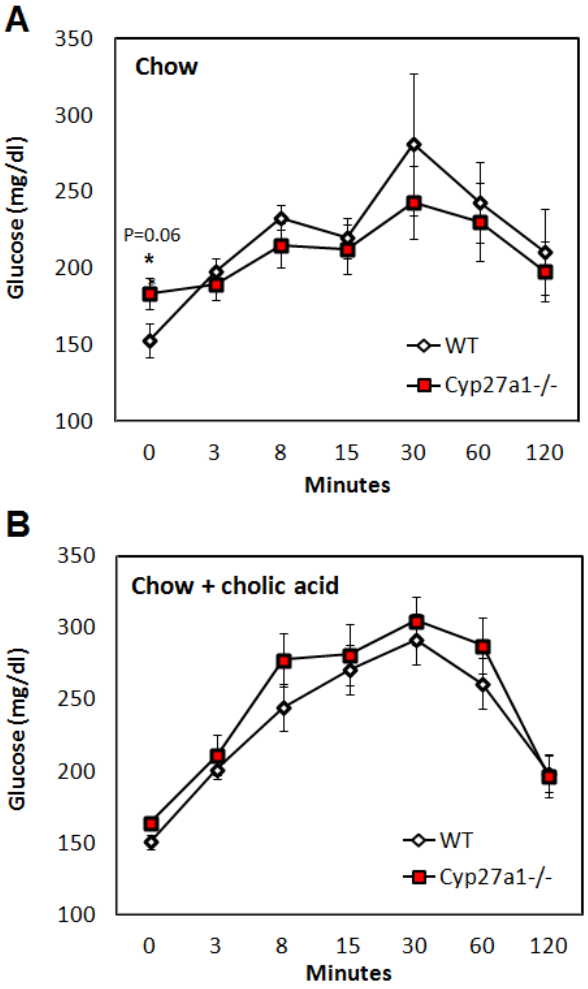

Figure. A.12. Gluose tolerance test in bile acid-deficient mice. Wildtype mice (white fill) and *Cyp27a* $^{-/-}$ mice (red fill) were fasted for 16 hours prior to GTT and baseline glucose reading was taken before mice received an IP injection of 2mg/Kg D-glucose in saline solution. Glucose reading was taken using AlphaTrak glucometer at 0, 3, 10, 15, 30, 60 and 120 minutes after glucose injection. A. IPGTT on mice fed regular chow. B. IPGTT on the same mice as in A but after recovering for one week and then receiving a rescue-diet containing cholic acid for one week. Data are shown as mean ± SEM. *n* = 6 mice per group.

Discussion and future direction

Our results clearly establish that bile acid receptors FXR and TGR5 are present and functional in mouse pancreatic islets. FXR does not appear to play a role in islet insulin secretion, however a global gene expression analysis suggests that FXR may affect islet cell proliferation, pathogen defense, or other novel biologic pathways. Importantly, bile acids, particularly the more physiologically relevant conjugated bile acids, do not appear to activate islet FXR, a finding consistent with an absence of bile acid transporters as revealed by qPCR analysis in this organ. Thus FXR may not play a significant role in coupling the changes in serum bile acids with islet function under normal physiologic states. However, serum bile acids are dramatically increased following gastric bypass surgery, and may reach significant levels under this condition. Our colleague, Dr. Vincent Aguirre, has developed the mouse version of Roux-enY Gastric Bypass surgery, and performing this technique in mice lacking FXR, TGR5, and/or bile acids ($CYP27A1^{-/-}$) while monitoring insulin secretion and glucose homeostasis could be very informative. In addition, synthetic FXR agonists are in preclinical testing, as agents to modulate serum cholesterol and/or glucose homeostasis. As these synthetic ligands can readily enter cells, they may affect FXR signaling pathways in the endocrine pancreas.

Collectively our data suggest that bile acids through TGR5 activation play a role in glucose stimulated insulin secretion. As TGR5 is a receptor present at the plasma membrane it does not rely on the bile acid transporters for access to these physiologic ligands. Plasma bile acid concentration is increased in the post-prandial state, and serum lithocholic acid (the most potent bile acid ligand for TGR5) is increased upon treatment

with bile acid sequestrants. Under these conditions, activation of TGR5 could contribute to enhanced insulin secretion and the anabolic state.

Future studies using mice with islet cell-selective deletion of FXR and/or TGR5, in conjunction with mouse models of increased/decreased serum bile acid levels should further elucidate the roles of these bile acid receptors in islet function.

Table A1. FXR regulated gene expression in mouse islets

#	Wildtype GW/Veh	*Fxr* $^{-/-}$ GW/Veh	Accession #	Gene symbol
1	4.47	1.03	NM_027950.1	**Osgin1**
2	2.99	0.90	NM_019471.1	Mmp10
3	2.66	1.09	NM_010517.2	Igfbp4
4	2.57	0.98	NM_013731.1	**Sgk2**
5	2.57	1.02	NM_013749.1	Tnfrsf12a
6	2.53	1.10	NM_009368.1	Tgfb3
7	2.35	1.01	NM_008160.1	Gpx1
8	2.26	1.02	NM_013900.1	Mfi2
9	2.25	0.97	NM_013731.1	**Sgk2**
10	2.23	0.90	NM_021352.2	Crybb3
11	2.18	1.04	NM_008350.1	Il11
12	2.11	1.07	NM_009366.1	Tgfb1i4
13	2.09	0.94	NM_013652.1	Ccl4
14	2.05	1.05	NM_016894.1	**Ramp1**
15	2.05	1.04	NM_138951.1	**Ttc36**
16	2.04	1.04	NM_016704.1	C6
17	2.02	1.05	NM_178600.2	Vkorc1
18	2.00	0.98	NM_201239	**Rnase4**
19	1.99	0.96	NM_133191.2	Eps8l2
20	1.98	0.93	NM_031869.1	Prkab1
21	1.92	1.01	NM_018777.2	Cldn6
22	1.87	0.99	NM_007447.2	Ang
23	1.86	1.05	NM_008610.1	Mmp2

24	1.86	1.08	NM_007440.2	**Alox12**
25	1.85	1.01	NM_008105.2	Gcnt2
26	1.83	0.96	NM_013606	**Mx2**
27	1.79	1.10	NM_008034.2	Folr1
28	1.79	1.07	NM_029035.2	Spsb1
29	1.77	0.97	NM_008449.2	Kif5c
30	1.76	1.09	NM_007843.2	Defb1
31	1.76	0.95	NM_001039387.1	Nelf
32	1.74	0.99	NM_001080935.1	**AK018341**
33	1.73	0.99	NM_182928.2	Adm2
34	1.66	0.94	NM_027450	Glipr2
35	1.66	0.95	NM_011468.2	Sprr2a
36	1.65	1.06	NM_026039.2	Med18
37	1.64	0.89	NM_010329.1	Pdpn
38	1.64	0.91	NM_133200.2	P2ry14
39	1.64	1.03	NM_175507.2	Tmem20
40	1.62	0.92	NM_080595.2	Emid1
41	1.62	0.95	NM_023268	Qsox1
42	1.61	1.02	NM_018731	Atp4a
43	1.61	1.04	NM_009505.2	Vegfa
44	1.61	1.02	NM_007707.2	Socs3
45	1.59	0.97	NM_027475.1	Ecd
46	1.56	0.94	NM_011337.1	Ccl3
47	1.53	1.15	NM_145539.1	**Tm4sf4**
48	1.53	0.98	NM_198111.2	Akap6
49	1.53	0.94	NM_007631.1	**Ccnd1**
50	1.52	1.03	NM_026418.1	Rgs10
51	1.52	1.12	NM_027475.1	Ecd
52	1.51	0.99	NM_146041.1	Gmds
53	1.50	0.95	NM_008003	**Fgf15**

Gene names in bold have been validated by qPCR and italicized genes showed no change when examined by qPCR.

APPENDIX B
Primers used for reporter assays and qPCR

Table C.1. Quantitative real-time PCR primer sequences for mouse mRNA measurement.

Gene Abbrev.	Accession Number	Sequence of Primers (5' to 3')	Amplicon position
36B4	NM_007475	F: CACTGGTCTAGGACCCGAGAAG R: GGTGCCTCTGAAGATTTTCG	502-574
ABCB11 (BSEP)	NM_021022	F: AGCTACATCTGCCTTAGACACAGAAA R: CAATACAGGTCCGACCCTCTCT	3858-3941
ADAM10	NM_007399	F: CTGCCTGGCCTATGTCTTCAC R: TCTCACATATTCCCCCAGAGCTT	1143-1243
ADAM17	NM_009615	F: TGAGGAAAGGGAAGCCATGT R: CAATTACGTCCTGTACTCGTTTCTC	2030-2107
AK018341	NM_001080935	F: GACAGAAGGGTCAGGAGTTCAAG R: TCTCCAGCCCCTCTCTAGAAGA	
AK5	NM_001081277	F: TTCCAAACAAAGAGGCTCCG R: CATCAAACATCATGGAAGGGTCA	1240-1299
ALOX12	NM_007440	F: AAACTGGAGCTGCAACTGCG R: TCGGGAACGTCGAAGTCAAACT	169-233
Amigo2	NM_178114	F: TGAGAAGCGACTGGCAAGAGAC R: GTTTGACAGCTCTAGGCAGGGTG	712-797
ARRB2	NM_145429	F: CAAGACCGTCAAGAAGATCAGAGT R: CTGCGCGGTGCTGAAG	759-828
CACNA1A (CaV2.1)	NM_007578	F: CGAGTGGCTCTCCGACTTC R:TTCGGACATAAAGAGTCCTAAGAAAA	1823-1886
CACNA1B (CaV2.2)	NM_007579	F: CGGGACCTGTGGAACATTCT R: CGCAGGACTCTCAGAGACTTGA	3715-3830
CACNA1C (CaV1.2)	NM_009781	F: GTGCGGTTGCTCAGGATCT R: GCAAGGATGCCACAAGGTT	2132-2201
CACNA1D (CaV1.3)	NM_028981	F: CGCCTGGAACACGTTTGAC R: GAGGGCCACGTCTATAATGCT	3922-3979
CACNA1E (CaV2.3)	NM_009782	F: CTGTGCCACCAAAGCCTCGT R: CAGGAGGTGGAGAGATGCCG	6363-6382
CACNA1F (CaV1.4)	NM_019582	F: CAGGCAGCCCAGTGTGATACAG R: AGCTGAATACTTCCTTCTTCCG	5179-5274
CACNA1G (CaV3.1)	NM_009783	F: CATTCTCGTGGAGGGTTTCCAG R: CTGTCCACTCGTATCTTCCCG	3464-3524
CACNA1H (CaV3.2)	NM_021415	F: TGTGAGGATGTTGAGTGCCG R: CTCCACAGCAAAGAAGGCAAAG	699-782
CACNA1I (CaV3.3)	NM_001044308	F: CCTCTCAAAGCCATCAACCG R: GTCCAGCAGCAGGTTCACCA	1108-1167
CACNA1S (CaV1.1)	NM_014193	F: TGAAATCGAAGGCTTGAACAAA R: AAGACGCGATTCCACTGTCG	1197-1262
CACNA2D1	NM_001110843	F: AGGACATGCTCATTCTGGTGGA R: GATGAGTTTCAGAGTCAATCCG	1078-1139

CACNA2D2	NM_001174047	F: GGTACTGGCAGGCAAGGACG R: GGGAGAGTTCCTGTTACCACCA	1617-1709
CACNA2D3	NM_009785	F: CTCAGGCCACTGTATGAAGAAGGA R: CTGTAGTTGGGTTTCCTCCG	1712-1761
CACNA2D4	NM_001033382	F: CCTCTCTCATCCTGACCTCCG R: TTGGGTTTGGGTCTCAGCTTCT	1809-1871
CACNB1	NM_031173	F: ACATCCAACAGCTTCGTCCG R: AGTCTGATGGTCGGCTCGTGT	350-410
CACNB2	NM_023116	F: CTCGGATGGAAGCACATCGTC R: GCTGGTGTAGGAGTCTGCCG	295-370
CACNB3	NM_007581	F: CGGCGAGAAGTGGAGAGTCA R: ACAGCAAATGCCACAGGTTTG	526-596
CACNB4	NM_001037099	F: GGCAAGAGCGAGAACAGCAAG R: GCTCACGTTCGTTTTCACCG	470-555
CACNG1	NM_007582	F: AAAGACAAGAGTTGTGAGCACG R: CCTGGGTTGAAGTGCCTGAAG	281-354
CACNG2	NM_007583	F: GGACTACGAAGCTGACACCG R: AGCAGGATCACACTCAGGATCG	650-733
CACNG3	NM_019430	F: CGCTGGCATCTTCTTCGTCT R: GCTGAGATATAAACTATGATGCCG	441-506
CACNG4	NM_019431	F: ATATTGTCCTCAGCGCGGGAAT R: TGGAAATGTAGACGATGATACCG	407-484
CACNG5	NM_080644	F: CATACTGGCCTTTGTCTCCG R: CAGGCCCACCACAAGAGAGAG	487-550
CACNG6	NM_133183	F: TGGAAGGTGTGCATCAAGCG R: CCCGTGGTGAAGAATTTGAAGT	250-368
CACNG7	NM_133189	F: ACTTGGTGACGGAAAACACG R: TGACCATAGGGAAGGGTGTAGC	251-319
CACNG8	NM_133190	F: GGACTACGACCACGACAGCG R: TGGCGCTCAGGATAGGAAAGAT	438-514
CCND1	NM_007631	F: GCGTACCCTGACACCAATCT R: CAGGTCTCCTCCGTCTTGAG	278-345
CSNK	NM_007786	F: AACTGCCGTGGTGAGAAGAATG R: ACAGGACTCTTTGCTCATCGTAC	136-187
CYCLO	NM_011149	F: TGGAGAGCACCAAGACAGACA R: TGCCGGAGTCGACAATGAT	642-707
CYP24A1	NM_009996	F: TGCCCTATTTAAAGGCCTGTCT R: CGAGTTGTGAATGGCACACTT	1485-1551
DOK5	NM_029761	F: CAGGGAGGATGTGTGAGACTGG R: CTTCTGGTAGATGGCCTCTCCG	909-982
FABP6	NM_008375	F: CAAGGCTACCGTGAAGATGGA R: CCCACGACCTCCGAAGTCA	240-317
FGF15	NM_008003	F: GGAGGACCAAAACGAACGAA R: TGACGTCCTTGATGGCAATC	381-454
FXR (NR1H4)	NM_009108	F: TGAGAACCCACAGCATTTCG R: GCGTGGTGATGGTTGAATGTC	1319-1390
GADD45a	NM_007836	F: CTGCAGAGCAGAAGACCGAAA R: GAGCCTTGCTGAGCACTTCCT	186-254

Galectin-1	NM_008495	F: GGGGAATGTCTCAAAGTTCG R: CCCAGGTTCAGCACAAAGCTC	114-178
GDF10 (BMP3b)	NM_145741	F: CAAATCCTTTGACGCCTACTACTG R: CTGACGATGCTCTGGATGGT	1494-1592
Glucagon	NM_008100	F: ATTCACCAGCGACTACAGCAA R: TCATCAACCACTGCACAAAATC	271-338
GLP1R	NM_021332	F: CTTTCTTTCTCCGCCTTGGT R: GGTGCAGTGCAAGTGTCTGA	470-535
GPBAR1	NM_174985	F: TCCTGCCTCCTTCTCCACTT R: ATGCACCAGCAGCAGATTG	247-318
GPC6	NM_011821	F: CGGAGTTCGAGTTTGTCACCAC R: TTCCTTCTTCTCTGCGGTCCG	2174-2236
H2-Bl	NM_008199	F: GCGAACGCTGTTCCTGCTACT R: ACTGCGGTCTCGAAATATCG	35-124
Het INSII	NT_039437 X04724	F: GGGGAGCGTGGCTTCTTCTA R: GGGGACAGAATTCAGTGGCA	1262-1347
HPRT1	NM_013556	F: GCCTAAGATGAGCGCAAGTTG R: TACTAGGCAGATGGCCACAGG	739-839
IBAT (SLC10A2)	NM_011388	F: TGGGTTTCTTCCTGGCTAGACT R: TGTTCTGCATTCCAGTTTCCAA	768-848
Ildr2*	NM_001154528	F: CCAGCAGTCCCAGCTATGAC R: CCTCCCTTTAAATGTTTCCTTTCA	6706-6777
InsulinI/II	NM_008386 NM_008387	F: TGAAGTGGAGGACCCACAAGT R: AGATGCTGGTGCAGCACTGAT	351-475 241-371
Klotho	NM_13823	F: AATTATGTGAATGAGGCTCGTAAAG R: TACGCAAAGTAGCCACAAAGG	2793-2860
MX2	NM_013606	F: CAGCATCTGAATGCCTACCG R: ATCAAGGGAACGTGGCTGGA	1833-1894
NEDD9	NM_017464	F: CCCAGGTCCACAGTAAGCCG R: GGTGGCTGGTCCTTGCTTAGAC	1921-1972
NTCP (SLC10A1)	NM_011387	F: GAAGTCCAAAAGGCCACACTATGT R: ACAGCCACAGAGAGGGAGAAAG	663-740
OSGIN1	NM_027950	F: GACTGGATGCGGAAGAAATGC R: TAGTAGTGGGCGATGTCACCG	639-709
OSTalpha	NM_145932	F: AACAGAACATGGGATCCAAGTTT R: CAGGGCGGTCAGGATGA	1103-1161
OSTbeta	NM_178933	F: GACAAGCATGTTCCTCCTGAGA R: TGTCTTGTGGCTGCTTCTTTC	198-265
PC1/3 (PCSK1)	NM_013628	F: TGGAGGCAAACCCAAATCTT R: GGGTCGTACTCAGAGGTCCAG	1262-1331
PC2 (PCSK2)	NM_008792	F: CAAGCGGAACCAGCTTCA R: ATTCCAGGCCAACCCCA	1606-1667
PRG-3	NM_178756	F: AACCGCGTCTCAGAGTACCG R: ATGAACCACACACATTCCCAAA	934-1032
RAMP1	NM_016894	F: CCATTACGGTCACGCTGCTC R: TACACGATGCCCTCTGTGCG	644-713
RNase4A	NM_201239	F: TCCCAGTCGGAGGAAAGCT R: CAAGAGCAGAAGCAA	445-530

SCL51094	SCL51094*	F: TTCGGGACCAGGGAGCTA R: CCCCCAGAGTCCTAAACAAAGA	*
SGK2	NM_013731	F: CAGCCCAGTTGGAGTTCCTAGC R: AAATCAAAGTCTGTGGGCCG	394-495
SHP (NR0B2)	NM_011850	F:CAGCGCTGCCTGGAGTCT R: AGGATCGTGCCCTTCAGGTA	492-565
SLITRK1	NM_199065	F: AACTTGCTGAGGTCCCTACCG R: GACTGAGCTTAGACAGGGAGACC	2403-2463
SST	NM_009215	F: CCCCCAAACCCCATATCTC R: TTTCTAATGCAGGGTCAAGTTGA	491-557
STX18	NM_026959	F: CCAGACTCCAAGAGATATTCACCG R: TGCTGTCGATCTCAGTTTCCTG	885-944
ST6Gal1	NM_145933	F: CTGTGTATCATGCAGACATTCCG R: GGGTGAAGCCTTCGGTAACTC	1564-1651
SYTL2	NM_031394	F: AAGACGCAGAAGTTGAACCTGTC R: TGTTGCGCTTAAATGTATCCCG	1017-1071
TACR3	NM_021382	F: AACTTCTTTCCCATCACAGCG R: GCCATATACCTGTCCACTGCAA	711-784
TGFB1	NM_011577	F: GCAGTGGCTGAACCAAGGA R: AGAGCAGTGAGCGCTGAATC	1482-1539
TM4SF4	NM_145539	F: GAGGAAAAGTGGTGAACGACAA R: CACAAGCGCAGGGAAGATC	300-400
TMEM27	NM_020626	F: GCCATAAGAAAGAATAGGAACCG R: TTCCAGAGTATGGTCATCCAGAAA	396-458
TRPV6	NM_022413	F: GGACAACACTCTGATGCAACAG R: CCACCAACCGGAGGTCAT	1381-1454
Ttc36	NM_138951	F: GTTGTTGGATTGGACCTGGAAG R: GAGTGCTCCAACTGTGCTTG	199-275
VDR	NM_009504	F: GGCTTCCACTTCAACGCTATG R: ATGCTCCGCCTGAAGAAAC	237-295

Table C.2. Oligonucleotides containing putative VDREs for analysis by cell reporter assay.

Gene Abbrev.	Species	Location	Oligonucleotide Sequence (5' to 3')	Genomic Localization
CACNA1E (CaV2.3)	human	3' UTR	F: agctt**TGAACTCCTTGAACT**tc R: agctga**AGTTCAAGGACTTCA**a	181770496-181770510
CACNA1E (CaV2.3)	human	Intron 6	F: agctt**GGTTGAGCAAGGTCA**tc R: agctga**TGACCTTGCTCAACC**a	181569812-181569826
CACNA1E (CaV2.3)	human	Intron 7	F: agctt**TGAACTCTATGACCT**tc R: agctga**AGGTCATAGAGTTCA**a	181673333-181673347
CACNA1E (CaV2.3)	human and mouse	Exon 13	F: agctt**AGGTCACAGTGGGCA**tc R: agctga**AGCCCACAGTGACCT**a	H:181688885-181688899 M:156330761-156330747
CACNA1E (CaV2.3)	human and mouse	Exon 18	F: agctt**AGGCCAAGGAGGTCA**tc R: agctga**AGCCCTCCTTGGCCT**a	H: 181695250-181695264 M: 156324944-156324930

CACNA1E (CaV2.3)	mouse	Intron 25	F: agctt**AGTTCACTGAGGTCA**tc R: agctga**TGACCTCAGTGAACT**a	156307171-156307157
CACNA1E (CaV2.3)	mouse	Intron 7	F: agctt**TGAACTGTGTGACCT**tc R: agctga**AGGTCACACAGTTCA**a	156348360-156348346
CACNA2D3	mouse	Intron 2a	F: agctt**AGTTCACTCAGTTCA**tc R: agctga**TGAACTGAGTGAACT**a	30425696-30425710
CACNA2D3	mouse	Intron 2b	F: agctt**TGAACTGCCTGACCT**tc R: agctga**AGGTCAGGCAGTTCA**a	30360546-30360560
CACNA2D3	mouse	Intron 16	F: agctt**AGGTCACACAGTTGA**tc R: agctga**TCAACTGTGTGACCT**a	29896753-29896767
CACNA2D3	mouse	3’	F: agctt**GGGTCAGAGGGGTCA**tc R: agctga**TGACCCCTCTGACCC**a	29710220-29710234

BIBLIOGRAPHY

1. Chuang J-C, Cha J-Y, Garmey JC, Mirmira RG, Repa JJ: **Nuclear hormone receptor expression in the endocrine pancreas.** *Molecular Endocrinology* 2008, **22**:2353-2363.

2. Suzuki Y, Landowski CP, Hediger MA: **Mechanisms and regulation of epithelial Ca2+ absorption in health and disease**. *Annu Rev Physiol* 2008, **70**:257-271.

3. Meyer MB, Goetsch PD, Pike JW: **A downstream intergenic cluster of regulatory enhancers contributes to the induction of CYP24A1 expression by 1alpha,25-dihydroxyvitamin D3**. *J Biol Chem* 2010, **285**(20):15599-15610.

4. Meyer MB, Goetsch PD, Pike JW: **Genome-wide analysis of the VDR/RXR cistrome in osteoblast cells provides new mechanistic insight into the actions of the vitamin D hormone**. *J Steroid Biochem Mol Biol* 2010, **121**(1-2):136-141.

5. Cavalier E, Delanaye P, Souberbielle JC, Radermecker RP: **Vitamin D and type 2 diabetes mellitus: where do we stand?** *Diabetes Metab* 2011, **37**(4):265-272.

6. Wolden-Kirk H, Overbergh L, Christesen HT, Brusgaard K, Mathieu C: **Vitamin D and diabetes: Its importance for beta cell and immune function**. *Mol Cell Endocrinol* 2011.

7. Ross AC, Manson JE, Abrams SA, Aloia JF, Brannon PM, Clinton SK, Durazo-Arvizu RA, Gallagher JC, Gallo RL, Jones G *et al*: **The 2011 report on dietary reference intakes for calcium and vitamin D from the Institute of Medicine: what clinicians need to know**. *J Clin Endocrinol Metab* 2011, **96**(1):53-58.

8. Jones G: **Pharmacokinetics of vitamin D toxicity**. *Am J Clin Nutr* 2008, **88**(2):582S-586S.

9. Holick MF: **Vitamin D status: measurement, interpretation, and clinical application**. *Ann Epidemiol* 2009, **19**(2):73-78.

10. Holick MF: **Vitamin D deficiency.** *New England Journal of Medicine* 2007, **357**:266-281.

11. Forrest KY, Stuhldreher WL: **Prevalence and correlates of vitamin D deficiency in US adults**. *Nutr Res* 2011, **31**(1):48-54.

12. Wang S: **Epidemiology of vitamin D in health and disease**. *Nutr Res Rev* 2009, **22**(2):188-203.

13. Knekt P, Laaksonen M, Mattila C, Harkanen T, Marniemi J, Heliovaara M, Rissanen H, Montonen J, Reunanen A: **Serum vitamin D and subsequent occurrence of type 2 diabetes**. *Epidemiology* 2008, **19**(5):666-671.

14. Anderson JL, May HT, Horne BD, Bair TL, Hall NL, Carlquist JF, Lappe DL, Muhlestein JB: **Relation of vitamin D deficiency to cardiovascular risk factors, disease status, and incident events in a general healthcare population**. *Am J Cardiol* 2010, **106**(7):963-968.

15. Pittas AG, Sun Q, Manson JE, Dawson-Hughes B, Hu FB: **Plasma 25-hydroxyvitamin D concentration and risk of incident type 2 diabetes in women**. *Diabetes Care* 2010, **33**(9):2021-2023.

16. Pittas AG, Harris SS, Stark PC, Dawson-Hughes B: **The effects of calcium and vitamin D supplementation on blood glucose and markers of inflammation in nondiabetic adults**. *Diabetes Care* 2007, **30**(4):980-986.

17. Nikooyeh B, Neyestani TR, Farvid M, Alavi-Majd H, Houshiarrad A, Kalayi A, Shariatzadeh N, Gharavi A, Heravifard S, Tayebinejad N *et al*: **Daily consumption of vitamin D- or vitamin D + calcium-fortified yogurt drink improved glycemic control in patients with type 2 diabetes: a randomized clinical trial**. *Am J Clin Nutr* 2011, **93**(4):764-771.

18. Mitri J, Dawson-Hughes B, Hu FB, Pittas AG: **Effects of vitamin D and calcium supplementation on pancreatic beta cell function, insulin sensitivity, and glycemia in adults at high risk of diabetes: the Calcium and Vitamin D for Diabetes Mellitus (CaDDM) randomized controlled trial**. *Am J Clin Nutr* 2011, **94**(2):486-494.

19. Norman AW, Frankel JB, Heldt AM, Grodsky GM: **Vitamin D deficiency inhibits pancreatic secretion of insulin**. *Science* 1980, **209**(4458):823-825.

20. Kadowaki S, Norman AW: **Dietary vitamin D is essential for normal insulin secretion from the perfused rat pancreas**. *J Clin Invest* 1984, **73**(3):759-766.

21. Kadowaki S, Norman AW: **Time course study of insulin secretion after 1,25-dihydroxyvitamin D3 administration**. *Endocrinology* 1985, **117**(5):1765-1771.

22. **Centers for Disease Control and Prevention. National diabetes fact sheet: national estimates and general information on diabetes and prediabetes in the United States, 2011**. In. Edited by Department of Health and Human Services CfDCaP. Atlanta, USA: 2011.

23. Weir GC, Bonner-Weir S: **Five stages of evolving beta-cell dysfunction during progression to diabetes**. *Diabetes* 2004, **53 Suppl 3**:S16-21.

24. WF G: **Endocrine Functions of the Pancreas and Regulation of Carbohydrate Metabolism**. In: *In Review of Medical Physiology.* Edited by Grawhill nEM, 22nd edn; 2005: 340-355.

25. Ishiki M, Klip A: **Minireview: recent developments in the regulation of glucose transporter-4 traffic: new signals, locations, and partners**. *Endocrinology* 2005, **146**(12):5071-5078.

26. Hauge-Evans AC, King AJ, Carmignac D, Richardson CC, Robinson IC, Low MJ, Christie MR, Persaud SJ, Jones PM: **Somatostatin secreted by islet delta-cells fulfills multiple roles as a paracrine regulator of islet function**. *Diabetes* 2009, **58**(2):403-411.

27. Hameed S, Dhillo WS, Bloom SR: **Gut hormones and appetite control**. *Oral Dis* 2009, **15**(1):18-26.

28. Andersson A: **Isolated mouse pancreatic islets in culture: effects of serum and different culture media on the insulin production of the islets**. *Diabetologia* 1978, **14**(6):397-404.

29. Stoffers KL, Sorg BL, Seuter S, Rau O, Radmark O, Steinhilber D: **Calcitriol upregulates open chromatin and elongation markers at functional vitamin D response elements in the distal part of the 5-lipoxygenase gene**. *J Mol Biol* 2010, **395**(4):884-896.

30. Kim S, Yamazaki M, Zella LA, Meyer MB, Fretz JA, Shevde NK, Pike JW: **Multiple enhancer regions located at significant distances upstream of the transcriptional start site mediate RANKL gene expression in response to 1,25-dihydroxyvitamin D3**. *J Steroid Biochem Mol Biol* 2007, **103**(3-5):430-434.

31. Mitri J, Muraru MD, Pittas AG: **Vitamin D and type 2 diabetes: a systematic review**. *Eur J Clin Nutr* 2011, **65**(9):1005-1015.

32. Pittas AG, Lau J, Hu FB, Dawson-Hughes B: **The role of vitamin D and calcium in type 2 diabetes. A systematic review and meta-analysis**. *J Clin Endocrinol Metab* 2007, **92**(6):2017-2029.

33. Li YC, Pirro AE, Amling M, Delling G, Baron R, Bronson RT, Demay MB: **Targeted ablation of the vitamin D receptor: an animal model of vitamin D-dependent rickets type II with alopecia.** *Proceedings of the National Academy of Sciences USA* 1997, **94**:9831-9835.

34. Poitout V, Stout LE, Armstrong MB, Walseth TF, Sorenson RL, Robertson RP: **Morphological and functional characterization of βTC-6 cells- an insulin-secreting cell line derived from transgenic mice.** *Diabetes* 1995, **44**:306-313.

35. Powers AC, Efrat S, Mojsov S, Spector D, Habener JF, Hanahan D: **Proglucagon processing similar to normal islets in pancreatic α-like cell line derived from transgenic mouse tumor.** *Diabetes* 1990, **39**:406-414.

36. Miyazaki J, Araki K, Yamato E, Ikegami H, Asano T, Shibasaki Y, Oka Y, Yamamura K: **Establishment of a pancreatic beta cell line that retains glucose-inducible insulin secretion: special reference to expression of glucose transporter isoforms.** *Endocrinology* 1990, **127**:126-132.

37. Ogihara T, Chuang JC, Vestermark GL, Garmey JC, Ketchum RJ, Huang X, Brayman KL, Thorner MO, Repa JJ, Mirmira RG *et al*: **Liver X receptor agonists augment human islet function through activation of anaplerotic pathways and glycerolipid/free fatty acid cycling**. *J Biol Chem* 2010, **285**(8):5392-5404.

38. Kurrasch DM, Huang J, Wilkie TM, Repa JJ: **Quantitative real-time polymerase chain reaction measurement of regulators of G-protein signaling mRNA levels in mouse tissues.** *Methods in Enzymology* 2004, **389**:3-15.

39. Valasek MA, Repa JJ: **The power of real-time PCR.** *Advances in Physiology Education* 2005, **29**:151-159.

40. Sandelin A, Wasserman WW: **Prediction of nuclear hormone receptor response elements.** *Molecular Endocrinology* 2005, **19**:595-606.

41. Willy PJ, Mangelsdorf DJ: **Unique requirements for retinoid-dependent transcriptional activation by the orphan receptor LXR.** *Genes & Development* 1997, **11**:289-298.

42. Christensen SE, Nissen PH, Vestergaard P, Heickendorff L, Rejnmark L, Brixen K, Mosekilde L: **Plasma 25-hydroxyvitamin D, 1,25-dihydroxyvitamin D, and parathyroid hormone in familial hypocalciuric hypercalcemia and primary hyperparathyroidism**. *Eur J Endocrinol* 2008, **159**(6):719-727.

43. Dardenne O, Prud'homme J, Arabian A, Glorieux FH, St-Arnaud R: **Targeted inactivation of the 25-hydroxyvitamin D(3)-1(alpha)-hydroxylase gene (CYP27B1) creates an animal model of pseudovitamin D-deficiency rickets**. *Endocrinology* 2001, **142**(7):3135-3141.

44. Kim S, Yamazaki M, Zella LA, Shevde NK, Pike JW: **Activation of receptor activator of NF-kappaB ligand gene expression by 1,25-dihydroxyvitamin D3 is mediated through multiple long-range enhancers**. *Mol Cell Biol* 2006, **26**(17):6469-6486.

45. Tarroni P, Villa I, Mrak E, Zolezzi F, Mattioli M, Gattuso C, Rubinacci A: **Microarray analysis of 1,25(OH)(2) D(3) regulated gene expression in human primary osteoblasts**. *J Cell Biochem* 2011.

46. Jurutka PW, Thompson PD, Whitfield GK, Eichhorst KR, Hall N, Dominguez CE, Hsieh JC, Haussler CA, Haussler MR: **Molecular and functional comparison of 1,25-dihydroxyvitamin D(3) and the novel vitamin D receptor ligand, lithocholic acid, in activating transcription of cytochrome P450 3A4**. *J Cell Biochem* 2005, **94**(5):917-943.

47. Nehring JA, Zierold C, DeLuca HF: **Lithocholic acid can carry out in vivo functions of vitamin D**. *Proc Natl Acad Sci U S A* 2007, **104**(24):10006-10009.

48. Meyer MB, Watanuki M, Kim S, Shevde NK, Pike JW: **The human transient receptor potential vanilloid type 6 distal promoter contains multiple vitamin D receptor binding sites that mediate activation by 1,25-dihydroxyvitamin D3 in intestinal cells**. *Mol Endocrinol* 2006, **20**(6):1447-1461.

49. Yang S-N, Berggren P-O: **The role of voltage-gated calcium channels in pancreatic β-cell physiology and pathophysiology.** *Endocrine Reviews* 2006, **27**:621-676.

50. Jing X, Li D-Q, Olofsson CS, Salehi A, Surve VV, Caballero J, Ivarsson R, Lundquist I, Pereverzev A, Schneider TL *et al*: **$Ca_v2.3$ calcium channels control second-phase insulin release.** *Journal of Clinical Investigation* 2005, **115**:146-154.

51. Holmkvist J, Tojjar D, Almgren P, Lyssenko V, Lindgren CM, Isomaa B, Tuomi T, Berglund G, Renstrom E, Groop L: **Polymorphisms in the gene encoding the voltage-dependent Ca(2+) channel Ca (V)2.3 (CACNA1E) are associated with type 2 diabetes and impaired insulin secretion**. *Diabetologia* 2007, **50**(12):2467-2475.

52. Muller YL, Hanson RL, Zimmerman C, Harper I, Sutherland J, Kobes S, Knowler WC, Bogardus C, Baier LJ: **Variants in the Ca V 2.3 (alpha 1E) subunit of voltage-activated Ca2+ channels are associated with insulin resistance and type 2 diabetes in Pima Indians**. *Diabetes* 2007, **56**(12):3089-3094.

53. Klugbauer N, Lacinova L, Marais E, Hobom M, Hofmann F: **Molecular diversity of the calcium channel α2δ subunit.** *Journal of Neuroscience* 1999, **19**:684-691.

54. Jangsangthong W, Kuzmenkina E, Khan IF, Matthes J, Hullin R, Herzig S: **Inactivation of L-type calcium channels is determined by the length of the N terminus of mutant beta(1) subunits**. *Pflugers Arch* 2010, **459**(3):399-411.

55. Cohen RM, Foell JD, Balijepalli RC, Shah V, Hell JW, Kamp TJ: **Unique modulation of L-type Ca2+ channels by short auxiliary beta1d subunit present in cardiac muscle**. *Am J Physiol Heart Circ Physiol* 2005, **288**(5):H2363-2374.

56. Kuro-o M, Matsumura Y, Aizawa H, Kawaguchi H, Suga T, Utsugi T, Ohyama Y, Kurabayashi M, Kaname T, Kume E *et al*: **Mutation of the mouse klotho gene leads to a syndrome resembling ageing**. *Nature* 1997, **390**(6655):45-51.

57. Kurosu H, Yamamoto M, Clark JD, Pastor JV, Nandi A, Gurnani P, McGuinness OP, Chikuda H, Yamaguchi M, Kawaguchi H *et al*: **Suppression of aging in mice by the hormone Klotho**. *Science* 2005, **309**(5742):1829-1833.

58. Chen CD, Podvin S, Gillespie E, Leeman SE, Abraham CR: **Insulin stimulates the cleavage and release of the extracellular domain of Klotho by ADAM10 and ADAM17**. *Proc Natl Acad Sci U S A* 2007, **104**(50):19796-19801.

59. Huang CL: **Regulation of ion channels by secreted Klotho: mechanisms and implications**. *Kidney Int* 2010, **77**(10):855-860.

60. Cha S-K, Ortega B, Kurosu H, Rosenblatt KP, Kuro-o M, Huang C-L: **Removal of sialic acid involving Klotho causes cell-surface retention of TRPV5 channel via binding to galectin-1.** *Proceedings of the National Academy of Sciences USA* 2008, **105**:9805-9810.

61. Ohtsubo K, Takamatsu S, Minowa MT, Yoshida A, Takeuchi M, Marth JD: **Dietary and genetic control of glucose transporter 2 glycosylation promotes insulin secretion in suppressing diabetes.** *Cell* 2005, **123**:1307-1321.

62. Farrow EG, White KE: **Recent advances in renal phosphate handling**. *Nat Rev Nephrol* 2010, **6**(4):207-217.

63. Utsugi T, Ohno T, Ohyama Y, Uchiyama T, Saito Y, Matsumura Y, Aizawa H, Itoh H, Kurabayashi M, Kawazu S *et al*: **Decreased insulin production and increased insulin sensitivity in the klotho mutant mouse, a novel animal model for human aging**. *Metabolism* 2000, **49**(9):1118-1123.

64. Mori K, Yahata K, Mukoyama M, Suganami T, Makino H, Nagae T, Masuzaki H, Ogawa Y, Sugawara A, Nabeshima Y *et al*: **Disruption of klotho gene causes an abnormal energy homeostasis in mice**. *Biochem Biophys Res Commun* 2000, **278**(3):665-670.

65. Tinsley FC, Taicher GZ, Heiman ML: **Evaluation of a quantitative magnetic resonance method for mouse whole body composition analysis**. *Obes Res* 2004, **12**(1):150-160.

66. Rondini TA, Rodrigues Bde C, de Oliveira AP, Bittencourt JC, Elias CF: **Melanin-concentrating hormone is expressed in the laterodorsal tegmental nucleus only in female rats**. *Brain Res Bull* 2007, **74**(1-3):21-28.

67. Tsujikawa H, Kurotaki Y, Fujimori T, Fukuda K, Nabeshima Y: **Klotho, a gene related to a syndrome resembling human premature aging, functions in a negative regulatory circuit of vitamin D endocrine system**. *Mol Endocrinol* 2003, **17**(12):2393-2403.

68. Urakawa I, Yamazaki Y, Shimada T, Iijima K, Hasegawa H, Okawa K, Fujita T, Fukumoto S, Yamashita T: **Klotho converts canonical FGF receptor intoa specific receptor for FGF23.** *Nature* 2006, **444**:770-774.

69. Morishita K, Shirai A, Kubota M, Katakura Y, Nabeshima Y, Takeshige K, Kamiya T: **The progression of aging in klotho mutant mice can be modified by dietary phosphorus and zinc**. *J Nutr* 2001, **131**(12):3182-3188.

70. Guillam MT, Hummler E, Schaerer E, Yeh JI, Birnbaum MJ, Beermann F, Schmidt A, Deriaz N, Thorens B: **Early diabetes and abnormal postnatal pancreatic islet development in mice lacking Glut-2**. *Nat Genet* 1997, **17**(3):327-330.

71. Kuro-o M: **Overview of the FGF23-Klotho axis**. *Pediatr Nephrol* 2010, **25**(4):583-590.

72. Forster RE, Jurutka PW, Hsieh JC, Haussler CA, Lowmiller CL, Kaneko I, Haussler MR, Kerr Whitfield G: **Vitamin D receptor controls expression of the anti-aging klotho gene in mouse and human renal cells**. *Biochem Biophys Res Commun* 2011, **414**(3):557-562.

73. Novelli M, De Tata V, Bombara M, Bergamini E, Masiello P: **Age-dependent reduction in GLUT-2 levels is correlated with the impairment of the insulin secretory response in isolated islets of Sprague-Dawley rats**. *Exp Gerontol* 2000, **35**(5):641-651.

74. Kramer J, Moeller EL, Hachey A, Mansfield KG, Wachtman LM: **Differential expression of GLUT2 in pancreatic islets and kidneys of New and Old World nonhuman primates**. *Am J Physiol Regul Integr Comp Physiol* 2009, **296**(3):R786-793.

75. Witkowski JM, Soroczynska-Cybula M, Bryl E, Smolenska Z, Jozwik A: **Klotho--a common link in physiological and rheumatoid arthritis-related aging of human CD4+ lymphocytes**. *J Immunol* 2007, **178**(2):771-777.

76. Li X, Liao L, Yan X, Huang G, Lin J, Lei M, Wang X, Zhou Z: **Protective effects of 1-alpha-hydroxyvitamin D3 on residual beta-cell function in patients with adult-onset latent autoimmune diabetes (LADA)**. *Diabetes Metab Res Rev* 2009, **25**(5):411-416.

77. Hypponen E, Laara E, Reunanen A, Jarvelin MR, Virtanen SM: **Intake of vitamin D and risk of type 1 diabetes: a birth-cohort study**. *Lancet* 2001, **358**(9292):1500-1503.

78. Stene LC, Joner G: **Use of cod liver oil during the first year of life is associated with lower risk of childhood-onset type 1 diabetes: a large, population-based, case-control study**. *Am J Clin Nutr* 2003, **78**(6):1128-1134.

79. **Vitamin D supplement in early childhood and risk for Type I (insulin-dependent) diabetes mellitus. The EURODIAB Substudy 2 Study Group**. *Diabetologia* 1999, **42**(1):51-54.

80. Mathieu C, Laureys J, Sobis H, Vandeputte M, Waer M, Bouillon R: **1,25-Dihydroxyvitamin D3 prevents insulitis in NOD mice**. *Diabetes* 1992, **41**(11):1491-1495.

81. Gysemans CA, Cardozo AK, Callewaert H, Giulietti A, Hulshagen L, Bouillon R, Eizirik DL, Mathieu C: **1,25-Dihydroxyvitamin D3 modulates expression of chemokines and cytokines in pancreatic islets: implications for prevention of diabetes in nonobese diabetic mice**. *Endocrinology* 2005, **146**(4):1956-1964.

82. Gregori S, Giarratana N, Smiroldo S, Uskokovic M, Adorini L: **A 1alpha,25-dihydroxyvitamin D(3) analog enhances regulatory T-cells and arrests autoimmune diabetes in NOD mice**. *Diabetes* 2002, **51**(5):1367-1374.

83. Giulietti A, Gysemans C, Stoffels K, van Etten E, Decallonne B, Overbergh L, Bouillon R, Mathieu C: **Vitamin D deficiency in early life accelerates Type 1 diabetes in non-obese diabetic mice**. *Diabetologia* 2004, **47**(3):451-462.

84. Benoist C, Mathis D: **Cell death mediators in autoimmune diabetes--no shortage of suspects**. *Cell* 1997, **89**(1):1-3.

85. Lemire JM: **Immunomodulatory actions of 1,25-dihydroxyvitamin D3**. *J Steroid Biochem Mol Biol* 1995, **53**(1-6):599-602.

86. Piemonti L, Monti P, Sironi M, Fraticelli P, Leone BE, Dal Cin E, Allavena P, Di Carlo V: **Vitamin D3 affects differentiation, maturation, and function of human monocyte-derived dendritic cells**. *J Immunol* 2000, **164**(9):4443-4451.

87. Mathieu C, Waer M, Laureys J, Rutgeerts O, Bouillon R: **Prevention of autoimmune diabetes in NOD mice by 1,25 dihydroxyvitamin D3**. *Diabetologia* 1994, **37**(6):552-558.

88. Odegaard JI, Chawla A: **Mechanisms of macrophage activation in obesity-induced insulin resistance**. *Nat Clin Pract Endocrinol Metab* 2008, **4**(11):619-626.

89. McDermott MF, Ramachandran A, Ogunkolade BW, Aganna E, Curtis D, Boucher BJ, Snehalatha C, Hitman GA: **Allelic variation in the vitamin D receptor influences susceptibility to IDDM in Indian Asians**. *Diabetologia* 1997, **40**(8):971-975.

90. Chang TJ, Lei HH, Yeh JI, Chiu KC, Lee KC, Chen MC, Tai TY, Chuang LM: **Vitamin D receptor gene polymorphisms influence susceptibility to type 1 diabetes mellitus in the Taiwanese population**. *Clin Endocrinol (Oxf)* 2000, **52**(5):575-580.

91. Pani MA, Knapp M, Donner H, Braun J, Baur MP, Usadel KH, Badenhoop K: **Vitamin D receptor allele combinations influence genetic susceptibility to type 1 diabetes in Germans**. *Diabetes* 2000, **49**(3):504-507.

92. Ban Y, Taniyama M, Yanagawa T, Yamada S, Maruyama T, Kasuga A: **Vitamin D receptor initiation codon polymorphism influences genetic susceptibility to type 1 diabetes mellitus in the Japanese population**. *BMC Med Genet* 2001, **2**:7.

93. Oh JY, Barrett-Connor E: **Association between vitamin D receptor polymorphism and type 2 diabetes or metabolic syndrome in community-dwelling older adults: the Rancho Bernardo Study**. *Metabolism* 2002, **51**(3):356-359.

94. Kajiwara Y, Buxbaum JD, Grice DE: **SLITRK1 binds 14-3-3 and regulates neurite outgrowth in a phosphorylation-dependent manner**. *Biol Psychiatry* 2009, **66**(10):918-925.

95. Katayama K, Yamada K, Ornthanalai VG, Inoue T, Ota M, Murphy NP, Aruga J: **Slitrk1-deficient mice display elevated anxiety-like behavior and noradrenergic abnormalities**. *Mol Psychiatry* 2010, **15**(2):177-184.

96. Xia D, Holla VR, Wang D, Menter DG, DuBois RN: **HEF1 is a crucial mediator of the proliferative effects of prostaglandin E(2) on colon cancer cells**. *Cancer Res* 2010, **70**(2):824-831.

97. Lucas JT, Jr., Salimath BP, Slomiany MG, Rosenzweig SA: **Regulation of invasive behavior by vascular endothelial growth factor is HEF1-dependent**. *Oncogene* 2010, **29**(31):4449-4459.

98. Aquino JB, Lallemend F, Marmigere F, Adameyko, II, Golemis EA, Ernfors P: **The retinoic acid inducible Cas-family signaling protein Nedd9 regulates neural crest cell migration by modulating adhesion and actin dynamics**. *Neuroscience* 2009, **162**(4):1106-1119.

99. Veugelers M, De Cat B, Ceulemans H, Bruystens AM, Coomans C, Durr J, Vermeesch J, Marynen P, David G: **Glypican-6, a new member of the glypican family of cell surface heparan sulfate proteoglycans**. *J Biol Chem* 1999, **274**(38):26968-26977.

100. Ono T, Sekino-Suzuki N, Kikkawa Y, Yonekawa H, Kawashima S: **Alivin 1, a novel neuronal activity-dependent gene, inhibits apoptosis and promotes survival of cerebellar granule neurons**. *J Neurosci* 2003, **23**(13):5887-5896.

101. Kuja-Panula J, Kiiltomaki M, Yamashiro T, Rouhiainen A, Rauvala H: **AMIGO, a transmembrane protein implicated in axon tract development, defines a novel protein family with leucine-rich repeats**. *J Cell Biol* 2003, **160**(6):963-973.

102. Luo X, Ding L, Xu J, Chegini N: **Gene expression profiling of leiomyoma and myometrial smooth muscle cells in response to transforming growth factor-beta**. *Endocrinology* 2005, **146**(3):1097-1118.

103. Birkenkamp-Demtroder K, Maghnouj A, Mansilla F, Thorsen K, Andersen CL, Oster B, Hahn S, Orntoft TF: **Repression of KIAA1199 attenuates Wnt-signalling and decreases the proliferation of colon cancer cells**. *Br J Cancer* 2011, **105**(4):552-561.

104. Zhao R, Lawler AM, Lee SJ: **Characterization of GDF-10 expression patterns and null mice**. *Dev Biol* 1999, **212**(1):68-79.

105. Larsen CM, Dossing MG, Papa S, Franzoso G, Billestrup N, Mandrup-Poulsen T: **Growth arrest- and DNA-damage-inducible 45beta gene inhibits c-Jun N-terminal kinase and extracellular signal-regulated kinase and decreases IL-1beta-induced apoptosis in insulin-producing INS-1E cells**. *Diabetologia* 2006, **49**(5):980-989.

106. Tajima A, Tanaka T, Ebata T, Takeda K, Kawasaki A, Kelly JM, Darcy PK, Vance RE, Raulet DH, Kinoshita K *et al*: **Blastocyst MHC, a putative murine homologue of HLA-G, protects TAP-deficient tumor cells from natural killer cell-mediated rejection in vivo**. *J Immunol* 2003, **171**(4):1715-1721.

107. Savaskan NE, Brauer AU, Nitsch R: **Molecular cloning and expression regulation of PRG-3, a new member of the plasticity-related gene family**. *Eur J Neurosci* 2004, **19**(1):212-220.

108. Consortium WTCC: **Genome-wide association study of 14,000 cases of seven common diseases and 3,000 shared controls.** *Nature* 2007, **447**:661-678.

109. Altirriba J, Gasa R, Casas S, Ramirez-Bajo MJ, Ros S, Gutierrez-Dalmau A, Ruiz de Villa MC, Barbera A, Gomis R: **The role of transmembrane protein 27 (TMEM27) in islet physiology and its potential use as a beta cell mass biomarker**. *Diabetologia* 2010, **53**(7):1406-1414.

110. Esterhazy D, Stutzer I, Wang H, Rechsteiner MP, Beauchamp J, Dobeli H, Hilpert H, Matile H, Prummer M, Schmidt A *et al*: **Bace2 is a beta cell-enriched protease that regulates pancreatic beta cell function and mass**. *Cell Metab* 2011, **14**(3):365-377.

111. Fukui K, Yang Q, Cao Y, Takahashi N, Hatakeyama H, Wang H, Wada J, Zhang Y, Marselli L, Nammo T *et al*: **The HNF-1 target collectrin controls insulin exocytosis by SNARE complex formation**. *Cell Metab* 2005, **2**(6):373-384.

112. Akpinar P, Kuwajima S, Krutzfeldt J, Stoffel M: **Tmem27: a cleaved and shed plasma membrane protein that stimulates pancreatic beta cell proliferation**. *Cell Metab* 2005, **2**(6):385-397.

113. Iinuma T, Aoki T, Arasaki K, Hirose H, Yamamoto A, Samata R, Hauri HP, Arimitsu N, Tagaya M, Tani K: **Role of syntaxin 18 in the organization of endoplasmic reticulum subdomains**. *J Cell Sci* 2009, **122**(Pt 10):1680-1690.

114. Okumura AJ, Hatsuzawa K, Tamura T, Nagaya H, Saeki K, Okumura F, Nagao K, Nishikawa M, Yoshimura A, Wada I: **Involvement of a novel Q-SNARE, D12, in quality control of the endomembrane system**. *J Biol Chem* 2006, **281**(7):4495-4506.

115. Yu M, Kasai K, Nagashima K, Torii S, Yokota-Hashimoto H, Okamoto K, Takeuchi T, Gomi H, Izumi T: **Exophilin4/Slp2-a targets glucagon granules to the plasma membrane through unique Ca2+-inhibitory phospholipid-binding activity of the C2A domain**. *Mol Biol Cell* 2007, **18**(2):688-696.

116. Saegusa C, Tanaka T, Tani S, Itohara S, Mikoshiba K, Fukuda M: **Decreased basal mucus secretion by Slp2-a-deficient gastric surface mucous cells**. *Genes Cells* 2006, **11**(6):623-631.

117. Holt O, Kanno E, Bossi G, Booth S, Daniele T, Santoro A, Arico M, Saegusa C, Fukuda M, Griffiths GM: **Slp1 and Slp2-a localize to the plasma membrane of CTL and contribute to secretion from the immunological synapse**. *Traffic* 2008, **9**(4):446-457.

118. Cai D, Dhe-Paganon S, Melendez PA, Lee J, Shoelson SE: **Two new substrates in insulin signaling, IRS5/DOK4 and IRS6/DOK5**. *J Biol Chem* 2003, **278**(28):25323-25330.

119. Tabassum R, Mahajan A, Chauhan G, Dwivedi OP, Ghosh S, Tandon N, Bharadwaj D: **Evaluation of DOK5 as a susceptibility gene for type 2 diabetes and obesity in North Indian population**. *BMC Med Genet* 2010, **11**:35.

120. Feng X, Wang W, Liu J, Liu Y: **beta-Arrestins: multifunctional signaling adaptors in type 2 diabetes**. *Mol Biol Rep* 2011, **38**(4):2517-2528.

121. Luan B, Zhao J, Wu H, Duan B, Shu G, Wang X, Li D, Jia W, Kang J, Pei G: **Deficiency of a beta-arrestin-2 signal complex contributes to insulin resistance**. *Nature* 2009, **457**(7233):1146-1149.

122. Kovac JR, Chrones T, Preiksaitis HG, Sims SM: **Tachykinin receptor expression and function in human esophageal smooth muscle**. *J Pharmacol Exp Ther* 2006, **318**(2):513-520.

123. Chu PJ, Best PM: **Molecular cloning of calcium channel alpha(2)delta-subunits from rat atria and the differential regulation of their expression by IGF-1**. *J Mol Cell Cardiol* 2003, **35**(2):207-215.

124. Stanojevic V, Habener JF, Holz GG, Leech CA: **Cytosolic adenylate kinases regulate K-ATP channel activity in human beta-cells**. *Biochem Biophys Res Commun* 2008, **368**(3):614-619.

125. Shekar PC, Goel S, Rani SD, Sarathi DP, Alex JL, Singh S, Kumar S: **kappa-casein-deficient mice fail to lactate**. *Proc Natl Acad Sci U S A* 2006, **103**(21):8000-8005.

126. Rampersaud E, Damcott CM, Fu M, Shen H, McArdle P, Shi X, Shelton J, Yin J, Chang YP, Ott SH *et al*: **Identification of novel candidate genes for type 2 diabetes from a genome-wide association scan in the Old Order Amish: evidence for replication from diabetes-related quantitative traits and from independent populations**. *Diabetes* 2007, **56**(12):3053-3062.

127. Rosmond R, Chagnon M, Bouchard C, Bjorntorp P: **Increased abdominal obesity, insulin and glucose levels in nondiabetic subjects with a T29C polymorphism of the transforming growth factor-beta1 gene**. *Horm Res* 2003, **59**(4):191-194.

128. Fuchs A, Cella M, Giurisato E, Shaw AS, Colonna M: **Cutting edge: CD96 (tactile) promotes NK cell-target cell adhesion by interacting with the poliovirus receptor (CD155)**. *J Immunol* 2004, **172**(7):3994-3998.

129. Gasa R, Mrejen C, Lynn FC, Skewes-Cox P, Sanchez L, Yang KY, Lin C-H, Gomis R, German MS: **Induction of pancreatic islet cell differentiation by the neurogenin-neuroD cascade.** *Differentiation* 2008, **76**:381-391.

130. Kim H, Toyofuku Y, Lynn FC, Chak E, Uchida T, Mizukami H, Fujitani Y, Kawamori R, Miyatsuka T, Kosaka Y *et al*: **Serotonin regulates pancreatic beta cell mass during pregnancy.** *Nature Medicine* 2010, **16**:804-808.

131. Imai J, Oka Y, Katagiri H: **Identification of a novel mechanism regulating beta-cell mass: neuronal relay from the liver to pancreatic beta-cells**. *Islets* 2009, **1**(1):75-77.

132. Imai J, Katagiri H, Yamada T, Ishigaki Y, Suzuki T, Kudo H, Uno K, Hasegawa Y, Gao J, Kaneko K *et al*: **Regulation of pancreatic beta cell mass by neuronal signals from the liver**. *Science* 2008, **322**(5905):1250-1254.

133. Wang Z, Thurmond DC: **Mechanisms of biphasic insulin-granule exocytosis - roles of the cytoskeleton, small GTPases and SNARE proteins**. *J Cell Sci* 2009, **122**(Pt 7):893-903.

134. Tront JS, Huang Y, Fornace AJ, Jr., Hoffman B, Liebermann DA: **Gadd45a functions as a promoter or suppressor of breast cancer dependent on the oncogenic stress**. *Cancer Res* 2010, **70**(23):9671-9681.

135. Michishita E, Garces G, Barrett JC, Horikawa I: **Upregulation of the KIAA1199 gene is associated with cellular mortality**. *Cancer Lett* 2006, **239**(1):71-77.

136. Hoffman B, Liebermann DA: **Gadd45 modulation of intrinsic and extrinsic stress responses in myeloid cells**. *J Cell Physiol* 2009, **218**(1):26-31.

137. Saisho K, Fukuhara A, Yasuda T, Sato Y, Fukui K, Iwahashi H, Imagawa A, Hatta M, Shimomura I, Yamagata K: **Glucose enhances collectrin protein expression in insulin-producing MIN6 beta cells**. *Biochem Biophys Res Commun* 2009, **389**(1):133-137.

138. Gordon DE, Bond LM, Sahlender DA, Peden AA: **A targeted siRNA screen to identify SNAREs required for constitutive secretion in mammalian cells**. *Traffic* 2010, **11**(9):1191-1204.

139. Assmann A, Ueki K, Winnay JN, Kadowaki T, Kulkarni RN: **Glucose effects on beta-cell growth and survival require activation of insulin receptors and insulin receptor substrate 2**. *Mol Cell Biol* 2009, **29**(11):3219-3228.

140. Bernal-Mizrachi E, Fatrai S, Johnson JD, Ohsugi M, Otani K, Han Z, Polonsky KS, Permutt MA: **Defective insulin secretion and increased susceptibility to experimental diabetes are induced by reduced Akt activity in pancreatic islet beta cells**. *J Clin Invest* 2004, **114**(7):928-936.

141. Kulkarni RN, Bruning JC, Winnay JN, Postic C, Magnuson MA, Kahn CR: **Tissue-specific knockout of the insulin receptor in pancreatic beta cells creates an insulin secretory defect similar to that in type 2 diabetes**. *Cell* 1999, **96**(3):329-339.

142. Kulkarni RN, Holzenberger M, Shih DQ, Ozcan U, Stoffel M, Magnuson MA, Kahn CR: **beta-cell-specific deletion of the Igf1 receptor leads to hyperinsulinemia and glucose intolerance but does not alter beta-cell mass**. *Nat Genet* 2002, **31**(1):111-115.

143. Otsuki M, Fujii M, Nakamura T, Tani S, Oka T, Yajima H, Baba S: **Effects of neuromedin B and neuromedin C on exocrine and endocrine rat pancreas**. *Am J Physiol* 1987, **252**(4 Pt 1):G491-498.

144. Morgan PE, Treweek TM, Lindner RA, Price WE, Carver JA: **Casein proteins as molecular chaperones**. *J Agric Food Chem* 2005, **53**(7):2670-2683.

145. Piccirillo CA, Chang Y, Prud'homme GJ: **TGF-beta1 somatic gene therapy prevents autoimmune disease in nonobese diabetic mice**. *J Immunol* 1998, **161**(8):3950-3956.

146. Suarez-Pinzon WL, Marcoux Y, Ghahary A, Rabinovitch A: **Gene transfection and expression of transforming growth factor-beta1 in nonobese diabetic mouse islets protects beta-cells in syngeneic islet grafts from autoimmune destruction**. *Cell Transplant* 2002, **11**(6):519-528.

147. Du W, Wong FS, Li MO, Peng J, Qi H, Flavell RA, Sherwin R, Wen L: **TGF-beta signaling is required for the function of insulin-reactive T regulatory cells**. *J Clin Invest* 2006, **116**(5):1360-1370.

148. Han B, Qi S, Hu B, Luo H, Wu J: **TGF-beta i promotes islet beta-cell function and regeneration**. *J Immunol* 2011, **186**(10):5833-5844.

149. Han S, Li T, Ellis E, Strom S, Chiang JY: **A novel bile acid-activated vitamin D receptor signaling in human hepatocytes**. *Mol Endocrinol* 2010, **24**(6):1151-1164.

150. Wood RJ: **Vitamin D and adipogenesis: new molecular insights**. *Nutr Rev* 2008, **66**(1):40-46.

151. Ceglia L: **Vitamin D and skeletal muscle tissue and function**. *Mol Aspects Med* 2008, **29**(6):407-414.

152. Russell DW: **The enzymes, regulation, and genetics of bile acid synthesis.** *Annual Reviews in Biochemistry* 2003, **72**:137-174.

153. Makishima M, Okamoto AY, Repa JJ, Tu H, Learned RM, Luk A, Hull MV, Lustig KD, Mangelsdorf DJ, Shan B: **Identification of a nuclear receptor for bile acids.** *Science* 1999, **284**:1362-1365.

154. Wang H, Chen J, Hollister K, Sowers LC, Forman BM: **Endogenous bile acids are ligands for the nuclear receptor FXR/BAR.** *Molecular Cell* 1999, **3**:543-553.

155. Parks DJ, Blanchard SG, Bledsoe RK, Chandra G, Consler TG, Kliewer SA, Stimmel JB, Willson TM, Zavacki AM, Moore DD *et al*: **Bile acids: natural ligands for an orphan nuclear receptor.** *Science* 1999, **284**:1365-1368.

156. Forman BM, Goode E, Chen J, Oro AE, Bradley DJ, Perlmann T, Noonan DJ, Burka LT, McMorris T, Lamph WW *et al*: **Identification of a nuclear receptor that is activated by farnesol metabolites.** *Cell* 1995, **81**:687-693.

157. Inagaki T, Choi M, Moschetta A, Peng L, Cummins CL, McDonald JG, Luo G, Jones SA, Goodwin B, Richardson JA *et al*: **Fibroblast growth factor 15 functions as an enterohepatic signal to regulate bile acid homeostasis.** *Cell Metabolism* 2005, **2**:217-225.

158. Inagaki T, Moschetta A, Lee Y-K, Peng L, Zhao G, Downes M, Yu RT, Shelton JM, Richardson JA, Repa JJ *et al*: **Regulation of antibacterial defense in small intestine by the nuclear bile acid receptor.** *Proceedings of the National Academy of Sciences USA* 2006, **103**:3920-3925.

159. Huang W, Ma K, Zhang J, Qatanani M, Cuvillier J, Liu J, Dong B, Huang X, Moore DD: **Nuclear receptor-dependent bile acid signaling is required for normal liver regeneration.** *Science* 2006, **312**:233-236.

160. Thomas AM, Hart SN, Kong B, Fang J, Zhong X, Guo GL: **Genome-wide tissue-specific farnesoid X receptor binding in mouse liver and intestine.** *Hepatology Research* 2010, **51**.

161. Chong HK, Infante AM, Seo Y-K, Jeon T-I, Zhang Y, Edwards PA, Xie X, Osborne TF: **Genome-wide interrogation of hepatic FXR reveals an asymmetric IR-1 motif and synergy with LRH-1.** *Nucl Acids Res* 2010, **38**:6007-6017.

162. Renga B, Mencarelli A, Vavassori P, Brancaleone V, Fiorucci S: **The bile acid sensor FXR regulates insulin transcription and secretion.** *Biochimica Biophysica Acta* 2010, **1802**:363-372.

163. Popscu IR, Hellboid-Chapman A, Lucas A, Vandewalle B, Dumont J, Bouchaert E, Derudas B, Kerr-Conte J, Caron S, Pattou F *et al*: **The nuclear receptor FXR is expressed in pancreatic β-cells and protects human islets from lipotoxicity.** *FEBS Lett* 2010, **584**:2845-2851.

164. Rieck S, White P, Schug J, Fox AJ, Smirnova O, Gao N, Gupta RK, Wang ZV, Scherer PE, Keller MP *et al*: **The transcriptional response of the islet to pregnancy in mice.** *Molecular Endocrinology* 2009, **23**:1702-1712.

165. Maruyama T, Miyamoto Y, Nakamura T, Tamai Y, Okada H, Sugiyama E, Nakamura T, Itadani H, Tanaka K: **Identification of membrane-type receptor for bile acids (M-BAR).** *Biochemical and Biophysical Research Communications* 2002, **298**:714-719.

166. Kawamata Y, Fujii R, Hosoya M, Harada M, Yoshida H, Miwa M, Fukusumi S, Habata Y, Itoh T, Shintani Y *et al*: **A G protein-coupled receptor responsive to bile acids.** *Journal of Biological Chemistry* 2003, **278**:9435-9440.

167. Sato H, Genet C, Strehle Z, Thomas C, Lobstein A, Wagner A, Mioskowski C, Auwerx J, Saladin R: **Anti-hyperglycemic activity of a TGR5 agonist isolated from *Olea europaea*.** *Biochem Biophys Res Commun* 2007, **362**:793-798.

168. Keitel V, Gorg B, Bidman HJ, Zemtsova I, Spomer L, Zilles K, Haussinger D: **The bile acid receptor TGR5 (Gpbar-1) acts as a neurosteroid receptor in brain.** *Glia* 2010, **58**:1794-1805.

169. Sato H, Macchiarulo A, Thomas C, Gioiello A, Une M, Hofmann AF, Saladin R, Schoonjans K, Pellicciari R, Auwerx J: **Novel potent and selective bile acid derivatives as TGR5 agonists: biological screening, structure - activity relationships, and molecular modeling studies.** *Journal of Medicinal Chemistry* 2008, **51**:1831-1841.

170. Herbert MR, Siegel DL, Staszewski L, Cayanan C, Banerjee U, Dhamija S, Anderson J, Fan A, Wnag L, Rix P *et al*: **Synthesis and SAR of 2-aryl-3-aminomethylquinolines as agonists of the bile acid receptor TGR5.** *Bioorganic & Medicinal Chemistry Letters* 2010, **20**:5718-5721.

171. Watanabe M, Houten SM, Mataki C, Christoffolete MA, Kim BW, Sato H, Messaddeq N, Harney JW, Ezaki O, Kodama T *et al*: **Bile acids induce energy expenditure by promoting intracellular thyroid hormone activation.** *Nature* 2006, **439**:484-489.

172. Katsuma S, Hirasawa A, Tsujimoto G: **Bile acids promote glucagon-like peptide-1 secretion through TGR5 in a murine enteroendocrine cell line STC-1.** *Biochemical and Biophysical Research Communications* 2005, **329**:386-390.

173. Thomas C, Gioiello A, Noriega L, Strehle A, Oury J, Rizzo G, Macchiarulo A, Yamamoto H, Mataki C, Pruzanski M *et al*: **TGR5-mediated bile acid sensing controls glucose homeostasis.** *Cell Metabolism* 2009, **10**:167-177.

174. Hansotia T, Maida A, Flock G, Yamada Y, Tsukiyama K, Seino Y, Drucker DJ: **Extrapancreatic incretin receptors modulate glucose homeostasis, body weight, and energy expenditure.** *Journal of Clinical Investigation* 2007, **117**:143-152.

175. Nguyen AD, Bouscarel B: **Bile acids and signal transduction: role in glucose homeostasis.** *Cellular Signalling* 2008, **20**:2180-2197.

176. Zhang Y, Lee FY, Barrera GC, Lee H-Y, Vales C, Gonzalez FJ, Willson TM, Edwards PA: **Activation of the nuclear receptor FXR improves hyperglycemia and hyperlipidemia in diabetic mice.** *Proceedings of the National Academy of Sciences USA* 2006, **103**:1006-1011.

177. Ma K, Saha PK, Chan L, Moore DD: **Farnesoid X receptor is essential for normal glucose homeostasis.** *Journal of Clinical Investigation* 2006, **116**:1102-1109.

178. Angelin B, Bjorkhem I, Einarsson K, Ewerth S: **Hepatic uptake of bile acids in man. Fasting and postprandial concentration of individual bile acids in portal venous and systemic blood serum.** *Journal of Clinical Investigation* 1982, **70**:724-731.

179. Ruaux CG, Steiner JM, Williams DA: **Postprandial changes in serum unconjugated bile acid concentrations in healthy Beagles.** *American Journal of Veterinary Research* 2002, **63**:789-793.

180. Patti M-E, Houten SM, Baianco AC, Bernier R, Larsen PR, Holst JJ, Badman MK, Maratos-Flier E, Mun EC, Pihlajamaki J *et al*: **Serum bile acids are higher in humans with prior gastric bypass: potential contribution to improved glucose and lipid metabolism.** *Obesity* 2009, **17**:1671-1677.

181. Zhang Y-KJ, Guo GL, Klaassen CD: **Diurnal variations of mouse plasma and hepatic bile acid concentrations as as expression of biosynthetic enzymes and transporters.** *PLoS One* 2011, **6**:e16683.

182. Maloney PR, Parks DJ, Haffner CD, Fivush AM, Chandra G, Plunket KD, Creech KL, Moore LB, Wilson JG, Lewis MC *et al*: **Identification of a chemical tool for the orphan nuclear receptor FXR.** *Journal of Medicinal Chemistry* 2000, **43**:2971-2974.